



AFCEC-CX-TY-TR-2020-0023

SELECTABLE CUTTING AND FRAGMENTATION OF DAMAGED RUNWAY SURFACES

Jonathan Parsons

Hyperion Technology Group
545 Commerce St.
Tupelo, Mississippi 38804

Phase I SBIR Technical Report

June 2020

DISTRIBUTION STATEMENT A: Approved for public release: Distribution unlimited.
AFCEC-202044, 29 October 2020

DESTRUCTION NOTICE. For unclassified, limited documents destroy by any method that will prevent disclosure of contents or reconstruction of the document.

**AIR FORCE CIVIL ENGINEER CENTER
READINESS DIRECTORATE**

DISCLAIMER

Reference herein to any specific commercial product, process, or service by trade name, trademark, manufacturer, or otherwise does not constitute or imply its endorsement, recommendation, or approval by the United States Air Force. The views and opinions of authors expressed herein do not necessarily state or reflect those of the United States Air Force.

This report was prepared as an account of work sponsored by the United States Air Force. Neither the United States Air Force, nor any of its employees, makes any warranty, expressed or implied, or assumes any legal liability or responsibility for the accuracy, completeness, or usefulness of any information, apparatus, product, or process disclosed, or represents that its use would not infringe privately owned rights.

NOTICE AND SIGNATURE PAGE

Using Government drawings, specifications, or other data included in this document for any purpose other than Government procurement does not in any way obligate the U.S. Government. The fact that the Government formulated or supplied the drawings, specifications, or other data does not license the holder or any other person or corporation; or convey any rights or permission to manufacture, use, or sell any patented invention that may relate to them.

Qualified requestors may obtain copies of this report from the Defense Technical Information Center (DTIC) (<http://www.dtic.mil>).

HAS BEEN REVIEWED AND IS APPROVED FOR
PUBLICATION IN ACCORDANCE WITH ASSIGNED DISTRIBUTION STATEMENT.

//SIGNED//

//SIGNED

This report is published in the interest of scientific and technical information exchange, and its publication does not constitute the Government's approval or disapproval of its ideas or findings.

REPORT DOCUMENTATION PAGE				<i>Form Approved OMB No. 0704-0188</i>	
<small>The public reporting burden for this collection of information is estimated to average 1 hour per response, including the time for reviewing instructions, searching existing data sources, gathering and maintaining the data needed, and completing and reviewing the collection of information. Send comments regarding this burden estimate or any other aspect of this collection of information, including suggestions for reducing the burden, to Department of Defense, Washington Headquarters Services, Directorate for Information Operations and Reports (0704-0188), 1215 Jefferson Davis Highway, Suite 1204, Arlington, VA 22202-4302. Respondents should be aware that notwithstanding any other provision of law, no person shall be subject to any penalty for failing to comply with a collection of information if it does not display a currently valid OMB control number.</small>					
PLEASE DO NOT RETURN YOUR FORM TO THE ABOVE ADDRESS.					
1. REPORT DATE (DD-MM-YYYY)		2. REPORT TYPE		3. DATES COVERED (From - To)	
4. TITLE AND SUBTITLE				5a. CONTRACT NUMBER	
				5b. GRANT NUMBER	
				5c. PROGRAM ELEMENT NUMBER	
6. AUTHOR(S)				5d. PROJECT NUMBER	
				5e. TASK NUMBER	
				5f. WORK UNIT NUMBER	
7. PERFORMING ORGANIZATION NAME(S) AND ADDRESS(ES)				8. PERFORMING ORGANIZATION REPORT NUMBER	
9. SPONSORING/MONITORING AGENCY NAME(S) AND ADDRESS(ES)				10. SPONSOR/MONITOR'S ACRONYM(S)	
				11. SPONSOR/MONITOR'S REPORT NUMBER(S)	
12. DISTRIBUTION/AVAILABILITY STATEMENT					
13. SUPPLEMENTARY NOTES					
14. ABSTRACT					
15. SUBJECT TERMS					
16. SECURITY CLASSIFICATION OF:			17. LIMITATION OF ABSTRACT	18. NUMBER OF PAGES	19a. NAME OF RESPONSIBLE PERSON
a. REPORT	b. ABSTRACT	c. THIS PAGE			19b. TELEPHONE NUMBER (Include area code)

TABLE OF CONTENTS

	Page
1. EXECUTIVE SUMMARY	1
2. PERFORMANCE PERIOD ACTIVITY	3
2.1. Task 1: System Trade Study	3
2.2. Task 2: Design High-fidelity SPICE Circuit Simulation Models of EHF System and Subcomponents	6
2.2.1. Summary: High-fidelity SPICE Circuit Simulation Models of EHF System and Subcomponents	7
2.2.2. EHF Circuit Topologies and SPICE Circuit Simulation Models.....	9
2.2.3. Detailed, High-Fidelity EHF SPICE Models.....	13
2.2.4. EHF Blasting Dynamic Loads and “Behavioral” SPICE Component Specifications	14
2.2.5. Comparison of EHF Field Testing Data to SPICE Simulations	16
2.3. Task 3: Proof-of-Principle Experiment(s) to Validate Performance	17
2.3.1. Ancillary HV Components:	26
3. CONCLUSIONS AND RECOMMENDATIONS	114
4. BIBLIOGRAPHY	115
LIST OF ABBREVIATIONS, SYMBOLS AND ACRONYMS.....	116

LIST OF FIGURES

	Page
Figure 1. Photograph Showing Deployed KAPRA System Set up to Fragment Large Boulder with Two Simultaneous Events	4
Figure 2. 20-ton Flatbed Military Truck Suitable for Carrying an Electrohydraulic Fragmenting System.....	5
Figure 3. Aquajet Systems AB Aqua Cutter 710V	6
Figure 4. Schematic and Photograph of Geometry of Pulsed-power Capacitor Bank for Igniting Plasma at the Probe.....	6
Figure 5. GAEP/Maxwell Series “C” 32349 Energy Storage Capacitor and Specifications.....	8
Figure 6. Maxwell Series “C” 32328 Energy Storage Capacitors	9
Figure 7. EHF SPICE Topology Models: Circuit (1.) B&M 4-cap, (2.) Single-sided 2-cap, (3.) Single-sided 4-cap, (4.) Bipolar 4-cap, ± 8 kV, (5.) Bipolar 4-cap, ± 16 kV, (6.) Bipolar 2-cap, ± 16 kV	10
Figure 8. Load Current (kA) Comparison for Topology Circuits 1–6.....	11
Figure 9. Load Power (GW) Comparison for Topology Circuits 1–6.....	11
Figure 10. (Left) Circuit 1: 2:2 B-M Circuit with $C1:C2 = 16$ kV, $C3:C4 = 0$ kV; Dual 412- μ F Cap Banks; (Right) Circuit 4: 2:2-Bipolar ± 8 -kV Charge Circuit with $C1$ and $C2 = +8$ kV, $C3$ and $C4 = -8$ kV.....	12
Figure 11. Circuit 3: Single-sided 16 kV with 4 Capacitors Parallel.....	12
Figure 12. Detailed “High Fidelity” SPICE Schematic of Circuit 3.....	13
Figure 13. Detailed Circuit 3 SPICE Model Results for 60-m Ω Load: Cap Bank Differential Voltage (red trace) and Current (blue trace)	14
Figure 14. (left) Modified Detailed SPICE Schematic Model for Maxwell 32328 Capacitor Bank ; (right) Time-varying EHF Blast Probe Load Resistance Approximated as a Piece-wise Linear Profile.....	15
Figure 15. Adjusted Circuit 3 SPICE Simulation Results	15
Figure 16. Voltage and Current Waveforms from Task 3 Field Test Shot 16.....	16
Figure 17. Voltage and Current Waveforms from Task 3 Field Test Shot 20.....	16
Figure 18. Approximated Power $P(t)$ from Task 3 Field Test Shot 20.....	17
Figure 19. Electro-Hydraulic Fracturing System Components Emphasized (red oval) in the Phase I Design Process	18
Figure 20. Comparisons of 206 μ F vs. 176 μ F for 2-, 3-, and 4-Capacitor Banks of the Phase I EHF System Capacitor Bank Energy vs. Charger Voltage.....	20
Figure 21. Phase I EHF Demonstration Platform Featuring Capacitor Bank, Main HV Switch, and Bus Plates for Interconnections.....	21
Figure 22. Details of a R.E. Beverly Spark Gap Model SG-172CM Spark Gap Trigratron.....	21
Figure 23. Beverly SG-172CM Operational Voltage Range Using N_2 as Its Dielectric Gas	22
Figure 24. Updated CAD Design for Phase I EHF Demonstration Platform	23
Figure 25. Updated EHF Probe Designs Including Some Changes Highlighted; (left) +Bus Addition Support, and (right) Back-force Thrust “Knee” (highlighted in red ellipse).....	24
Figure 26. Machined EHF Plasma Probe Parts (left) and Inertial Blast Restraint Plates (right).	24
Figure 27. EHF Plasma Blasting Probe Shown Partially Assembled.....	25
Figure 28. EHF Pulse Transmission Line, Dielectric Sciences 2198 Coaxial Cable Cross-Section and Overall Coil.....	25
Figure 29. Dielectric Sciences 2198 Pulse Coaxial Cable Cross-section Specifications	25

Figure 30. HV Capacitor Charging Power Supply (CCPS); TDK-Lambda ALE 102A	27
Figure 31. “Fault-Mode” Stairstep Charge Cycle Pattern of a Standard TDK 102A CCPS without an LCA (Long-charge Adapter).....	27
Figure 32. Simulated Charge Cycle Characteristics of Standard TDK 102A 20 kV(max)	28
Figure 33. Simulated <i>V</i> -charge and <i>I</i> -charge Cycle Characteristics of an LCA-controlled TDK 102A 20 kV(max) CCPS Charging a 704-μF Capacitor Bank to 16 kV	29
Figure 34. Simulated <i>V</i> -charge and Power Cycle Characteristics of an LCA-controlled TDK 102A 20-kV(max) CCPS, Charging a 704-μF Capacitor Bank to 16 kV.....	29
Figure 35. Constructed Field-portable HV Charge/Dump Control Switches.....	30
Figure 36. 12-in-thick Concrete Padsfor EHF Testing: (top) 6-ft x 12-ft Slab, (bottom) Three 6-ft x 6-ft Slabs.....	31
Figure 37. EHF System Set up for Field Testing.....	32
Figure 38. EHF Main HV System.....	32
Figure 39. Plasma Blasting Probe Set up.....	33
Figure 40. HVProbes and Pearson Current Monitor.....	33
Figure 41. Four 4000-lb/in ² Strength Concrete Test Slabs for the Test Set	34
Figure 42. Crack Propagation in Concrete Test Slab 2 from Shot 6.....	36
Figure 43. Sequence of Three Shots: (left) 2 Broke off a Section of Test Slab 1, (center) 4 Cracked along the Same Line; 5 (right) Left a Reasonably Straight Edge.....	36
Figure 44. Remaining Section of Test Slab 1 Split into Two Pieces by Shot 5.....	37
Figure 45. Lines Sawed in a Diagonal Pattern Intersecting the Borehole Centered in Test Slab 3 (a) prior to, (b) preparing for and (c) after Shot 7.....	37
Figure 46. Shot 8; Lines Cut to Set the Desired Separation Path in Test Slab 4; Probe Borehole Centered in Section to Be Separated (a) before and (b) after Shot 8.....	38
Figure 47. Shot 13 in Test Slab 4.....	39
Figure 48. Exploding Wire Test Conducted for Shot 12	39
Figure 49. EHF Main HV System Assembly.....	40
Figure 50. Dielectric Plate over Ground Bus Plate Insulates Positive Bus Plate from Ground.....	41
Figure 51. Positive Bus Plate Connects Positive Terminals of Capacitors in Parallel through Positive Terminal Risers	41
Figure 52. Connection of EHF Coaxial Pulse Transmission Line to EHF Pulser	42
Figure 53. Plasma Blasting Probe Connection to EHF Main HV System.....	42
Figure 54. Plasma Blasting Probe 4 Shown Just prior to Use in Field Testing	43
Figure 55. Field Test Setup.....	43
Figure 56. Debris Barrier to Shield EHF Main HV System and Instrumentation	44
Figure 57. The EHF System Included Three HV Probes.....	45
Figure 58. Pearson 1423 Wideband Current Monitor Installed on Output Lead of Coaxial Pulse Transmission Line.....	45
Figure 59. Block Schematic Diagram of EHF Electrical System Setup for Field Tests	45
Figure 60. HV Power Supply and Connection to the EHF Capacitor	46
Figure 61. Copper Sulfate Sink Contained in a 5-gal Bucket.....	46
Figure 62. Electrical Safety Features	46
Figure 63. Four 4000-PSI Concrete Test Slabs Poured for the Test Set.....	47
Figure 64. Makita Hammer Drill and 1-in-diameter Borehole in Concrete Slab	47
Figure 65. Plasma Blasting Probe Weight Plate	48
Figure 66. Precut Lines in Concrete Test Slab	48

Figure 67. Plot of Peak Current as a Function of Capacitor Bank Charge Voltage for EHF Shots 1–20; Presumed Outlier Points Are Plotted in Blue	51
Figure 68. Plot of Peak Current as a Function of Capacitor Bank Charge Energy for EHF Shots 1–20; Presumed Outlier Points Plotted in Blue	52
Figure 69. Test Shot 1–20 Positions in Concrete Samples S1–S4.....	53
Figure 70. Shot 1: Concrete Test Slab and Plasma Blasting Probe Setup	54
Figure 71. Shot 1: Charge and Output Voltage for Time of Trigger of EHF System	55
Figure 72. Shot 1: Current Reading for Time of Trigger from Output of EHF System to Plasma Blasting Probe.....	55
Figure 73. Plasma Blasting Probe Tip post Fire on Shot 1 (after Clean-up); No Visible Damage to Probe from the Shot	55
Figure 74. Shot 2: Charge and Output Voltage for Time of Trigger of the EHF System.....	57
Figure 75. Shot 2: Current Reading (Clipped) for Time of Trigger from EHF System Output to Plasma Blasting Probe	57
Figure 76. Shot 2: Concrete Test Slab Successfully Fractured.....	58
Figure 77. Shot 2: Fracture Lines	58
Figure 78. Shot 2: Fractured Section after Separated Concrete Section Pulled Back	59
Figure 79. Shot 2: Closeup Image of Separated Borehole Section.....	59
Figure 80. Shot 2: Test Concrete Slab Showing Separation of Corner Section	59
Figure 81. Photo of Plasma Blasting Test Probe after Shot 2; No Damage Noted to Probe	59
Figure 82. Shot 3: Plasma Blasting Probe Set up in Chunk of Concrete Separated by Shot 2.....	60
Figure 83. Shot 3: Charge and Output Voltage for Time of Trigger of the EHF System.....	61
Figure 84. Shot 3: Time of Trigger from EHF System Output to Plasma Blasting Probe	61
Figure 85. Shot 3: Completely Fractured Debris from Chunk of Concrete from Shot 2.....	62
Figure 86. Shot 3: Debris; Fragments of Chunk of Concrete Separated by Shot 2	62
Figure 87. Plasma Blasting Test Probe after Shot 3	62
Figure 88. Shot 4: Setup in Concrete Test Slab 1	63
Figure 89. Shot 4: Charge and Output Voltage for Time of Trigger of EHF System	64
Figure 90. Shot 4: Current–Time Plot of Trigger from EHF System to Plasma Probe	64
Figure 91. Shot 4: Separated Corner of Test Slab; Repeats Shot 2 Result	65
Figure 92. Shot 4: Fracture Lines in Concrete Test Slab 1	65
Figure 93. Plasma Blasting Test Probe after Shot 4	65
Figure 94. Shot 5: Charge and Output Voltage for Time of Trigger of the EHF System.....	67
Figure 95. Shot 5: Time–Current Plot of Trigger from EHF System to Plasma Probe	67
Figure 96. Shot 5: Borehole for Plasma Blasting Probe Located between Shot 2 and 4 Boreholes	68
Figure 97. Shot 5: Sliver between Sections Separated from Test Slab by Shots 2 and 4	68
Figure 98. Shot 5: Remaining Section of Concrete Test Slab 1 after Debris Removal	68
Figure 99. Shot 5: Conical Section Separated below Borehole	68
Figure 100. Remaining Pieces of Test Slab 1 Shown with Fault Line up	68
Figure 101. Shot 6: Setup; Borehole Drilled in Center of 4-ft x 4-ft Concrete Test Slab 2	69
Figure 102. Shot 6: Charge and Output Voltage for Time of Trigger of the EHF System.....	70
Figure 103. Shot 6: Time–Current Plot for Trigger from EHF System to Plasma Probe.....	70
Figure 104. Shot 6: Concrete Test Slab Cracked into Three Sections.....	71
Figure 105. Plasma Blasting Test Probe after Shot 6.	71
Figure 106. Shot 7: 2-in-deep Diagonal Pre-cuts in Concrete Test Section 3	72

Figure 107. Shot 7: Plasma Blasting Probe Set into Concrete Test Slab 3 with 2-in-deep Pre-cuts along the Diagonals.....	72
Figure 108. Shot 7: Charge and Output Voltage for Time of Trigger of the EHF System.....	73
Figure 109. Shot 7: Time–Current Plot for Trigger from EHF System to Plasma Probe.....	74
Figure 110. Shot 7: Crack Separation along the Pre-cuts of Test Slab 3.....	74
Figure 111. Shot 7: Close-up of an Unintended Transverse Crack in Test Slab 3	75
Figure 112. Shot 7: Corner Crack along the 2-in-deep Pre-cut Lines in Test Slab 3	75
Figure 113. Shot 7: Test Concrete Slab 3 Section Separated by Shot along Pre-cut Lines.....	75
Figure 114. Shot 7: Crack Cross-section of Chunk Separated along Pre-cut Diagonal Lines.....	76
Figure 115. Shot 7: Unintended Cracks in Two Other Chunks Separated along Pre-cuts	76
Figure 116. Shot 8: Placement of 2-in-deep Pre-cuts and Plasma Blasting Probe	77
Figure 117. Shot 8: Charge and Output Voltage for Time of Trigger of EHF System	78
Figure 118. Shot 8: Time–Current Plot for Trigger from EHF System to Plasma Probe.....	78
Figure 119. Shot 8: Central EHF Blast Location Setup and Pre-cuts Failed to Control Path of Crack Propagation.....	79
Figure 120. Shot 8: Crack Propagating Perpendicularly through Pre-cut Line	79
Figure 121. Shot 9: Setup Building on Shot 8 Setup	79
Figure 122. Shot 9: Charge and Output Voltage for Time of Trigger of EHF System	80
Figure 123. Shot 9: Time–Current Plot for Trigger from EHF System to Plasma Probe.....	81
Figure 124. Plasma Blasting Test Probe after Shot 9	81
Figure 125. Shot 10: Setup Built on Shot 9 Setup.	82
Figure 126. Shot 10: Charge and Output Voltage for Time of Trigger of EHF System	83
Figure 127. Shot 10: Time–Current Plot for Trigger from EHF System to Plasma Probe.....	83
Figure 128. Shot 10: Large Cracks Did Not Follow Pre-cut Lines.	84
Figure 129. Shot 11: Placement of Plasma Blasting Probe in Borehole.....	84
Figure 130. Shot 11: Charge and Output Voltage for Time of Trigger of EHF System	85
Figure 131. Shot 11: Time–Current Plot for Trigger from EHF System to Plasma Probe.....	86
Figure 132. Shot 11: Cracks and Chunk Separation from Concrete Test Slab.....	86
Figure 133. Shot 11: Slab after Removal of Large Concrete Chunks Separated by Shots 8–11	87
Figure 134. Shot 11: Probe 4 Shows Signs of Wear, but Is Still Useable	87
Figure 135. Copper Wire Connected across Terminals of EHF Coaxial Pulse	88
Figure 136. Shot 12: 2-in-deep Pre-cut Line for Exploding Wire Test	88
Figure 137. Shot 12: Copper Wire in Slit Line for Exploding Wire Test.....	88
Figure 138. Shot 12: Charge and Output Voltage for Time of Trigger of EHF System	89
Figure 139. Shot 12: Time–Current Plot for Trigger from EHF System to Plasma Probe.....	90
Figure 140. Shot 12: Exploding Wire Blasted out Shallow Divot along Wire in Pre-cut Line...	90
Figure 141. Shot 13: Pre-cut Lines End Close to (~0.5 in), but Do Not Connect to Borehole ...	91
Figure 142. Shot 13: Plasma Blasting Probe Borehole at Intersection of Pre-cut Lines	91
Figure 143. Shot 13: Charge and Output Voltage for Time of Trigger of EHF System	92
Figure 144. Shot 13: Time–Current Plot for Trigger from EHF System to Plasma Probe.....	93
Figure 145. Shot 13: Cracked along Both Pre-cut Lines on 4 Concrete Test Slab.....	93
Figure 146. Shot 13: Fracture Lines from Borehole to Edge of Concrete Test Slab.....	94
Figure 147. Shot 13: Separated Section of Concrete with Crack	94
Figure 148. Shot 13: Unintentional Crack from Borehole into Concrete Test Slab	94
Figure 149. Shot 14: Plasma Blasting Probe in Concrete Section Separated by Shot 13.....	95
Figure 150. Shot 14: Charge and Output Voltage for Time of Trigger of the EHF System.....	96

Figure 151. Shot 14: Time–Current Plot for Trigger from EHF System to Plasma Probe.....	96
Figure 152. Shot 14: Debris And Concrete Chunks from Separated Concrete Section	97
Figure 153. Shot 14: Debris And Concrete Chunks from Separated Concrete Section	97
Figure 154. Shot 15: Plasma Blasting Probe in Borehole.....	97
Figure 155. Shot 15: Charge and Output Voltage for Time of Trigger of EHF System	98
Figure 156. Shot 15: Time–Current Plot for Trigger from EHF System to Plasma Probe.....	99
Figure 157. Shot 15: Plasma Blasting Probe after Dry Fire (Left) Probe Tip Is Slightly Bent, Significant Carbon Buildup. (Right) Cleaned Probe Shows Adhesive Delamination.....	99
Figure 158. Shot 16: Same Setup and Borehole as Shot 15.....	100
Figure 159. Shot 16: Charge and Output Voltage for Time of Trigger of EHF System	101
Figure 160. Shot 16: Time–Current Plot for Trigger from EHF System to Plasma Probe.....	101
Figure 161. Shot 16: Plasma Blasting Probe Failed; Cracks Did Not Follow Pre-cut Line	102
Figure 162. Shot 16: Failed Plasma Blasting Probe Tip and Cracks Formed from Borehole ...	102
Figure 163. Shot 17: Probe in Hole between Hole for Shots 15 & 16, and Cut in Test Slab 4.	103
Figure 164. Shot 17 Charge and Output Voltage for Time of Trigger of EHF System.....	104
Figure 165. Shot 17: Time–Current Plot for Trigger from EHF System to Plasma Probe.....	104
Figure 166. Shot 17. Crack Propagation Did Not Follow Offset Pre-cut Lines	105
Figure 167. Shot 17. Crack Propagation Did Not Follow Offset Pre-Cut Lines	105
Figure 168. Shot 18: Exploding Wire for Installation in Cut in Slab	105
Figure 169. Shot 18:~ Cut into Concrete Test Slab 13 to Hold Exploding Wire	106
Figure 170. Shot 19: Chunk of Concrete over Wire and Cut to Contain Pressure Pulse	106
Figure 171. Shot 18: Charge and Output Voltage for Time to Trigger the EHF System	107
Figure 172. Shot 18: Time–Current Plot for Trigger from EHF System to Plasma Probe.....	107
Figure 173. Shot 18: Pressure Pulse of Exploding Wire Only Lifted Concrete Chunk.....	108
Figure 174. Shot 19: Test Setup; as for Shot 13, Plus Second Borehole to Stop Crack.....	108
Figure 175. Shot 19: Test Setup with Plasma Blasting Probe Installed.....	109
Figure 176. Shot 19 Charge and Output Voltage for Time of Trigger of EHF System.....	110
Figure 177. Shot 19: Time–Current Plot for Trigger from EHF System to Plasma Probe.....	110
Figure 178. Shot 19: Two Unintentional Cracks Formed in the Concrete Test Section	111
Figure 179. 6-in-deep Pre-cuts Directed Crack Propagation.....	111
Figure 180. Shot 19: Crack Propagation along Pre-cut Lines from Borehole	111
Figure 181. Shot 20: Plasma Blasting Probe in Concrete Section Separated by Shot 19.....	112
Figure 182. Shot 20: Charge and Output Voltage for Time of Trigger of EHF Ssystem.....	113
Figure 183. Shot 20: Time–Current Plot for Trigger from EHF System to Plasma Probe.....	113
Figure 184. Shot 20: Debris and Chunks from 36-in by 36-in Shot 19 Fragment.....	113
Figure 185. Shot 20: Debris and Chunks from 36-in by 36-in Shot 19 Fragment.....	113

LIST OF TABLES

	PAGE
Table 1 Topology Circuits Cases 1–6 Simulated Electrical Performance Specifications for a 75-m Ω Load	11
Table 2. Initial Phase I “Proof-of-Principle” Test Demonstration Capacitor Candidates	19
Table 3. Comparison of CCPS Ratings vs. Capacitor Bank Charge Voltage and Charging Time	26
Table 4. Summary of Testing Shots.....	34
Table 5. Test Shot Summary Table by Test Shot Number	50
Table 6. Test Shot Summary by Test Shot Number	50
Table 7. Data for Shot 1: Test Setup and Results	54
Table 8. Data for Shot 2: Test Setup and Results	56
Table 9. Data for Shot 3: Test Setup and Results	60
Table 10. Data for Shot 4: Test Setup and Results	63
Table 11. Data for Shot 5: Test Setup and Results	66
Table 12. Data for Shot 6: Test Setup and Results	69
Table 13. Data for Shot 7: Test Setup and Results	73
Table 14. Data for Shot 8: Test Setup and Results	77
Table 15. Data for Shot 9: Test Setup and Results	80
Table 16 Data for Shot 10: Test Setup and Results	82
Table 17. Data for Shot 11: Test Setup and Results	85
Table 18. Data for Shot 12: Test Setup and Results	89
Table 19. Data for Shot 13: Test Setup and Results	92
Table 20. Data for Shot 14: Test Setup and Results	95
Table 21. Data for Shot 15: Test Setup and Results	98
Table 22. Data for Shot 16: Test Setup and Results	100
Table 23. Data for Shot 17: Test Setup and Results	103
Table 24. Data for Shot 18: Test Setup and Results	106
Table 25. Data for Shot 19: Test Setup and Results	109
Table 26. Data for Shot 20: Test Setup and Results	112

1. EXECUTIVE SUMMARY

The Phase I SBIR “Selectable Cutting and Fragmentation of Damaged Runway Surfaces,” Contract No. FA8051-19-CA002, a demonstration of the Electro-Hydraulic Fracture (EHF) method has been completed successfully. As proposed, Hyperion constructed and demonstrated a “Proof-of-Principle” (PoP) EHF laboratory system that effectively fragmented large concrete block sections approximately 3-ft x 3-ft x 1-ft, from a larger 6-ft x 12-ft x 1-ft thick concrete slab into pieces sufficiently small that they could be removed easily by such standard equipment as a front end loader. The use of user-controlled, variable power was demonstrated to affect the degree of concrete slab fragmentation. In addition, techniques to use the EHF system in a controlled manner to segment off 90°-corner sections without the use of a water-jet cutter was also demonstrated.

The Task 1 “EHF System Trade Study” consisted of an extensive literature review including physics and historical review of EHF R&D development, a summary of project-specific example, a review of EHF system design and necessary components, and Phase II and Phase III system design needs.

In Task 2, “High Fidelity SPICE Circuit Simulation Models of EHF System and Subcomponents,” the two primary Phase I Task 2 SPICE circuit simulation efforts were: (1.) Topologies—examine the performance characteristics of multiple capacitance bank design topologies, and (2.) High-Fidelity SPICE Circuit Schematic development. In Task 2 Hyperion worked initially and concurrently within the context of the Task 1 Trade Study efforts. The SPICE circuit simulation efforts gradually included more-specific system design and component details based upon initial feedback from the Task 1 trade study and initial parts/components selections likely to be used during the Task 3 PoP Experiment. For Task 2, Hyperion also reviewed some electrical test data (Task 3) acquired during the EHF field PoP demonstration testing phase to help further understand the EHF blasting dynamics better to improve the simulation models fidelity. In some cases, the simulation results matched quite well with the experimental data, which can be fine-tuned to better match the dynamic load characteristics.

For Task 3, “PoP Experiment(s) to Validate Performance,” work started with the selection and purchases of primary components including main pulse capacitors, high-energy switch, and high-current coaxial cable, which would drive the hardware design phase. Other efforts involved the design planning for CAD-machined parts for EHF blast probe, bus plates, and capacitor bank frame. After a few in-lab system checkouts, the completed Phase I EHF system was successfully field tested on 3–5 December 2019 through a series of 20 test shots into four test section slabs of 12-in-thick concrete. Note that as originally proposed in the Phase I proposal, Hyperion intended that field demonstration would have combined the use of a waterjet cutting system for completely pre-cutting slabs followed by use of the EHF system to fragment the cut concrete slabs into small fragments for easy handling and disposal. However, at the time for the field testing, short-term rental use of the qualified waterjet cutting systems was not available as vendors were interested only in long-term use agreements. Therefore, Hyperion modified the EHF field demonstration tests using no waterjet cutting system, and instead to show the results of having no, or only shallow pre-cuts into the concrete to be followed by EHF system plasma blasts.

During these tests, the user-selectable energy applied to each blast demonstrated the way an operator may control and tailor the blast mechanics to produce and limit the desired level of crack formation and fragmentation. Testing proved that the EHF system effectively fragmented large concrete blocks approximately 3 ft x 3 ft x 1 ft into small pieces that could be easily removed by standard equipment such as skid-steers or front end loaders. These successful field tests demonstrated that not only does the EHF determine significant fragmentations of large sections of cut concrete slabs, but that it also may in addition be used effectively for breaking out 3 ft sections of 12-in-thick concrete with clean 90° corners when used in conjunction with the shallow saw cuts.

If selected for Phase II, the Phase I PoP system will be used as a laboratory tool for probe development. In Phase II, the drilling, cutting, and fracturing process may become stand-alone individual systems that would be further integrated into the optimum configuration for a Phase III effort to produce a TRL-9 system. All of the separate elements in this approach are readily adaptable to robotic platforms, which has the potential to be a cost-effective technique that significantly reduces operator personnel needs.

2. PERFORMANCE PERIOD ACTIVITY

The following section discusses the progress toward proposed objectives (cited in Italics), accomplishments, and activities completed during this project.

2.0 Task 0: Program Management

In the proposal, Task 0 focuses on *“the items to be completed as part of the overall program management. The proposed effort is based on a 9 month period of performance with 6 months of technical performance and 3 months for review and finalization of the final report documentation. The program management task will focus on a Kick-off meeting, monthly reports, a draft Final Report, and Final Report.”*

During the reporting periods, a series of six monthly reports were written and submitted for approval; a brief kickoff introduction was made with the Technical Point of Contact (TPOC) as well. In addition, a Field Test Data Summary Report was submitted to the TPOC.

2.1. Task 1: System Trade Study

“Hyperion will perform trade studies to define each subsystem’s architecture and the performance requirements necessary from each subcomponent to generate the required EHF parameters while allowing for integration into a laboratory device with eventual traceability and integration onto a common robotic platform with a high pressure Hydrodemolition water jet like the Aquajet Systems Aqua Cutter 710V. The following is a short list of potential trade studies that Hyperion has completed during this effort. The trade studies examined the relevant literature on primary switches including gas sparkgaps, dielectric puncture, high voltage solid state silicon carbide insulated-gate bipolar transistor, thyristor, ignitrons as well as laser-triggered pseudo sparkgaps. Hyperion performed a literature review of IEEE with regards to EHF techniques previously explored and current state of the art. The second focus of the trade study examined how the size, weight, volume, and power requirements of EHF match those of a chosen robotic platform. The last area of focus of the trade study examined how operational requirements, environmental factors, safety, employment requirements impact the various subsystems.”

Months 1–3

Determined EHF waveform parameters necessary to generate the desired effects. Quantified the ranges of rise time, pulse width, di/dt , dV/dt etc. to be covered for scalability

Examined available subcomponents and performance characteristics of each from the available literature

Performed mechanical packaging and integration trade studies that examined packaging of the EHF subsystems with special attention to size, weight, and energy requirements as well as performance and safety limitations

Provided suitable options/down selected key components including, prime energy supply, energy conditioning and storage, switching, transmission line, safety system, fire control, and probe.

The Task 1 System Trade Study was accomplished during months 1–3. At that time, Hyperion did not have detailed specifications for a system that will fragment concrete rubble sufficient for runway repair. However, based on the trade study, an order of magnitude “strawman” set of requirements was derived as follows:

- Operating voltage range 10–50 kV
- Peak current range 40–100 kA
- Stored single pulse energy 50–100 kJ
- Single pass Coulomb transport – 6–10 C
- Switch life ~ 10,000 shots

Summary:

The trade study suggested that an EHF system applicable to bomb damage repair on aircraft runways is technically feasible and, in some cases, could be an adaptation of a COTS item (KAPRA Korean unit). It is instructive to look at a picture of the COTS item and compare it briefly with the “strawman” system described above. Figure 1 is a picture of the KAPRA system along with its specifications.

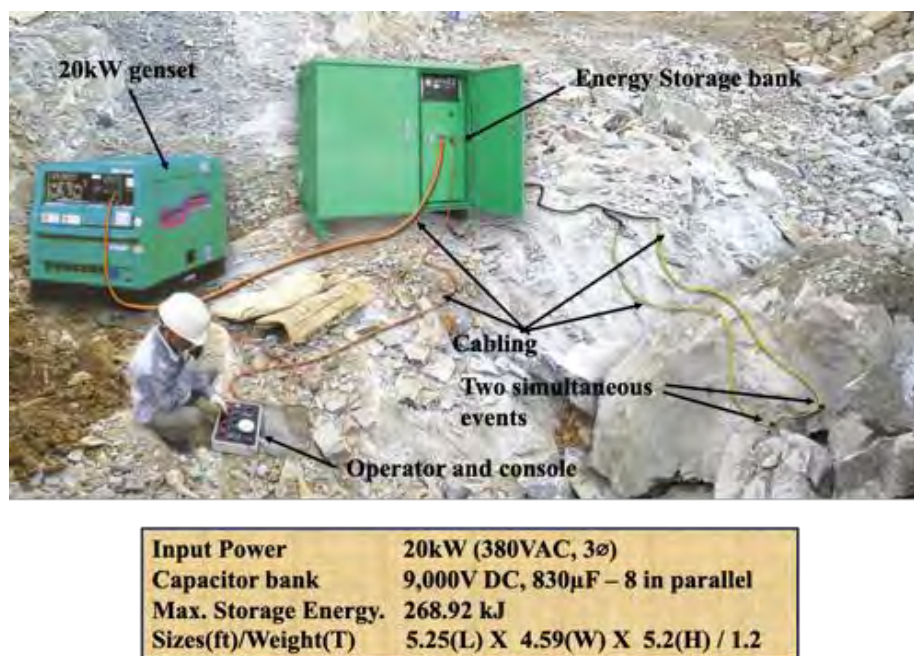


Figure 1. Photograph Showing Deployed KAPRA System Set up to Fragment Large Boulder with Two Simultaneous Events

In Figure 1 the operator is only ~8 ft from the event, which implies that it creates no flying fragments. It is interesting to note that the power requirements for the strawman system above, which has a total mass of 1.25 T, are very similar to those for the KAPRA system’s 1.2-T capacitive energy storage system. This is reasonable in that the strawman system operates at considerably higher voltage but uses only four capacitors. That the Korean system power train has been implemented safely in the field provided confidence that the proposed Hyperion EHF system would be equally safe.

The next question is how to integrate the EHF system into any of the mobility platforms. The weight of the unit is modest at 1.25 T but the addition of a hydraulically driven arm and probe assembly would add considerable weight. It is also possible and probably practical to palletize the total assembly and place it on a military flatbed truck such as that shown below in Figure 2.



Figure 2. 20-ton Flatbed Military Truck Suitable for Carrying an Electrohydraulic Fragmenting System

If Phase II of this work is funded, a working first prototype system can be built for Air Force evaluation.

Additional requirements for the complete cutting-and-fragmenting system:

Two other pieces of equipment will be needed in the ensemble used for runway repair.

Shallow drilling apparatus: The two most promising embodiments of an EHF system require a pre-drilled hole in debris to be broken up. Drilling in stone and concrete is a highly developed technique and readily adaptable to the problem of runway repair. As it is highly probable that suitable drills exist within the military equipment inventory it will not be covered further.

Waterjet cutting and erosion of concrete: While the waterjet technology was not a part of this trade study (total COTS systems are available from numerous vendors), it must be integrated into the total equipment ensemble that will be needed to repair runway damage. Surveying the literature shows that waterjet concrete processing is an established technology with semi-annual conferences sponsored by the WaterJet Technology Association (WJTA). In these conferences, advances in the state of the art are described and the latest in equipment is presented and demonstrated (see for example the “*Proceedings of the 2017 WJTA-IMCA Conference & Expo*,” New Orleans, Louisiana, 2017).

Reviewing these and other proceedings indicates that there are several variables associated with the concrete to be processed, including the presence of aggregate materials, rebar, and concrete strength. Nevertheless, removal rates cited range from 1–3 m³/h.

The waterjet system will replace the diamond saw to separate the area to be repaired, so it is useful to estimate its linear rate for cutting to a depth of 12 in. If a single jet, with a processing width of 3 in aligned along the cut line could remove 1 m³/h, a linear cut 3 in wide, 1 ft deep and 142 ft long is possible. The most optimistic cut rate would be on the order of 400 linear ft/h. *Numbers such as the above can be misleading—they do not consider the depth-of-cut per pass in the cut rates—however, they should be correct to an order of magnitude.* Waterjet cutting and

processing of concrete is in widespread use for a variety of tasks such as removing damaged concrete from such structures as buildings, bridges, pillars, dams, roadways, and airport runways.

An ample body of literature describes application of waterjet technology specific to these tasks. In general, the use of waterjets has been proven to be a cost-effective, minimally hazardous technique. Figure 3, taken from the Hyperion Phase I proposal, is an example of a robotic unit manufactured by Aquajet Systems.



Figure 3. Aquajet Systems AB Aqua Cutter 710V

Whereas the unit shown in Figure 3 is typical of what is available, such a system can be modified to produce the linear cut typical of what is used for runway repair. In the target application waterjet technology will be part of a complete system to selectively cut a line inside which all concrete debris is to be shattered to the point that it can serve as aggregate or effectively be removed by standard machines like front end loaders.

In Phase II, the drilling, cutting, and fracturing process will probably use stand-alone individual systems that would be further integrated into the optimum configuration in a Phase III effort to produce a TRL-9 system. *Each of the separate elements in this approach is readily adaptable to robotic platforms, which have the potential to be a cost-effective technique that significantly reduces operator personnel needs.*

2.2. Task 2: Design High-fidelity SPICE Circuit Simulation Models of EHF System and Subcomponents

The proposal specifies: “...*SPICE circuit simulation models will be developed of the EHF components and subcomponents based on the system proposed herein. ... Successful model simulation results will serve as verification of the conceptual design outlined in Figure 4.*”

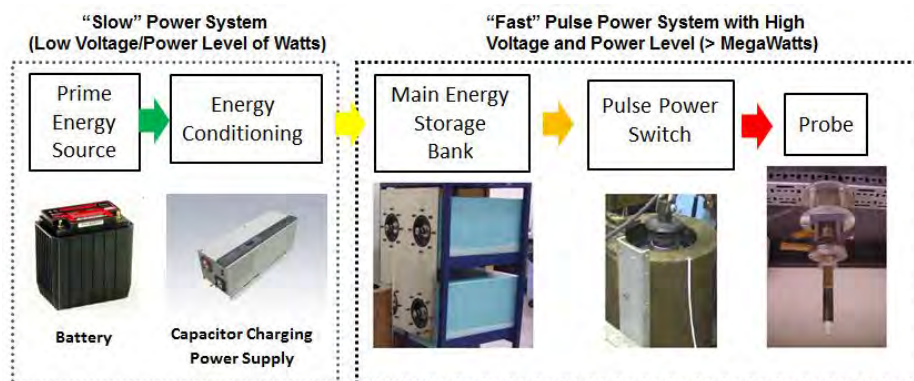


Figure 4. Schematic and Photograph of Geometry of Pulsed-power Capacitor Bank for Igniting Plasma at the Probe

2.2.1. Summary: High-fidelity SPICE Circuit Simulation Models of EHF System and Subcomponents

The two primary Phase I Task 2 SPICE circuit simulation efforts were: (1) Topologies - examine the performance characteristics of multiple capacitance bank design topologies, and (2) High-fidelity SPICE Circuit Schematic development. In Task 2 Hyperion worked initially and concurrently within the context of the Task 1 Trade Study efforts. SPICE circuit simulation efforts gradually included more-specific design detail based upon initial feedback from the Task 1 Trade Study and initial part/component selections to be used during the Task 3 PoP Experiment. For Task 2, Hyperion also reviewed electrical test data acquired during the EHF field PoP testing phase to better understand the EHF blasting dynamics to improve the simulation model's fidelity.

Initial SPICE simulation models studied early in Phase I used fixed (static) load parameters, primarily a static resistance. The EHF blasting probe has a gap between electrodes separated by a dielectric insulator and some blasting fluid, typically as common as water. When the electrical potential increases sufficiently, electrical current starts to flow as the dielectric–water barrier starts to ionize and break down. The water vaporizes into an ionized gas (or plasma) and develops into an intense electric arc. This causes an abrupt pressure increase in the virtually incompressible blasting fluid, resulting in pressures of approximately 1 GPa (145 kpsi) or more, depending on the system energy E , instantaneous power $P(t)$, rise-time (dI/dt), and the media's physical properties (tensile and compressive strength, moduli, homogeneity), mass, and geometry. The transient pressure pulse generates a shock wave and pressure fractures to the rock or concrete. Both the gas expansion and kinetic inertia continue to develop the rock/concrete crack fractures.


More-sophisticated SPICE models based partially on high-current underwater spark gaps can improve the circuit performance fidelity leading to system optimization. A limited review of published research papers related to plasma arc channel development for application to SPICE “Behavioral” component modeling of this EHF dynamic load was made. For high-fidelity simulations, provision for a *dynamic, time-varying load model* for the EHF blasting probe load were incorporated. These optimizations were varied based upon different design interests that arise from the Task 1 System Trade Study, and Task 3 PoP laboratory test demonstrations. These addition simulation results were compared to actual data acquired from these laboratory test demonstrations. These were used to improve the SPICE model's fidelity and to predict improved built system performance designs.

The basis of the EHF system can be conceptually divided into two subsystems: 1) the “slow,” low-power, and mostly (but not exclusively) low-voltage side, and 2) the “fast” HV, high-power Pulse Power System that is the heart of the EHF system. The low-voltage side of the system provides the prime energy source such as the AC-grid, or off-grid sources such as batteries or inverter systems including an alternator or small generator. Next after the Prime energy source, any required power conditioning circuitry required to match the requirements of the pulsed power train, typically an HV capacitor–charging power supply (CCPS). The “fast” HV side of the pulsed system generally includes a bank of HV capacitors storing energy at a low-power rate, and then discharging quickly at a much higher power level, to produce a short time duration (microsecond timescale) energy release in the GW range. Another key element of the EHF system is the electro-hydraulic plasma blasting “probe,” which inserts into a fluid-filled bored hole in the substrate—in this project, concrete—and discharges the stored energy as an electric plasma arc. When the electrical arc is exposed to a pre-emplaced fluid such as water, it creates a high-brisance shockwave, fracturing the surrounding substrate.

Figure 4 is a system functional block diagram from the prime energy input components through the power conditioning for the low-power system and on to the HV system pulsed power capacitors, which are switched through a transmission line to the electro-hydraulic probe.

The primary energy storage source will consist of low-inductance, HV, pulse-power-rated capacitors. A range of voltages and capacitance values will be considered. Several capacitor manufacturers such as General Atomics (GA) and National Winding Labs (NWL) sell high-energy-density pulsed-power capacitors within the voltage and capacitance range, and physical size envelope needed for an EHF Third-Generation System design. For over 50 years GA has continued to manufacture high-energy-density capacitors, originally produced by Maxwell Laboratories, and collectively continued pulsed power technology development. For the Phase I effort, two candidate capacitor models, both manufactured by Maxwell/GA, were used to illustrate the energy storage performance options.

One of the most likely best options for high-energy density capacitors for this EHF approach are dielectric-oil-filled, metal-cased capacitors similar to those from the Maxwell/GA “Series C” product line. Two different Maxwell/GA candidate capacitors were studied during this Ph. I Task 2 effort. The Maxwell/GA 32349 is a low-inductance, 206- μ F, 22-kV capacitor Hyperion personnel have experience with is shown in Figure 5 along with its electrical specifications. The 32349 capacitor is designed internally with a low equivalent series inductance (ESL) of ~ 40 nH and high peak current of 150 kA resulting in fast current rise-times.



Part Number	Cap (μ F)	Max Voltage (kV)	Energy (kJ)	Voltage Rev %	Peak Current (kA)	Design Life
32349	206.0	22	50	10	150	3×10^3

Approx. Inductance (nH)	Case Dimensions H x W x L	Approx Weight	Case Detail (pdf)
45	12.0 x 16.0 x 27.4 in. (305 x 407 x 696 mm)	320 lbs (145.2 kgs)	C2

Figure 5. GAEP/Maxwell Series “C” 32349 Energy Storage Capacitor and Specifications

During the Phase I project, absent readily available 32349 capacitors, Hyperion opted for a similar Maxwell series-C capacitor 32328 (Figure 6). The Maxwell 32328 is a similarly low-inductance 176- μ F, 21.3-kV capacitor. While the 32328 has somewhat higher ESL inductance of 70 nH, and lower peak current estimated to be ~ 75 kA per capacitor (manufacturer original specifications not available), those values make it a good capacitor candidate given that the other overall system ESL inductance characteristics will influence the capacitor specifications in use.

The “Series C” capacitor packaging often has a central output bushing/post with the metallic case serving as the circuit return, often also grounded. In the case of the 32328, a dual-output bushing is used and the “dead” case is not used in the current return circuit. The unique bushing material used to insulate the HV center post on the capacitors can be a low-profile design or optionally a lower-inductance “bowl” design referred to as Scyllac bushings, tailored for direct coaxial-fed spark-gap switches.



Figure 6. Maxwell Series “C” 32328 Energy Storage Capacitors

GA’s capacitor data sheets list several capacitors that are suitable to meeting a wide range of design requirements for a third-generation EHF device, either as modules that would be bussed to the desired capacitance, or as single packages similar to those used in previous designs. The output can be configured in a number of geometries. Each approach has unique advantages, which were explored through modeling to determine the optimal approach for this application. Different capacitor topologies were considered during simulations including a dual-sided Bernardes–Merryman (B-M) first-generation system scheme, as well as a conventional single-sided capacitor system (second- and third-generation systems) for the EHF. The B-M scheme offers the advantage of preventing capacitor voltage reversals without introducing energy-limiting fuses or requiring the additional complexities of crowbar circuits. A first-generation system developed for NASA used the B-M topology for the effectiveness of the EHF approach.

2.2.2. EHF Circuit Topologies and SPICE Circuit Simulation Models

The following sections describe the first set of discussed SPICE simulation analysis comparing various capacitor bank topologies. Presented first is a summary of six (6) different capacitor bank topologies. Presented second is a more detailed high-fidelity SPICE model for an EHF system.

Circuit Topologies: In this first topology summary section, six different capacitor bank topologies are shown (see Figure 7), all using the specifications for the Maxwell/GA 32349 capacitor. The topologies look initially at different capacitor bank layout (B-M, 2- or 4-caps., single-sided or bipolar) and different capacitor charge–voltage schemes. In this first series of multiple-topology SPICE circuit simulations, early approximated fixed-load inductance (1 μH) and load resistance (75 $\text{m}\Omega$) values are used collectively for the switch, transmission line, and load values. To summarize, a circuit number description is given followed by schematics of each. Following that, a table of predicted electrical performance specifications is shown followed by various graphs of capacitor voltage $V(t)$, load current $I(t)$, and load power $P(t)$.

Circuit No. 1: B-M (Figure 7) with dual 412- μF cap banks @ 16 kV; most conservative topology with no V -reversal, initial charges: $C1\text{-}C2 = 16 \text{ kV}$, $C3\text{-}C4 = 0 \text{ kV}$, $I_{\text{pk}} \sim 119 \text{ kA}$ @ 17.5 μs . *Assuming discharge probe does not re-open early*, the B-M scheme ends discharge with both cap banks resting at $\sim <8 \text{ kV}$; 52.7-kJ starting energy with 26.35 kJ remaining after shot (23.35 kJ consumed). Peak load 1.07 GW.

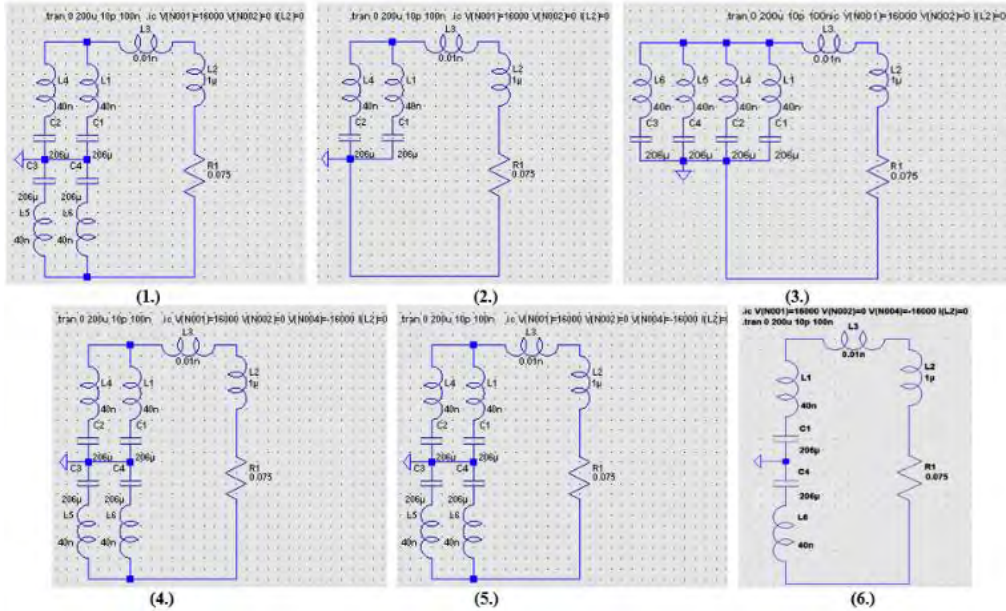


Figure 7. EHF SPICE Topology Models: Circuit (1.) B&M 4-cap, (2.) Single-sided 2-cap, (3.) Single-sided 4-cap, (4.) Bipolar 4-cap, ± 8 kV, (5.) Bipolar 4-cap, ± 16 kV, (6.) Bipolar 2-cap, ± 16 kV

Circuit 2: Single-sided 16 kV, 2 caps. parallel, 412 μF ; $I_{\text{pk}} \sim 140 \text{ kA}$ @ 21.7 μs . Ends discharge with caps. @ $\sim 0 \text{ kV}$; 52.7-kJ charge energy, all dissipated if no early probe openings. Peak load power, 1.48 GW.

Circuit 3: Single-sided 16 kV, 4 caps. parallel, 824 μF ; $I_{\text{pk}} \sim 159 \text{ kA}$ @ 28.0 μs . Ends discharge with cap bank $\sim 0 \text{ kV}$; 105.5 kJ charge energy, all dissipated if no early probe openings. Peak Load power, 1.9 GW.

Circuit 4: Bipolar ± 8 -kV charge; Modified use of B-M topo. assembly with dual 412- μ F cap banks; $I_{pk} \sim 119$ kA @ 17.0 μ s; voltage reversal possible. Ends discharge with the one cap bank resting at ~ 0 kV; 26.4-kJ charge energy, all dissipated if no early probe openings. Peak Load power, 1.06 GW.

Circuit 5: Bipolar ± 16 -kV charge; Modified use of B-M topo. assembly with dual 412- μ F cap banks; $I_{pk} \sim 238$ kA @ 17.4 μ s; voltage reversal possible. Ends discharge with one cap bank resting at ~ 0 kV; 105.5-kJ charge, all dissipated if no early probe openings. Peak Load power, 4.24 GW.

Circuit 6: Bipolar ± 16 -kV charge; Modified use of B-M topo. assembly with dual 206- μ F capacitors; $I_{pk} \sim 194.4$ kA @ 13.4 μ s; voltage reversal possible. Ends discharge with one cap bank resting at ~ 0 kV; 52.7-kJ charge energy, all dissipated if no early probe openings. Peak load power, 2.8 GW.

Table 1 shows a compiled summary of Topology Circuits Case 1 to 6 simulated electrical performance specifications, followed by various graphs of capacitor bank voltage $V(t)$, load current $I(t)$, and load power $P(t)$ for a 75-m Ω static load.

Table 1 Topology Circuits Cases 1–6 Simulated Electrical Performance Specifications for a 75-mΩ Load

Topology Circuit #	Desc.	Total # Caps	# Chrgd Caps	Cap. Chrgd (μF)	Voltage (kV)	Energy (kJ)	Load ESL:ESR (μH:mΩ)	Peak Ipk Current I(t), (kA)	Peak I(t) Time (μs)	dI/dt (kA/μs)	Peak Power Ppk (GW)	Peak P(t) Time (μs)
1	2:2-B&M	4	2	412	16	52.7	(1.0 : 75)	119.2	17.5	15.1	1.07	17.5
2	2:Single-Side	2	2	412	16	52.7	(1.0 : 75)	140.3	21.7	15.3	1.48	21.6
3	4:Single-Side	4	4	824	16	105.5	(1.0 : 75)	159.0	28.0	15.5	1.9	28.5
4	2:2-Bi-Polar	4	4	824	8	26.4	(1.0 : 75)	119.0	17.0	15.1	1.06	17.6
5	2:2-Bi-Polar	4	4	824	16	105.5	(1.0 : 75)	237.7	17.4	30	4.24	17.2
6	1:1-Bi-Polar	2	2	412	16	52.7	(1.0 : 75)	194.4	13.4	28.8	2.8	13.4

Comparing graphs of capacitor voltage $V(t)$, load current $I(t)$, and load power $P(t)$ for these six topology circuits are in Figures 8 and 9. Figure 8 shows the load current $I(t)$ for the example 75-mΩ load, followed by $P(t)$ in Figure 9. For the topologies presented, note that the B-M and the bipolar designs have the faster rise times. The bipolar circuits 5 and 6 have the highest peak currents (238 and 194 kA, respectively) and power (4.2 and 2.8 GW, respectively) with dI/dt (30 and 28.8 kA/μs, respectively) approximately double circuits 1–4. The reason for this is that the bipolar capacitor bank is at the higher (32 kV) differential voltage. While this is attractive energetically, in practical EHF application such a system would require precise synchronization of two switches to flash a coaxial-style blasting probe barrel to high potential with respect to the earth-grounded concrete. Unless insulated, this system likely would lose some of its energy to the borehole walls.

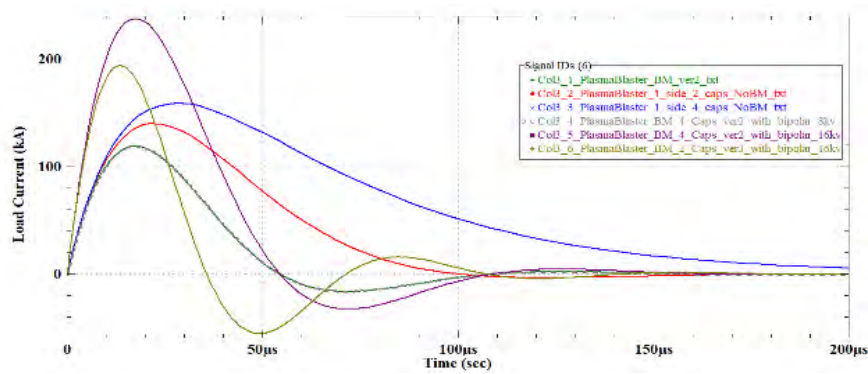


Figure 8. Load Current (kA) Comparison for Topology Circuits 1–6

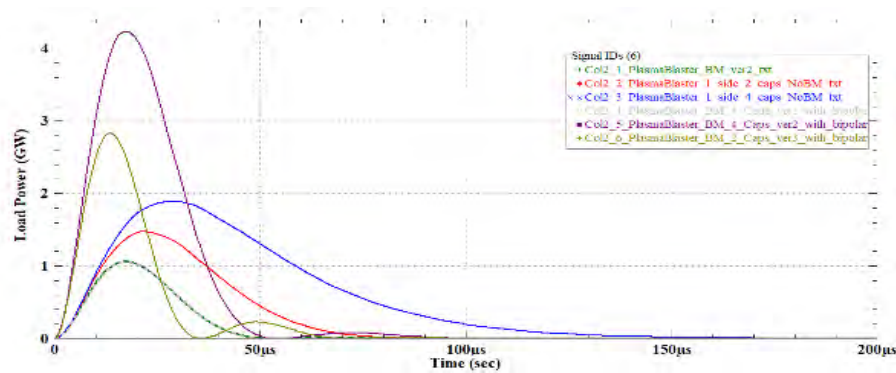


Figure 9. Load Power (GW) Comparison for Topology Circuits 1–6

Note in both circuits 1 and 4, $I(t)$ and $P(t)$ are the same and overlie each other (the graph traces are dashed so both are visible). Both sides of the capacitor bank voltages $V(t)$ and $I(t)$ are plotted. The effective parallel/series capacitance is the same for both, as is $V(t)$ at all times. The difference is only in the initial charge states of the capacitors with Circuit 1 (Left) B-M system capacitors at +16 kV and 0 kV, respectively, vs. the Circuit 4 (Right) capacitors at +8 kV and -8 kV, respectively (16 kV differential voltage).

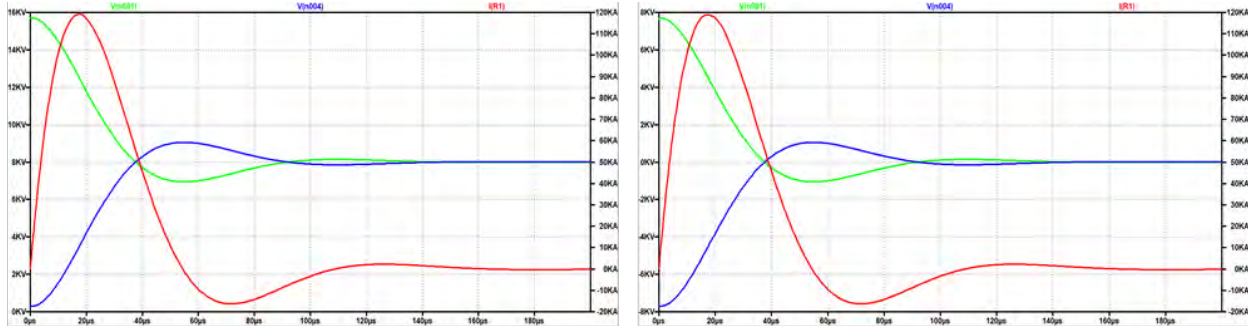


Figure 10. (Left) Circuit 1: 2:2 B-M Circuit with C1:C2 = 16 kV, C3:C4 = 0 kV; Dual 412-μF Cap Banks; (Right) Circuit 4: 2:2-Bipolar ±8-kV Charge Circuit with C1 and C2 = +8 kV, C3 and C4 = -8 kV

In Phase I, Circuit 3 was chosen for the Task 3 field demonstration PoP design for the assembled EHF system. A graph for Circuit 3 $V(t)$, $I(t)$, and $P(t)$ appears in Figure 11, 824 μF; $I_{pk} \sim 159$ kA @ 28 μs, 1.9 GW @ 28.7 μs; Energy; 105.5 kJ Charge, All Dissipated. Computations and graphs of Circuit 2, 5 and 6 topologies, and waveforms for $V(t)$, $I(t)$, and $P(t)$, are not included here for brevity.

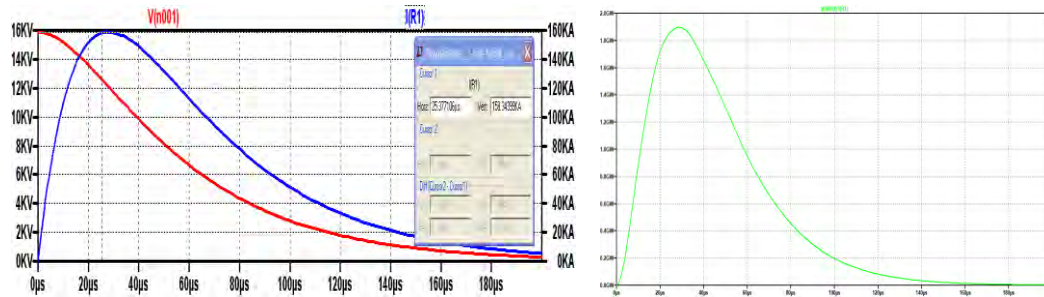


Figure 11. Circuit 3: Single-sided 16 kV with 4 Capacitors Parallel

Results from initial various topology simulations suggested different design approaches based on the pulsed system performance needs. For example, if slower, high-energy pulses are required, circuits 2 and 3 are good options with energies of ~53 and 105 kJ, respectively. If a direct blasting effect performance comparison of the lower vs. higher energy is desired, circuits 4, 1 and 5 have the same current dI/dt rise times with energies of ~26, 53 and 105 kJ, respectively. Of course, applying different charge voltages varies the energy but a range of different $I(t)$ rise times and therefore, different action integrals (I^2t), can be achieved.

Different EHF applications are likely to respond differently and more effectively, depending on the details of the plasma blasting resulting from different pulsed power profiles. For example, large rock-boulder blasts where the mass may be considered to approach that of a “semi-infinite”

mass may sometimes respond well to higher-energy, slower-pulse rise time, and long pulse time profiles. Alternatively, EHF applications of thinner structures (<1 ft) such as with this project's concrete runway repair may benefit from much faster pulse rise times, while also using EHF blasting probes designed to optimize the lateral shockwave profiles.

2.2.3. Detailed, High-Fidelity EHF SPICE Models

A much more detailed, high-fidelity SPICE model of Circuit 3 was developed as an example for the EHF system using the specifications for the Maxwell/GA 32349 capacitor. The individual detailed electrical specifications of system primary subcomponents (capacitors, switch, transmission line, and load) are broken out in this high-fidelity SPICE model to allow more specific design space studies/comparisons to be made—e.g., the effects of using a lower-inductance transmission cable or different switching topologies. Additional details capturing different capacitor bank bus-work design-feeds were also evaluated. As an example, Figure 12 illustrates the detailed SPICE model for topology Circuit 3 with a unipolar (“single-side”) scheme using four 32349 capacitors, connected in parallel. Most of the component values represent actual component values while others are used as place holders for future, more specific evaluation. The EHF blasting probe load is 10 m Ω , 250 nH inductance.

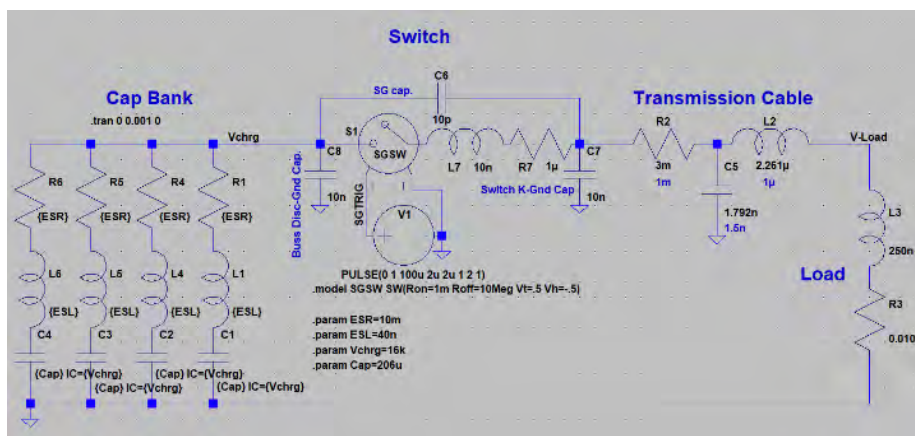
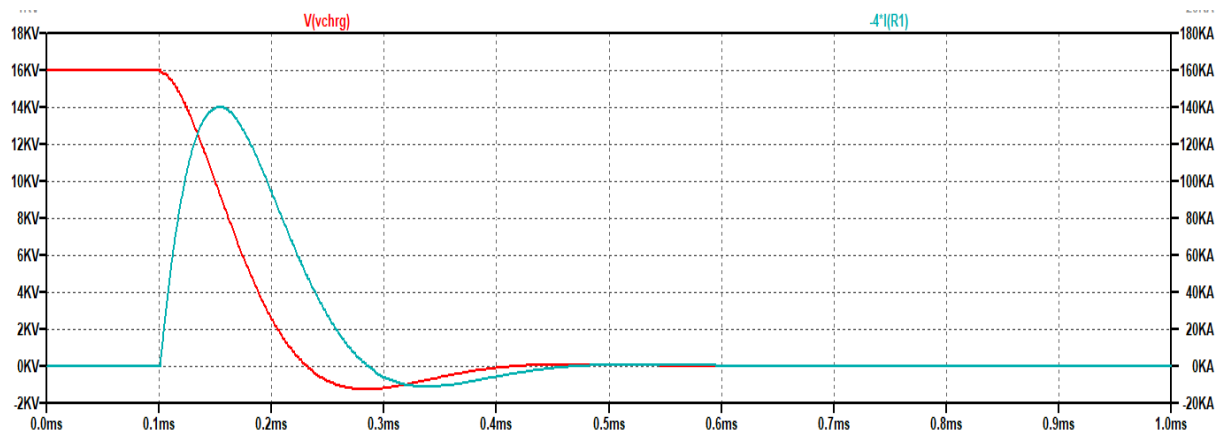


Figure 12. Detailed “High Fidelity” SPICE Schematic of Circuit 3

As an example of such a design space, the system electrical responses to changes of the R3 load resistances to 10, 35, or 60 m Ω were computed. With a 10-m Ω load resistance, the circuit is under-damped ($Q \sim 3$) and the capacitor banks experience $\sim 60\%$ voltage reversal (V_{rev}). With a 35-m Ω load, V_{rev} is down to $\sim 25\%$ and peak power is ~ 1 GW at 60 μ s. However, when the load resistance is 60 m Ω , the circuit is almost critically damped and the capacitors experience only $\sim 6\%$ V_{rev} (Figure 13). This is well below the specified maximum V_{rev} % rating, and promises longer capacitor life due to the reduced dielectric film voltage-relaxation stress.

The detailed SPICE simulation waveform results such as those shown for the 60-m Ω load resistance in Figure 13 with only $\sim 10\%$ V_{rev} are nearly identical to those recorded in some actual Auburn University laboratory tests described below. This provides good initial indication that the detailed, high-fidelity, SPICE model shown in Figure 12 closely emulates the original first-generation system.



**Figure 13. Detailed Circuit 3 SPICE Model Results for 60-mΩ Load:
Cap Bank Differential Voltage (red trace) and Current (blue trace)**

2.2.4. EHF Blasting Dynamic Loads and “Behavioral” SPICE Component Specifications

Further enhancement of the high-fidelity model should include considerations for the dynamic load characteristics of EHF system applications, primarily at the blasting probe load. SPICE models were updated to include some SPICE behavioral components for dynamic EHF probe load resistance simulation. This allowed for simulations of some previously observed plasma arc channel development testing effects.

In SPICE, components such as resistors may be assigned certain nonstatic properties including *behavior*, definitions which may be based upon equation models, time-integrated (cumulative) dissipated power or peak current effects, or even simple tabular data for a PWL LUT (piece-wise linear look-up table) based on measured data. Such circuit elements were incorporated into the original, detailed, high-fidelity, EHF model presented above, and included exact specifications for Task 3 selected sub-components.

In addition, during Phase I, Task 2, the high-fidelity SPICE circuit simulations were modified to reflect the selected 176-μF (each) capacitor bank components (four 176-μF capacitors vs. previous 206-μF). Though the surplus 176-μF Maxwell 32328 capacitors have ~15% less capacitance than the Auburn University Space Research Institute (A.U. SRI) 206-μF 32317 capacitors, if equivalent energy test comparisons are desired, a nominal charge voltage of ~17.3 kV would provide the same energy from the 32328s as from a 32317/32349 capacitor bank at 16-kV charge voltage. From the standpoint of an equal peak dI/dt rate test, given the lower capacitance of the 32328 bank and corresponding faster LC frequency, a slightly lower charge voltage may achieve fractures due to the higher ESL (internal equivalent series inductance (L)) of 70 nH for the 32328 vs. the 32349s’ 45 nH each. This was confirmed in SPICE simulations. Test measurements of the Maxwell 32328 capacitors rated at 176 μF indicated that the actual average capacitance is ~170 μF each. It is assumed the ESL inductance is still 70 nH each, as indicated on the name-plaque. Figure 14 shows one of the modified dynamic load SPICE models developed under Task 2 for the lower 680-μF bank capacitance, higher 70-nH (each) ESL and 17.3-kV charge voltage, added bus inductance, and time-varying EHF blast probe resistance.

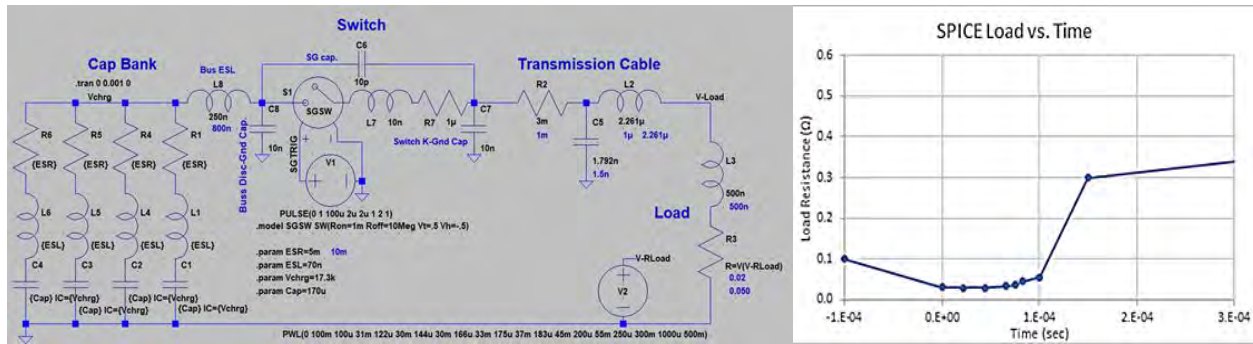


Figure 14. (left) Modified Detailed SPICE Schematic Model for Maxwell 32328 Capacitor Bank ; (right) Time-varying EHF Blast Probe Load Resistance Approximated as a Piece-wise Linear Profile

In this example, the varying load resistance was approximated by using some previously acquired test data to develop the Piece-Wise Linear profile shown in Figure 14. Note that initially the EHF blast probe resistance decreases as ionization and current density increases, and then a little after current peaks, the resistance starts to rapidly increase representing highly gasified water-based blasting media and expansion of the plasma.

The improved SPICE model results in performance as in Figure 15. The SPICE simulation results: 174-kA I -peak @ 61 μ s, 4.83 kA/ μ s, and 135- μ s pulse width using 680- μ F capacitance, 70-nH ESL, 17.3-kV charge voltage, added 250-nH bus inductance, and time-varying EHF blast probe resistance profile shown in Figure 15. The voltage reversal simulated is -4 kV (~23%) for a pulse differential voltage of 21.3 kV, which is the standard rated voltage for 32328 capacitors.

The SPICE simulations indeed confirmed the slightly greater performance level if charged to the higher 17.3 kV. Simulation predicts I -peak of 174 kA vs. the 32317/32349's 160 kA. Due to the lower capacitance, despite the higher 70-nH ESL inductance (each, vs. 45 nH), the I -peak is achieved ~ 10% faster. At 174-kA total, the per-capacitor current load is 43.5 kA, which should be very conservative for these capacitors, given that, due to their age, the I -peak ratings might have drifted from their original value.

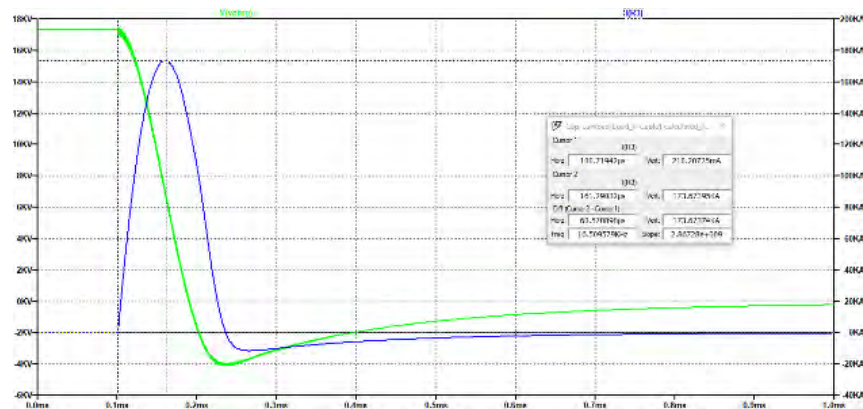


Figure 15. Adjusted Circuit 3 SPICE Simulation Results

2.2.5. Comparison of EHF Field Testing Data to SPICE Simulations

These higher-fidelity simulation results confirmed the predicted performance, and that the system performs within ratings. The simulation results were briefly compared to actual field test data acquired from Task 3 laboratory PoP test demonstration test data. In Figure 16, the waveforms from Task 3 field test shot 16 indicate a nearly shorted probe impedance causing voltage reversal. This allows for the approximation of the EHF system inductance. From the first half-cycle corresponding to ~ 6024 Hz and given the $704\text{-}\mu\text{F}$ capacitor bank, the approximate EHF system inductance is 992 nH . This is a lower physical system ESL inductance given the attention and care used in sub-component selection and design and assembly of the EHF PoP system. The simulation in Figure 15 had assumed close to $3\text{ }\mu\text{H}$ for an overall ESL compared to the final constructed EHF PoP system's $\sim 1\text{ }\mu\text{H}$, resulting in faster rise times.

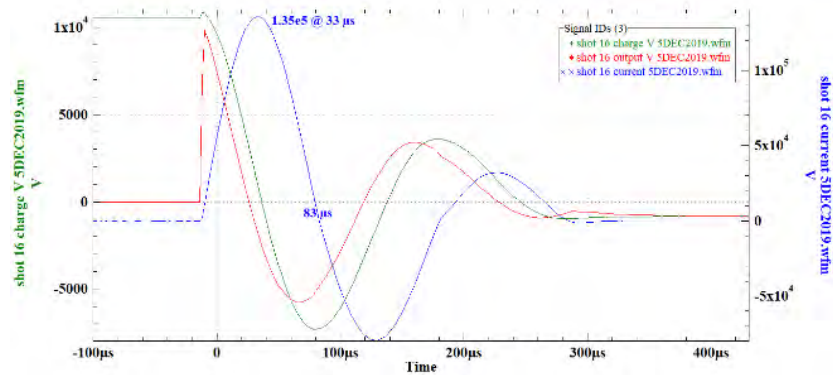


Figure 16. Voltage and Current Waveforms from Task 3 Field Test Shot 16

Figure 17 shows voltage and current waveforms from Task 3 field test shot 20, which fragmented a 3-ft x 3-ft x 12-in concrete slab with 15.7-kV charge, 86.8 kJ , resulting in peak current of 153.6 kA at $54\text{ }\mu\text{s}$. When compared to one Circuit 3 simulation result in Figure 15 and scaled for 15.7 kV vs. simulation 17.3 kV , the simulation's predicted peak $I(t)$ would be 158 kA vs. the measured 154 kA . Due to the lower overall EHF PoP system ESL inductance, this peak current appears sooner, $54\text{ }\mu\text{s}$ vs. $60.6\text{ }\mu\text{s}$ predicted by simulation.

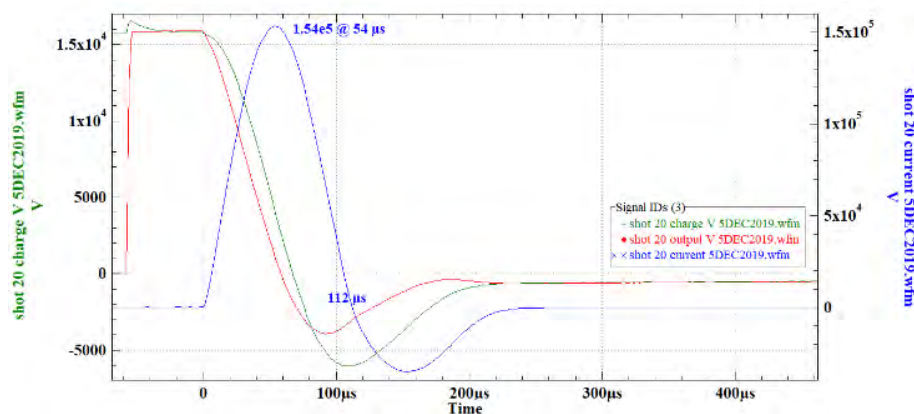


Figure 17. Voltage and Current Waveforms from Task 3 Field Test Shot 20

Figure 18 shows the approximated $P(t)$ from Task 3 field test shot 20, which fragmented a 3-ft x 3-ft x 12-in concrete slab with 15.7-kV charge, 86.8 kJ, resulting in peak power of 915 MW at 26 μ s compared to the peak $P(t)$ of 28.5 μ s that simulation predicted.

Overall these initial comparisons of the EHF system SPICE simulations compare very well to the actual field test data acquired. More comparisons of EHF SPICE simulation to actual field test data were used to recalculate updated simulation runs to better predict future system design performance improvements. Other field data analysis yielded more information regarding the probe load's dynamic resistive loading attributes.

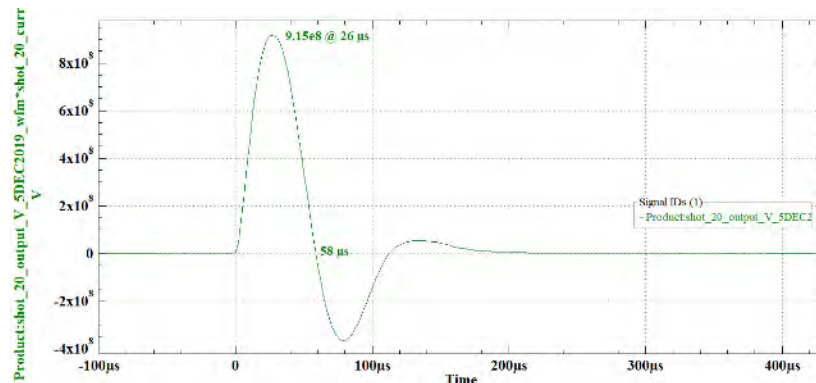


Figure 18. Approximated Power $P(t)$ from Task 3 Field Test Shot 20

2.3. Task 3: Proof-of-Principle Experiment(s) to Validate Performance

The proposal specifies that the contractor will “...construct a scaled, third-generation proof-of-principle device suitable for conducting a live fire demonstration experiment rendering a 3-ft. x 3-ft. x 1-ft. section of concrete. This device will validate the circuit model, benchmark performance for the chosen subcomponents/approach, and determine optimal future designs. Tests to determine attainable pulse parameters from each subsystem, peak voltage, pulse rise time, and pulse width possible will be conducted, as well as a series of characterization experiments to quantify rendering capability per discharge event yield, aggregate size, and fracturing efficiency (i.e. size of remaining aggregate). A commercially available Hydrodemolition high-pressure water-jet system will be utilized to produce the boundary line section cut for the Phase I demonstration prior to actuation of the EHF system.”

Summary:

Task 3 was accomplished in two broad phases. The first was component selection, which started with the purchase of primary components including main pulse capacitors, a high-energy switch, and a high-current coaxial cable, which drove the hardware design phase. Other intense efforts involved design planning for CAD-machined parts for the EHF blast probe, bus plates, and capacitor bank frame. Second was the field demonstration, for which test setup, data, and results are presented.

The EHF system was assembled through Oct–Dec 2019. After a few in-lab system check-outs, the completed Ph I EHF system was successfully field tested on 3–5 December 2019 through a series of 20 test shots into four test section slabs of 12-in-thick concrete. As originally proposed,

Hyperion intended that field demonstration would have combined the use of a waterjet cutting system for completely pre-cutting slabs followed by use of the EHF system to fragment the cut concrete slabs into small fragments for easy handling and disposal. However, at the time of field testing, short-term rental use of the qualified waterjet cutting systems was not available, so, Hyperion modified the EHF field demonstration tests to eliminate waterjet cutting, and instead to show the results of having no, or only shallow pre-cuts into the concrete to guide separation caused by EHF system plasma blasts.

During these tests, the user-selectable energy applied to each blast demonstrated how an operator may control and tailor the blast mechanics to produce and limit the desired level of crack formation and fragmentation. Testing proved that the EHF system effectively fragmented large concrete blocks approximately 3-ft x 3-ft x 1-ft into small pieces that could be easily removed by standard equipment such as skid-steers or front-end loaders. These successful field-test days proved that not only does the EHF cause significant fragmentations of large sections of cut concrete slabs, but also can in addition be used effectively for breaking out 3-ft sections of 12-in-thick concrete with clean 90° corners in conjunction with the shallow saw cuts.

Scope of Ph I EHF System Design:

Design work on Task 3 concentrated primarily on the high-energy elements, which are essential for the test demonstration. Figure 19 shows the primary test components of the intended Phase I PoP system design, highlighted from the overall Phase II Electro-Hydraulic Fracturing System schematic previously seen in the Task 1 Trade Study.

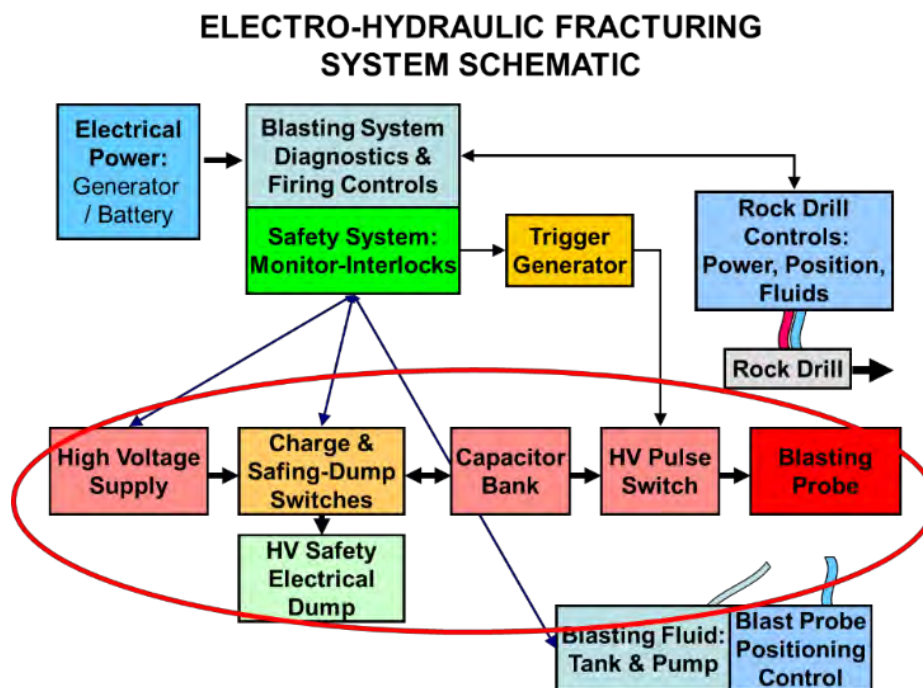


Figure 19. Electro-Hydraulic Fracturing System Components Emphasized (red oval) in the Phase I Design Process

After the capacitors, HV switch, and pulse transmission coaxial line were received, and the key pieces of hardware were on hand, planning and CAD design of the capacitor rack, EHF blasting probe, and purchase of balance of necessary components could continue. The following sections contain some of the component selection analysis and considerations.

Ph I EHF Capacitor Bank:

Table 2 lists initial capacitor candidates considered for the Phase I demonstration. Original Auburn U/Radiance work by members of this Phase I project used the Maxwell 32317, 22-kV-rated capacitors. Four capacitors were used with two pairs paralleled, and only one pair charged in the Bernardes–Merryman topology. This allowed a charged capacitance of 412 μF , and 52.7 kJ energy at a conservative 16-kV charge voltage. For this Phase I demonstration, a larger $\sim 800 \mu\text{F}$ capacitance is desired with topology options for non-voltage reversals or bipolar charging circuits.

Table 2. Initial Phase I “Proof-of-Principle” Test Demonstration Capacitor Candidates

Capacitor Mfg / PN	Capacitance (μF)	Max. Voltage (kV)	Peak Current (kA)	ESL (nH)
Maxwell 32317	206	22	200	45
Maxwell/GA 32349	206	22	150	45
GA 32349-LL	206	18	150	45
Maxwell 32328	176	21.3	100+?	70
Aerovox PM223YW099D01	100	22	100+?	TBD

The initial choice for the part of the Phase I effort at Hyperion was the Maxwell 32349 capacitor; however, it was not available on the surplus market. As discussed in the Task 1 Trade Study, when GA was contacted regarding price and delivery lead-times for the 32349, Hyperion was informed that the 32349 was no longer at the 22-kV rating, but available only as a derated, lower 18-kV voltage model 32349-LL (“Long-Life”). This -LL model is specified with a 6000 life-cycle rating compared to the 3000 of the 22-kV 32349 model. However, purchasing these for the Phase I demonstration would have broken both the Phase I materials budget and the time schedule. Aerovox PM223- 100 μF were available but would have required that 8 capacitors be bussed to reach the nominal goal of 800 μF .

Finally, a quantity of four surplus Maxwell 32328 capacitors, 176 μF each, rated 21.3 kV max., were purchased. All five capacitor options discussed are summarized in Table 2. Though the 32328s are $\sim 15\%$ less capacitance, if equivalent energy test comparisons are desired, a nominal charge voltage of ~ 17.3 kV would provide the same energy from the 32328s as a 32349 bank at 16-kV charge voltage. From the standpoint of an equal peak dI/dt rate test, given the lower capacitance of the 32328 bank and corresponding faster LC frequency, a slightly lower charge voltage may suffice. This component option was compared in SPICE simulations, discussed previously, due to the higher ESL of 70 nH for the 32328 vs. the 32349’s 45 nH each. Due to older production dates, the peak rated current of the 32328’s is not known or available to GA personnel/database.

The structural design comparisons of the other Maxwell/GA Series-C capacitors imply that the 32328s’ peak current rating is slightly less than or equal to 100 kA each. As it is unlikely that in

Phase I testing the total bank peak current will exceed 250 kA, or 62.5 kA/capacitor, these are expected to be conservatively safe. One caveat however is that these are used surplus capacitors with an unknown usage history, and therefore if previously heavily stressed, they could experience an early mortality during the course of Ph I testing.

Figure 20 compares 206 μF vs. 176 μF for 2-, 3-, and 4-capacitor banks of the Phase I EHF system capacitor bank energy vs. charger voltage. For example, though the 32328s are ~15% less capacitance, if equivalent energy test comparisons are desired, a nominal charge voltage of ~17.3 kV would provide the same energy from the 32328s as from a 32349 bank at 16 kV charge voltage. Considering capacitor bank energy, a 2-capacitor 32317/32349 system (charged B-M topology) at 16 kV as used by Auburn U/Radiance systems, has the same energy as 32328 capacitors in 2-cap. bank @ 17.3 kV, 3-cap. bank @ 14.1 kV, or 4-cap. bank @ 12.1 kV. Note that the latter two systems (32328 caps. in 3-cap. or 4-cap. configurations) would be a longer, slower pulse time due to total capacitance and higher ESL.

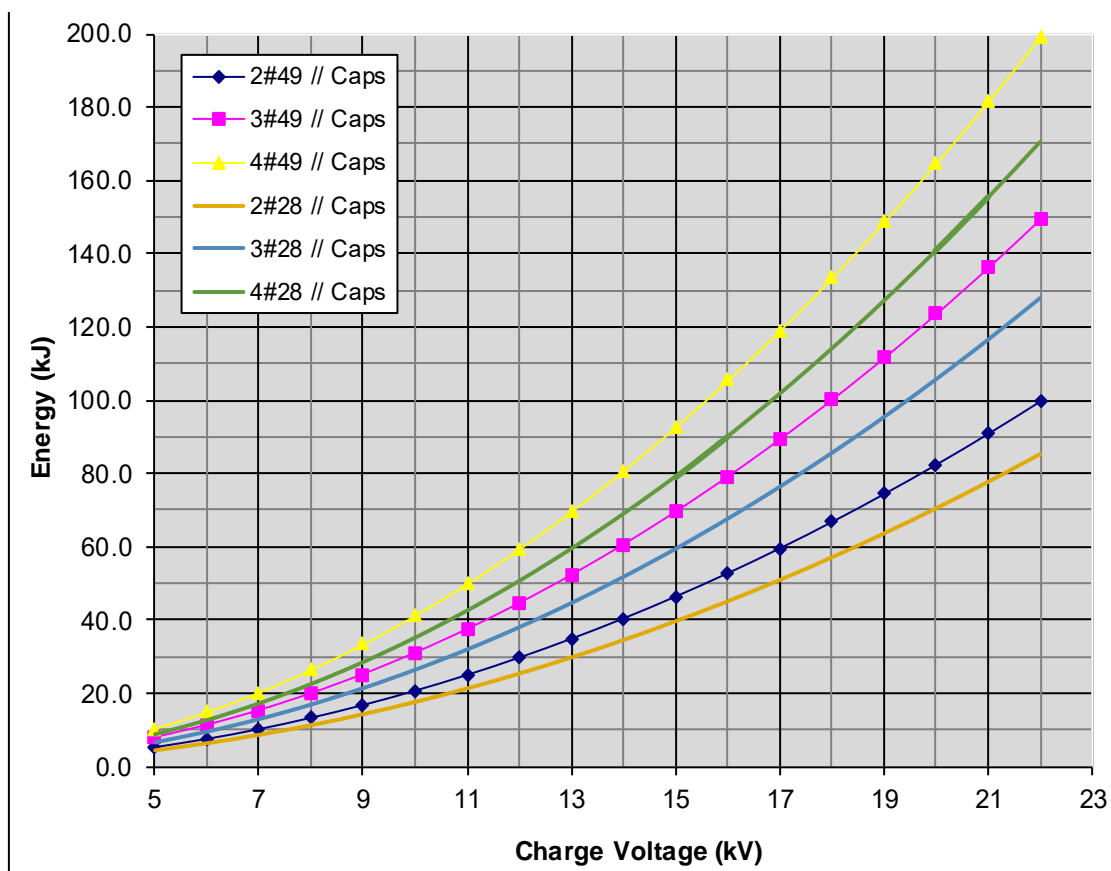


Figure 20. Comparisons of 206 μF vs. 176 μF for 2-, 3-, and 4-Capacitor Banks of the Phase I EHF System Capacitor Bank Energy vs. Charger Voltage

With the capacitors and spark gap switch selection completed, CAD design and fabrication could proceed. Figure 21 shows an early rough concept design for the Phase I EHF demonstration platform featuring the 4-capacitor bank, main HV switch, and bus plates for interconnections.

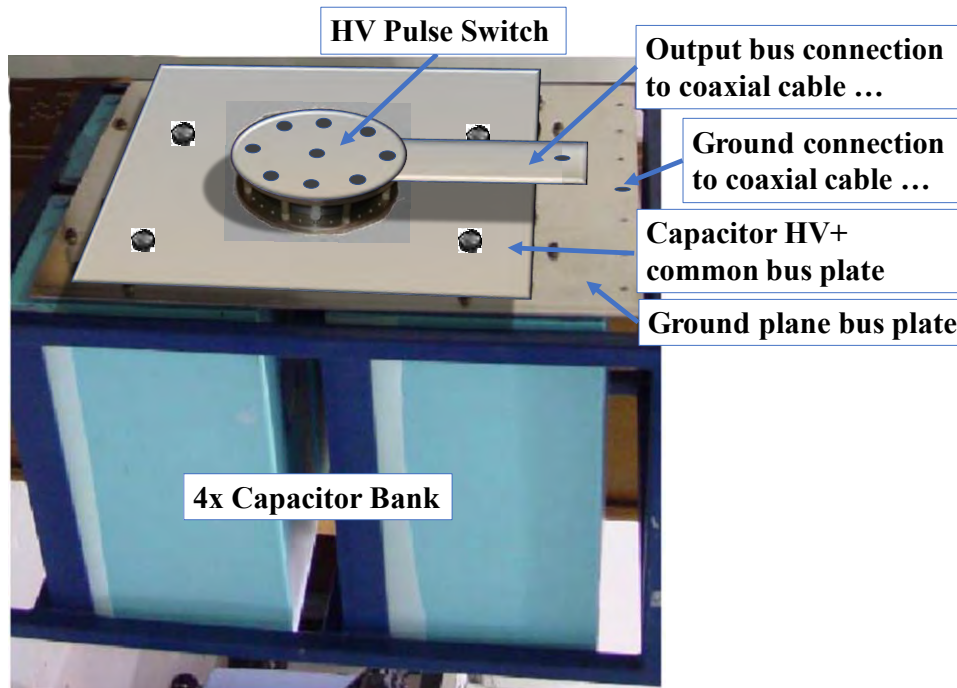


Figure 21. Phase I EHF Demonstration Platform Featuring Capacitor Bank, Main HV Switch, and Bus Plates for Interconnections

HV Pulse Switch:

The high-voltage, high-energy pulse switch purchased for use in these Phase I test demonstrations was the R.E. Beverly SG-172CM trigatron-style spark gap switch with a large 20-C (coulombs) per shot charge transfer rating, 5–30 kV voltage range, 250 kA peak current, and a low 50-nH inductance. Its total lifetime charge transfer ranges from 8–32 kC, depending on gas environment and peak current.. Figure 22 shows a summary of its specifications and a photograph of a SG-172CM.

Model Number ^a	Trigger Method	Operating Voltage Range, ^b kV	Max Peak Current, ^c kA	Max Charge Transfer, Coulomb	Switch Inductance, nH	Trigger Jitter, ^d ns	Dimensions (dia x hgt) ^e inches millimeters	Repetition Rate (max), ^f Hz
SG-172CM	Trigatron	5–30	250 (250)	20	<50	<250	10.5 x 3.23 267 x 82.0	0.02




Figure 22. Details of a R.E. Beverly Spark Gap Model SG-172CM Spark Gap Trigatron

The Beverly SG-172CM can be used with various gas combinations including N₂, compressed dry air, N₂–Ar and SF₆–Ar mixes. For the operational voltage ranges anticipated for the Ph I demonstration tests, N₂ or compressed dry air allow the SG-173CM to operate over its higher voltage ranges. An example of the SG-172CM operational voltage range when using N₂ is shown in Figure 23. V_{sb} refers to self-breakdown, V_{op} refers to recommended triggered operation range (typically ~ 85% V_{sb}), and V_{min} Modes A and B refer to minimum reliable triggered voltages (depending on trigger voltage/energy method), though with increased delay and jitter. Since the self-breakdown V_{sb} is approximately 17 kV for 0 lb/in², triggering by simple “gas-release” is not a good option. The use of “vacuum triggering” is an option whereby the spark gap switch is

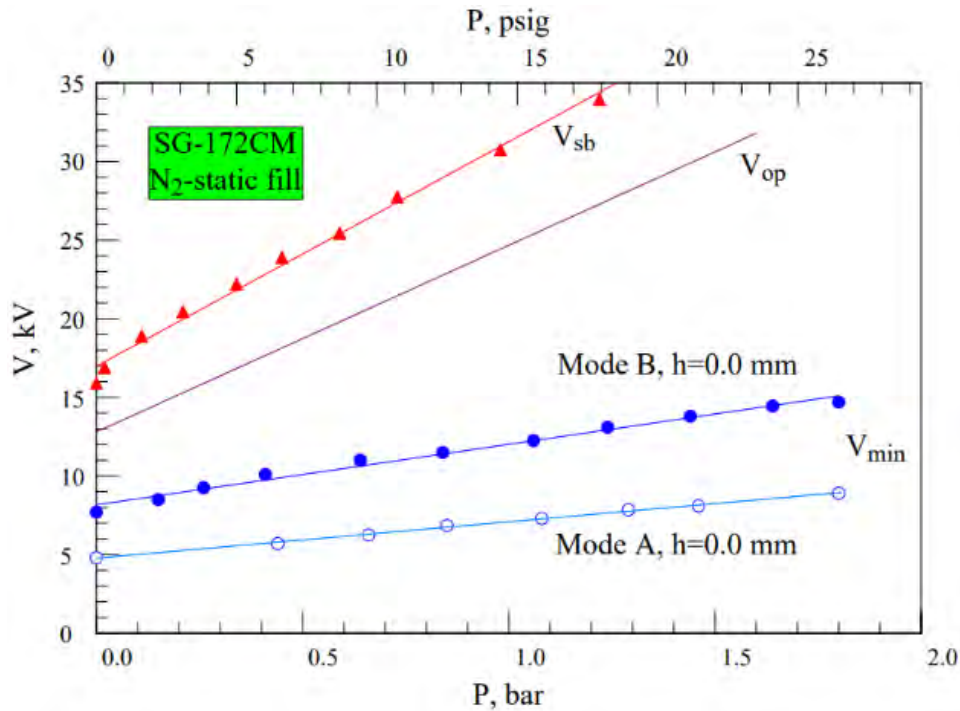


Figure 23. Beverly SG-172CM Operational Voltage Range Using N₂ as Its Dielectric Gas

pressurized for standoff. Then, when ready to discharge the capacitor bank, a three-way valve is rotated from pressurize to vacuum suction. For capacitor bank charge voltages below the 0-lb/in² self-breakdown voltage, when a spark-gap is partially evacuated (<0 psig), then the spark-gap channel will switch. Active gas flow post-trigger to flush the chamber is strongly recommended.

Main HV System Assembly:

Design Integration of Capacitor Bank with Spark Gap Switch:

Figure 24 shows an updated design for the main HV system hardware. The CAD designs were updated for HV pulsed-power engineering details and also for manufacturing, mostly adding such design details as verifying holes, threads, and tolerance stack-up fitment. Attention was also given to the bus-work edge radii and insulators to reduce high *E*-field stress and surface tracking. The layout of the capacitor bank assembly was partially modified to allow for an easy, progressive translation of the test assembly parallel to the concrete pad. The revised parts designs included:

- * Ground Dielectric Plate
- * Revised Stanchions based on preliminary assembly of Capacitor Frame
- * Accommodated power supply and diagnostics connections
- * Accommodated connection for Shipping / Storage Safety grounding strap
- * Accommodations for universal skid-steer pickup plate mounting.

A CAD/CAM manufacturing package was created, including the generic CAD, and sent to the manufacturers.

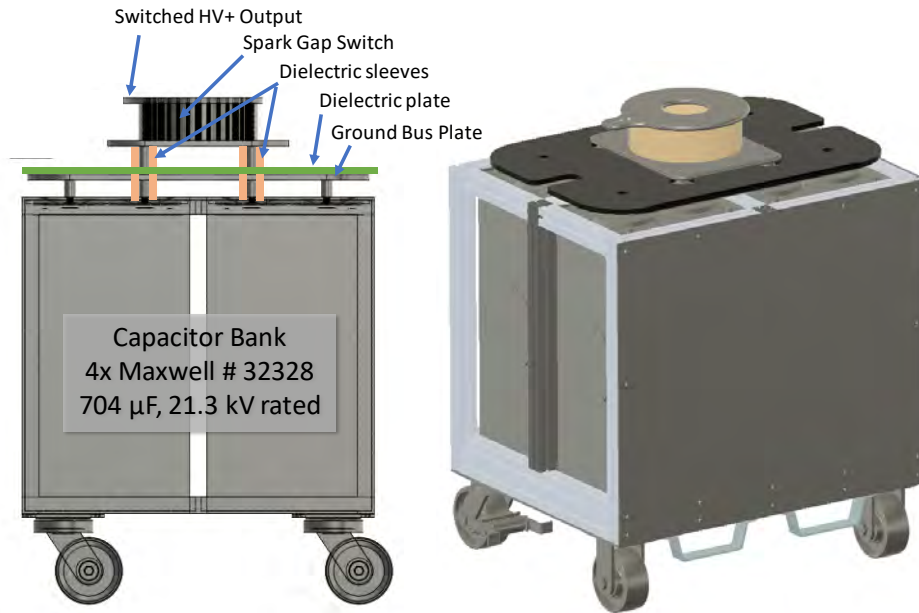


Figure 24. Updated CAD Design for Phase I EHF Demonstration Platform

Phase I EHF Plasma Blasting Probe Design:

The second major EHF system build effort was for the EHF plasma blasting probes. The CAD designs were updated for HV pulsed power engineering details and also for manufacturing, mostly adding more design details, verifying manufactured tube/cylinder tolerance stack-up fitment, etc. The EHF plasma probe assembly revised parts designs included:

- Redesign for manufacturing
- Detailed design; verifying holes, threads, fitment etc.
- Revised shield and weight plate to square, larger area, stock as purchased
- Revised bus bar clamps and lug connections
- Added + bus bar force support knee and eliminated nut joint
- Modified probe nose cone and/or steel tube end-radius on two of four probes.

Some changes included (Figure 25) addition of support for the +bus terminal and dielectric back-force thrust “knee” behind the center conductor. The center electrode previously used a threaded portion above the +bus bar (upper). The added G10 fiberglass block acts as a back-force thrust–impulse block to prevent the center conductor from being forced back.

A CAD/CAM manufacturing package was created including the generic CAD and 2-D drawings and sent to the manufacturers. Figure 26 displays parts received from machine shops.

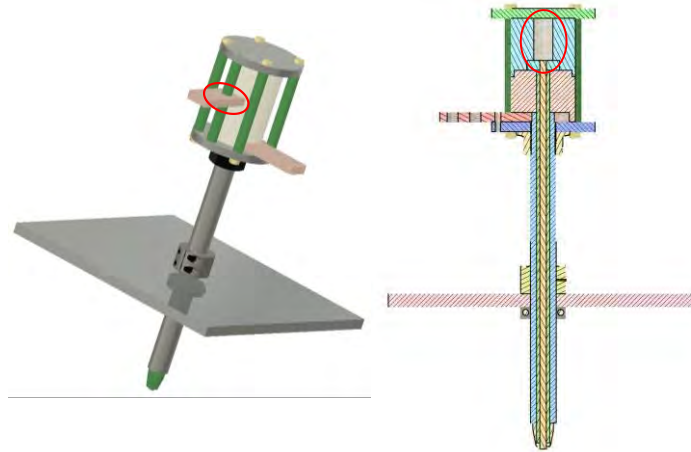


Figure 25. Updated EHF Probe Designs Including Some Changes Highlighted; (left) +Bus Addition Support, and (right) Back-force Thrust “Knee” (highlighted in red ellipse)



Figure 26. Machined EHF Plasma Probe Parts (left) and Inertial Blast Restraint Plates (right)

Figure 27 shows an example of the partially assembled EHF plasma blasting probe. The image did not include the G10 dielectric sleeves, the G10 inner tubes, center conductor and nose cone.

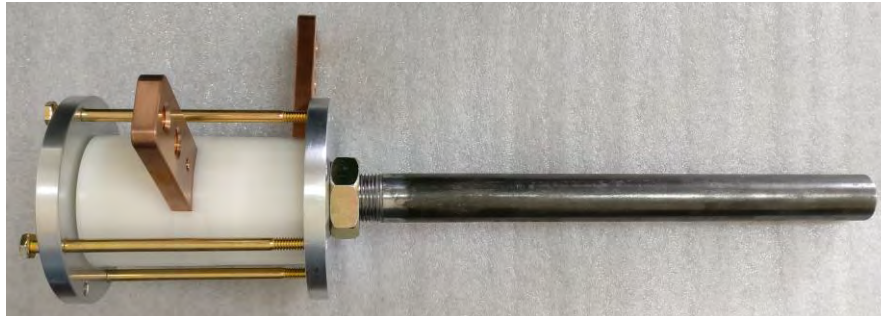


Figure 27. EHF Plasma Blasting Probe Shown Partially Assembled

Transmission Line:

Stock for a heavy coaxial pulse cable selected was the Dielectric Sciences 2198 coaxial cable; rated at 75 kV (DC), 300-kA peak pulse current. Cross-section end views and overall coil are in Figure 28 with detailed specifications in Figure 29. The visible specifications, detailed in the drawing, are the braid strands of aramid fiber used to help withstand the impulse magnetic forces within the cable and prevent cable “ballooning.”



Figure 28. EHF Pulse Transmission Line, Dielectric Sciences 2198 Coaxial Cable Cross-Section and Overall Coil

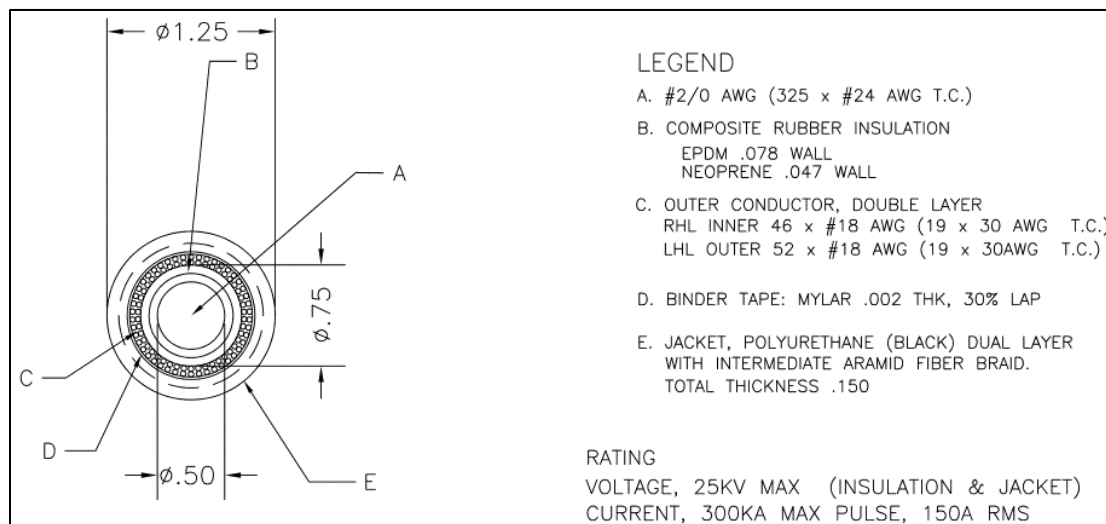


Figure 29. Dielectric Sciences 2198 Pulse Coaxial Cable Cross-section Specifications

2.3.1. Ancillary HV Components:

HV Power Supply (HVPS):

Hyperion's initial plan for an HVPS needed to charge the capacitor bank included use of an existing in-house HVPS, a Glassman EW40P15. This unit has a 0–40 kV range with power limited at a stated maximum 600-W output. Glassman's documentation states that the EW-series of power supplies have extended current up to 84% of rated output voltage and that higher currents are derated to maintain a constant 500-W maximum output. Because of this lower rating, charging the capacitor bank to 16–17 kV range would require >15 min, so a higher-power HVPS was acquired.

Table 3 lists an example comparison of CCPS charge-rates vs. capacitor bank charge voltage and charging times. All cases are for four, parallel connected, 176-μF capacitors for a total 704-μF bank. The first four rows are for 16-kV charge follow by four more rows at 17.3-kV charge. The stored bank energies are 90.1 and 105.4 kJ, respectively. Different charging times (seconds) were entered corresponding to different kJ/s charge rates and peak AC line power kW ratings. For 16-kV charge voltage, a 10 s charge time requires a 9-kJ/s CCPS and peak AC power 18 kW. For 17.3 kV, the same 10-s time would require 10.5 kJ/s and 21.1 kW. At the slower end, a much smaller 2-kJ/s CCPS would charge the 704-μF bank to 16 kV in 45 s, or 17.3 kV in 53 s. When gensets are considered, their intermittent surge load rating characteristics must also be considered.

Table 3. Comparison of CCPS Ratings vs. Capacitor Bank Charge Voltage and Charging Time

# of Caps*	Total Capacitance (μF)	Charge Voltage (kV)	Stored Energy (kJ)	**Charging Time (sec)	Required CCP rating (kJ/sec)	Peak AC Line Power (kW)	NOTE: Peak AC Power required by CCP supplies during charging is approx. (>) 2x (2-times) kJ/sec rating (Ex. 10 kJ/s CCP requires >20 kW peak power). An AC generator's rating must take this into account.			
4	704	16	90.1	10	9.0	18.0	** Times are approximate; actual time will be slightly longer to account for capacitor settling time, in-line protection current limiting resistors, CCP supply Power Factor (PF) ratings and inefficiencies...			
4	704	16	90.1	18	5.0	10.0				
4	704	16	90.1	23	3.9	7.8				
4	704	16	90.1	45	2.0	4.0				
4	704	17.3	105.4	10	10.5	21.1				
4	704	17.3	105.4	21	5.0	10.0				
4	704	17.3	105.4	27	3.9	7.8				
4	704	17.3	105.4	53	2.0	4.0				

For this project, a CCPS rated for peak 1.1 kJ/s, a TDK-Lambda A.L.E. 102A, Figure 30, was acquired and integrated with the other HV power control components. It has an OEM package and is controlled remotely with line level and analog control signals and provides feedback signal for current, voltage, and fault states. The electrical input: 115 or 230 V, and HV output: 0–20 kV DC. With the small package dimensions: 5-3/4-in x 5-5/8-in H x 14-in D, it will be connected with the ancillary HV switching components, a pair of N.O./N.C. 25-kV rated Ross relays being assembled inside portable, modular plastic cases



Figure 30. HV Capacitor Charging Power Supply (CCPS); TDK-Lambda ALE 102A

The procured TDK-Lambda ALE 102A CCPS, rated for peak 1.1 kJ/s, is a rather low-charging power capacity given the size of our capacitor bank; however, this was a necessary compromise given the cost hit vs. Phase I budget and lead time for a new and larger-capacity CCPS supply. In addition, this CCPS has a long-term average-power-limitation protection scheme when used to charge large capacitor banks requiring longer charging times exceeding its standard default 500-ms time limit to achieve programmed targeted V -charge level. After that 500 ms, a temporary fault-state inhibits the CCPS for another 500 ms, after which it enables the CCPS to resume charging. The TDK HVPS alternates in this stair-stepped mode until V -charge is achieved as in Figure 31.

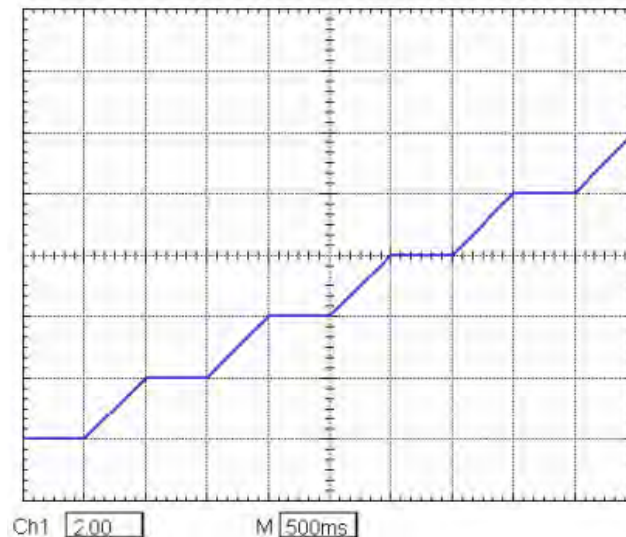


Figure 31. “Fault-Mode” Stairstep Charge Cycle Pattern of a Standard TDK 102A CCPS without an LCA (Long-charge Adapter)

The TDK 102A operated in this mode results in the effective long-term power supply being <450 J/s instead of its ideally rated 1-kJ/s rating. Figure 32 shows the simulated charge cycle characteristics of the stock TDK 102A 20-kV(max) CCPS charging a 704- μ F capacitor bank to 16 kV would require 205 s.

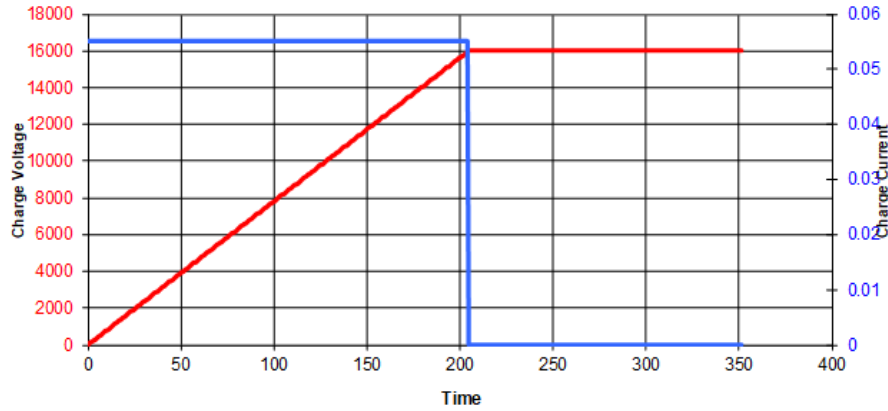


Figure 32. Simulated Charge Cycle Characteristics of Standard TDK 102A 20 kV(max)

A work-around devised by TDK–Lambda gradually rolls in this maximum power limit feature by starting a pro-rated reduction at the 50% V_{max} design level. Above this 50% V_{max} voltage levels during the charge cycles, an automatic time-proportionally (PWM) charged duty-cycle adjustment gradually transitions I -charge from 99 to 50% (@ V_{max}). For this, TDK–Lambda produces a control plug-in module referred to as an LCA

The following equations illustrate the relationship between output voltage and current:

If $V_{out} \leq 50\%$ of rated V_{max} ,

$$I_{charge} = I_{rated} \quad (1)$$

If $V_{out} > 50\%$ of rated V_{max} ,

$$I_{charge} = I_{rated} \times (V_{rated} - V_{out}) / V_{rated} \quad (2)$$

Using this power-limiting control scheme, Figure 33 shows the simulated V -charge and I -charge cycle characteristics of a standard TDK 102A 20-kV(max) CCPS, with an LCA, charging a 704- μ F capacitor bank to 16 kV requires 110 s, 54% of the time required without the LCA. Note the gradual decrease of I -charging current begins when V -charge > 10 kV. Figure 34 shows the V -charge and power profile for the same conditions (standard TDK 102A 20-kV(max) CCPS, with an LCA, charging a 704- μ F capacitor bank to 16 kV).

Due to budget, schedule, and delivery time limitations, Hyperion opted not to use a TDK LCA. Instead, Hyperion managed this by modulating the average I -charge to be the equivalent of the LCA-imposed limit at 16 kV (assuming that is our planned V -charge). Applying equation (2) to a 20-kV rated CCPS charging to 16 kV, the adjusted I -charge level needs to be reduced to 70% of the nominally specified I -charge current $(0.5 + (20-16)/20) = 0.7$). One way to reduce the time-averaged charging current is to modulate the TDK 102A's "INHIBIT" line with a 70% duty-cycle signal (350 ms enabled, 150 ms disabled). For a 17.3-kV V -charge level, a 63.5% duty-cycle pulse train would be required. Higher % effective duty cycles may be realized at lower charge voltages.

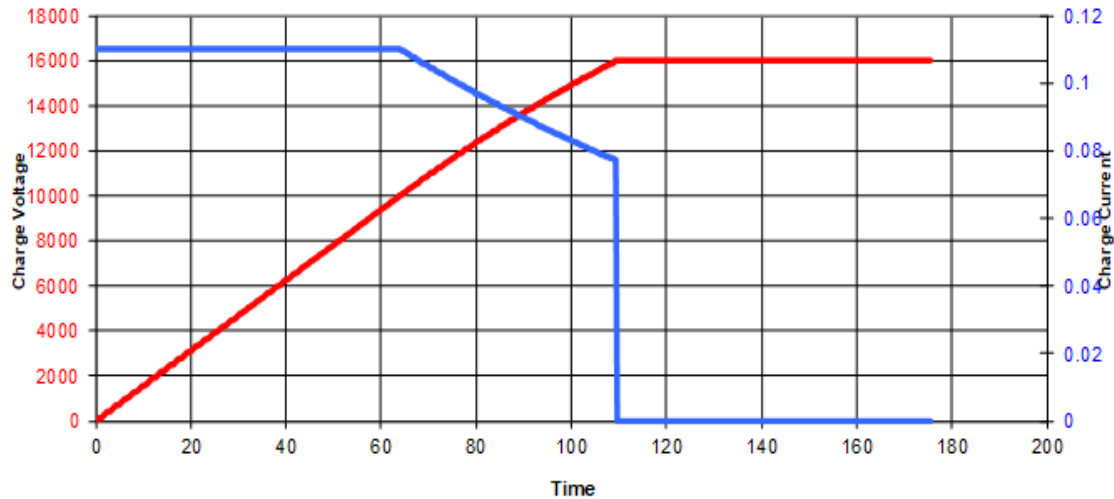


Figure 33. Simulated *V*-charge and *I*-charge Cycle Characteristics of an LCA-controlled TDK 102A 20 kV(max) CCPS Charging a 704- μ F Capacitor Bank to 16 kV

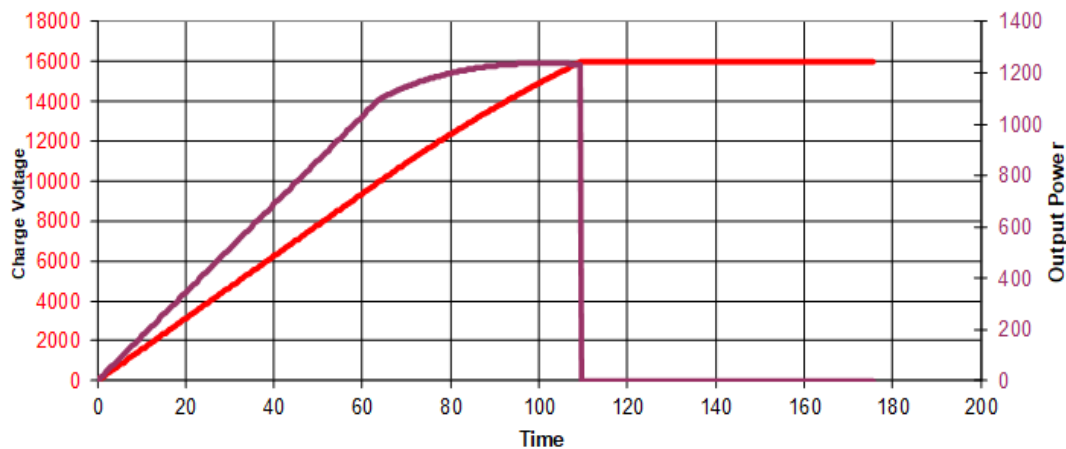


Figure 34. Simulated *V*-charge and Power Cycle Characteristics of an LCA-controlled TDK 102A 20-kV(max) CCPS, Charging a 704- μ F Capacitor Bank to 16 kV This duty cycle limit of 70% or 63.5% is imposed only after *V*-charge has reached 50% of the CCPS V_{\max} (20 kV in this case, or 10 kV); however, for simplicity and conservative operation, the INHIBIT signal's pulse train may be applied throughout the entire charge cycle using a digital delay generator (DDG) or function generator (FG).

The TDK-102A was packaged in a plastic field-portable box and included a small protective default load HV capacitor and a voltage-reversal HV rectifier. In addition, an ancillary HV charge/dump field-portable switch box was assembled as in Figure 35. A large 5-gal copper sulfate (CuSO_4) current-limiting charge/dump resistor was also assembled.



Figure 35. Constructed Field-portable HV Charge/Dump Control Switches

EHF Field Testing Summary

The EHF system was successfully tested in the field 3–5 December 2019 through a series of 20 test shots into four test section slabs of 12-in-thick concrete. During these tests, the user-selectable energy applied to each blast demonstrated the way an operator may control and tailor the blast mechanics to produce and limit the desired level of crack formation and fragmentation. These initial tests over only two field-test days (plus one for setup) show that not only does the EHF cause significant fragmentations of large sections of cut concrete slabs, but also may in addition be used effectively for breaking out 3-ft sections of 12-in-thick concrete with clean 90° corners when used in conjunction with the shallow saw cuts. Since these initial 90° tests also produced a diagonal crack into the main test slab.

Demonstration Site Concrete Pads:

The demonstration 12-in-thick concrete pads, Figure 36, were poured and cured for > 30 days before the demonstration tests. Three smaller, 6-ft x 6-ft square, concrete slabs allowed some initial system checks, fine-tuning tests before initiation of the main demonstration tests on the large 6-ft x 12-ft slab.



**Figure 36. 12-in-thick Concrete Pads for EHF Testing:
(top) 6-ft x 12-ft Slab, (bottom) Three 6-ft x 6-ft Slabs**

The 704- μ F capacitor bank was assembled in a low-inductance bus design and connected through a coaxial pulse transmission line to the EHF main HV system to the plasma blasting probe. A high-energy nitrogen-gas-pressurized spark gap as the switch was integrated into the EHF main HV system as the control trigger of the system. Figure 37 shows the EHF system assembled and set up for testing in the field.

As in Figure 38, the EHF main HV system was packaged to for easy transport and maneuverability in the field. The system can be moved using either a forklift, a skid steer, or other equipment with lifting forks. Lifting pockets are bolted to the bottom of the EHF main HV system for this purpose.

Four plasma blasting probes were made for the testing series. The probes proved to be very rugged and only two probes were used during testing. Probe 4 was the first probe connected to the EHF system as in Figure 39. Probe 4 was used for 15 of the 20 total test shots reported. Two shots of the 15 were “dry-fire” shots in which water was not present in the borehole. These two shots did significantly more damage to the probe than a normal shot with the borehole filled with water. If the probe had not been “dry-fired” twice, probe 4 could have been used for additional testing. After probe 4 was damaged on the higher energy shot 16, it was replaced by probe 3, which was used for the remainder of the testing shots and was still in excellent working shape, capable of being used for more shots. Other than the damage due to the “dry-fire” shots to probe 4, the EHF system experienced damage or degradation from the series of 20 field test shots it was tested over.

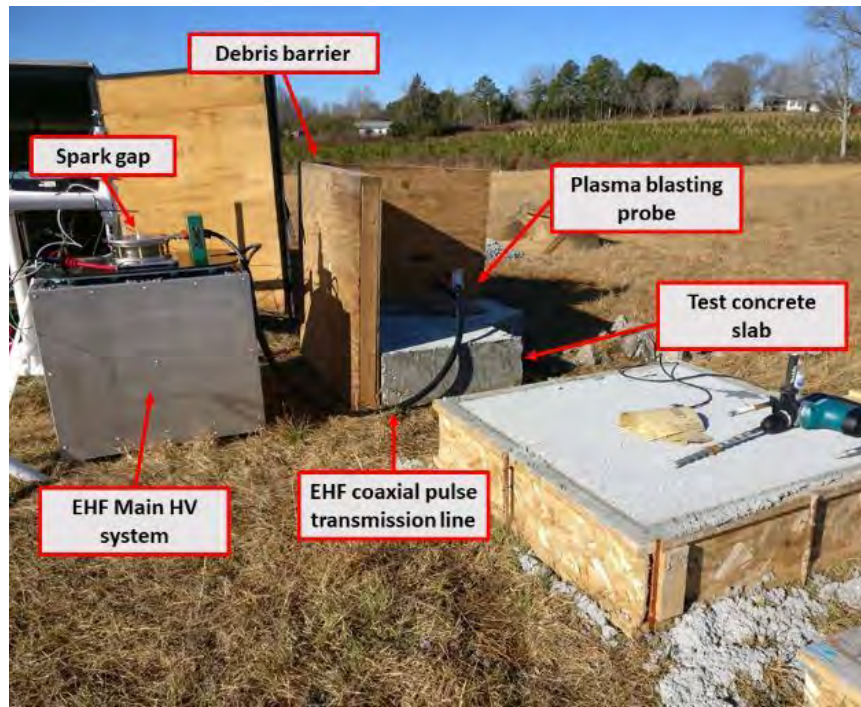


Figure 37. EHF System Set up for Field Testing



Figure 38. EHF Main HV System

The EHF system is potentially capable of firing a charge voltage of up to 20 kV, equating to a charge energy of 140.8 kJ. For the testing series conducted, the maximum voltage used was 16.55 kV, equating to a charge energy of 96.4 kJ. Maximum peak current achieved for the test shots was 153.6 kA on shot 20. For the majority of the testing a maximum of 10.5-kV charge voltage (38.8-kJ charge energy) often proved adequate for the purpose of cracking the concrete where desired while not cause excessive destructive fragmenting. When large chunks of detached concrete were to be further fragmented for disposal, at higher charge voltage of 16 kV was used.

This testing series the EHF Main system was instrumented for voltage and current measurement as in Figure 40. In addition, photos of the test setup and post shot effects were recorded. Video of each of the shots was recorded and is available separate from this technical report.

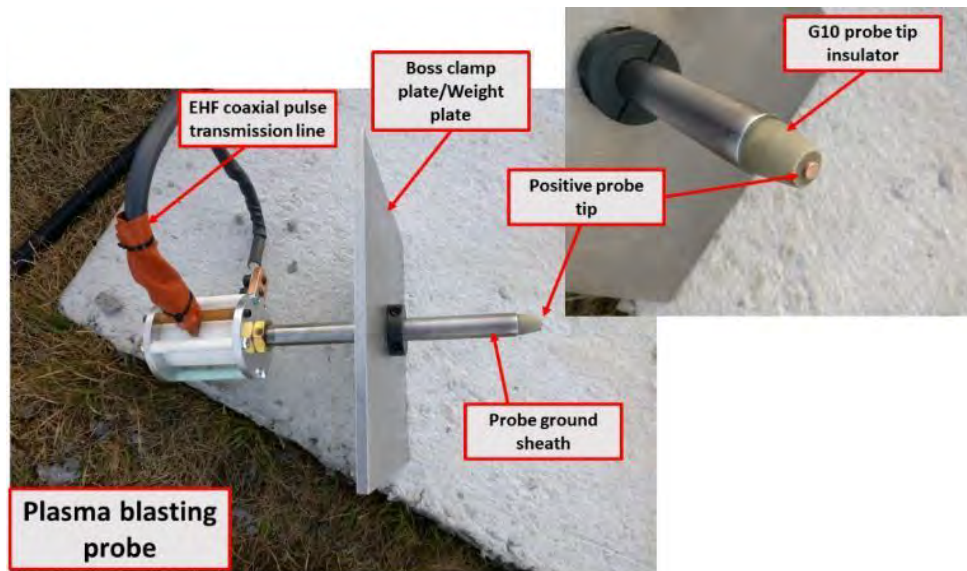


Figure 39. Plasma Blasting Probe Set up

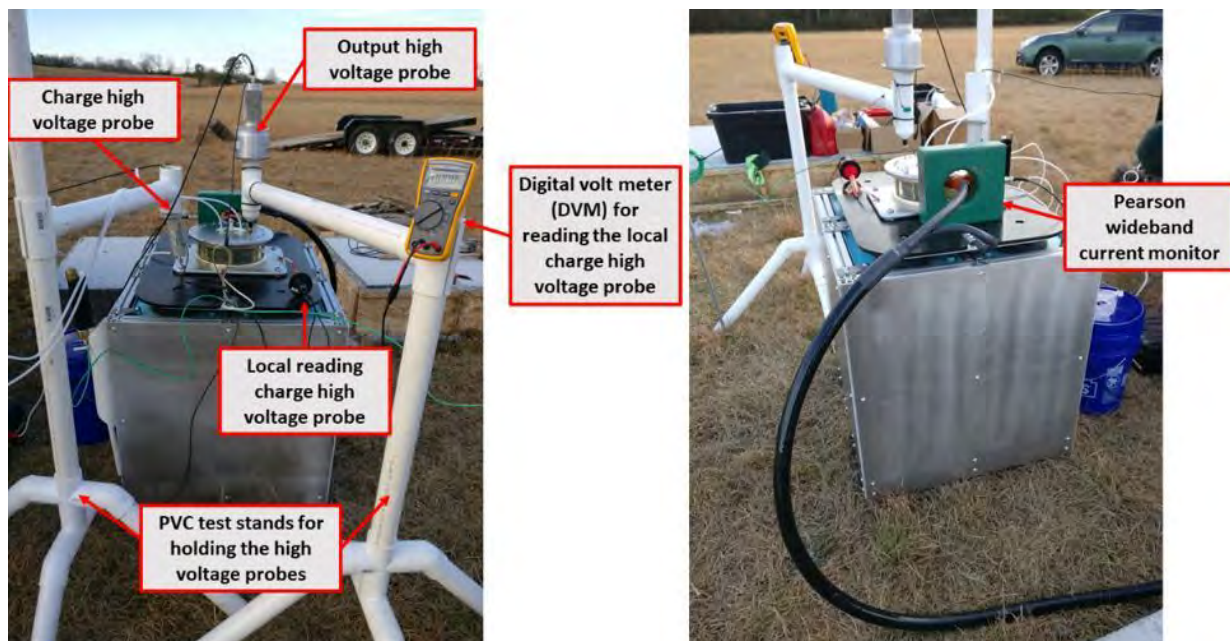


Figure 40. HVProbes and Pearson Current Monitor

Four concrete test slabs of 4000-lb/in² strength concrete were poured for the EHF system testing. This included three identical concrete test slabs 4 ft x 4 ft x 12 in thick, and one larger concrete test slab measuring 6 ft x 12 ft x 12 in thick (Figure 41). The number convention for the concrete test slabs shown in Figure 41 is used for discussing the test setup and testing results.

A summary table of the EHF system testing is provided in Table 4, with a short description for each shot.

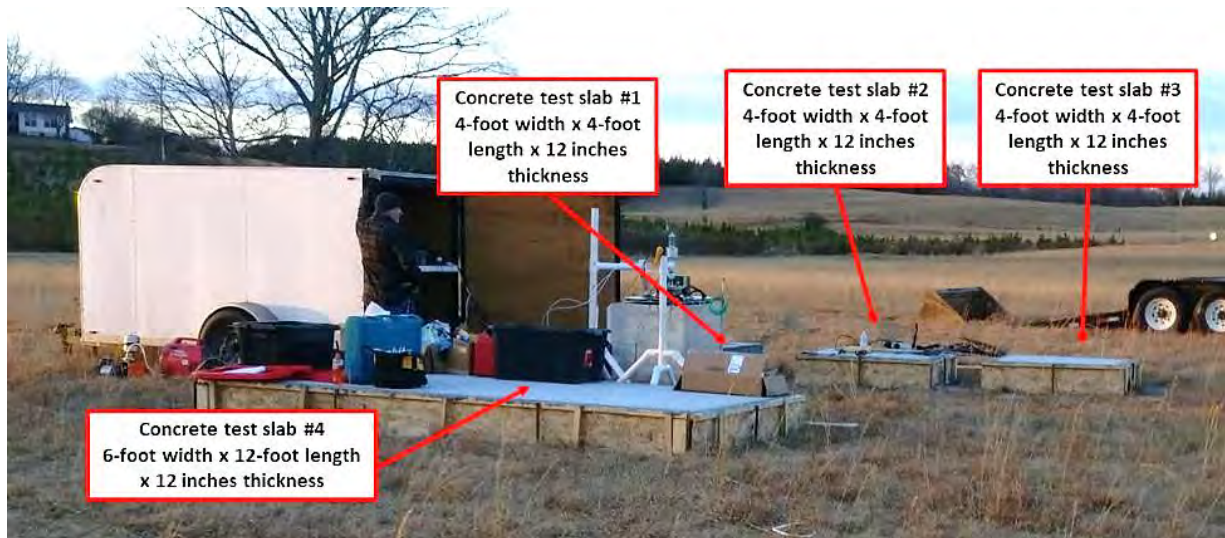


Figure 41. Four 4000-lb/in² Strength Concrete Test Slabs for the Test Set

Table 4. Summary of Testing Shots

Shot	Shot Summary
1	Initial low-voltage diagnostic instrumentation test; concrete slab did not visibly crack
2	Successful shot, separated the corner off the test concrete slab along two main cracks
3	Successful shot, broke up separated section of concrete. Borehole depth changed from 6 in to 7 in to add 1-in water volume under the tip of the plasma blasting probe
4	Successful shot, repeated result of shot 2. Corner of the slab was separated off the larger concrete slab successfully
5	Attempt to separate remaining section between the sections separated in shots 2 & 4. Occurred, but large crack formed in remaining portion of test slab 1 and split the slab
6	Done to look at natural crack propagation from the shot. Charge energy for this shot was double that used in shots 2–5
7	First shot to look at controlling crack propagation, pre-cut the concrete test slab using a diamond concrete saw. Showed that cracking can be directed using this method. Additional cracks occurred. Further testing will improve control of crack propagation.
8	Used 2-in-depth pre-cuts to attempt to section off 36-in by 36-in section from concrete test slab with probe placed at the center of the chunk to be sectioned off. Failed to control path of crack propagation. Main cracks propagate outward from the borehole, ignoring pre-cuts made at a distance from plasma blasting probe. Pre-cuts must start and/or intersect probe location to be effective in controlling propagation path
9	2-in-depth pre-cut added to section off end of concrete test slab after shot 8. Plasma blasting probe was placed in the through hole drilled for shot 8
10	Using shot 9 test setup, drilled new borehole in center of slab width (36 in from sides) and 18 in from edge of the length of the slab along one of the 2-in-deep lines cut for shot 8. Crack lines did not follow pre-cut line intersecting borehole, possibly due to cracking from shots 8 & 9 prior to shot 10.
11	Mainly used to break-up and remove section of test slab used for shots 8–10. Charge energy increased significantly to observe the effect of using higher energy shots

Shot	Shot Summary
12	Conducted to test use of exploding wire to fracture concrete test slab. Wire was pressed down to the bottom of 2-in-deep pre-cut the length of and in the center of the test slab. Leads of EHF coaxial pulse transmission line (to Plasma blasting probe) connected to the length of copper wire. Test blew out small divot in the concrete around the cut and wire.
13	As above, but ~6-in-deep pre-cut. Charge energy of shot reduced to 39.6 kV to avoid stray cracks in the concrete. Successfully sectioned off 36-in by 36-in section from the slab. Still one small, unintentional crack remote from the pre-cut section.
14	Delivered 87.9-kJ charge energy to fragment the 36-in by 36-in section separated in shot 13 into smaller chunks. A was used for this shot to get more fragmentation of concrete section. Successfully broke up separated section into smaller chunks.
15	Execution error---neglected to put water in borehole, no effect realized
16	Repeat 15. 4 to 6-in-deep pre-cut to steer separation line in remaining 36-in by 36-in section attached to 4 concrete test slab after shot 13. G10 probe tip blew off plasma blasting probe. As in 8, cracks formed remote from the borehole.
17	Repeat 16 with same 4 to 6 in deep pre-cut. Offset pre-cuts again failed to control crack propagation path, confirms pre-cut(s) must either intersect or terminate near the borehole for pre-cut to set the crack propagation path.
18	Wire pressed down into 2-in-deep pre-cut the length of the test slab down the center and connected to the two leads of the EHF coaxial pulse transmission line. Section of concrete was added over the cut to hold pressure in and create pressure spike.
19	Crack ran through hole 4 in from probe borehole meant to stop crack propagation. 6-in-deep pre-cuts directed crack propagation to separate 36-in by 36-in section, so pre-cut lines that pass through or end at the borehole can direct crack propagation. Two unintentional cracks also formed.
20	Charge energy of 86.8kJ successfully broke up separated section into smaller chunks.

The main portion of the EHF system testing evaluated the ability of the system to break up the test concrete slabs using the plasma blasting probes. For these tests, a 1-in hammer drill was used to create a borehole for installation of the plasma blasting probe into the concrete test slab. Several different combinations of the borehole depth and plasma blasting probe depth were tried. Based on the testing results, a borehole depth of 8 in and a plasma blasting probe depth of 7 in was found to be most effective for the testing conducted and this combination was used for 12 of the 18 total test shots using the plasma blasting probe. This combination leaves 1 in of water below the plasma blasting probe depth and 4 in of concrete below the borehole.

Overall, the system was found very capable of cracking and breaking up sections of the concrete test slabs. As an example, the relatively low voltage/energy used for shot 6, the resultant cracks are in Figure 42. This shot easily broke the full concrete test section into three large sections with no damage to the probe at roughly 30% of the EHF systems maximum rated charge energy. After the subsequent tests, it certain that had the higher voltage/energy settings been used, the fragmentation damage would have been significantly more.

In addition to proving that the system is able to effect breakup of the concrete test slabs, the testing focused also on determining how the system could be used to section off straight lines in the test concrete slabs. In the early test shots, three separate shots were used to crack off a section of test slab 1, leaving a reasonably straight edge as in Figure 43.

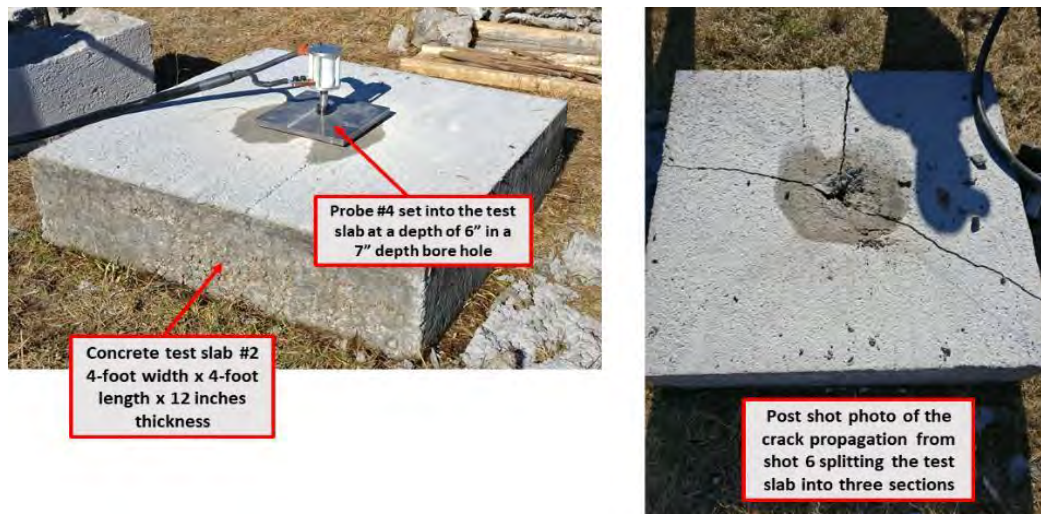


Figure 42. Crack Propagation in Concrete Test Slab 2 from Shot 6



Figure 43. Sequence of Three Shots: (left) 2 Broke off a Section of Test Slab 1, (center) 4 Cracked along the Same Line; 5 (right) Left a Reasonably Straight Edge

In Figure 43, the respective top and bottom photos show the test setup and the results of each test shot. By shot 5 in Figure 43, a section of the concrete slab had been removed leaving a relatively straight crack line. Unfortunately, shot 5 also cracked the remaining section of test slab 1, leaving the remaining concrete split into two pieces (Figure 44).



Figure 44. Remaining Section of Test Slab 1 Split into Two Pieces by Shot 5

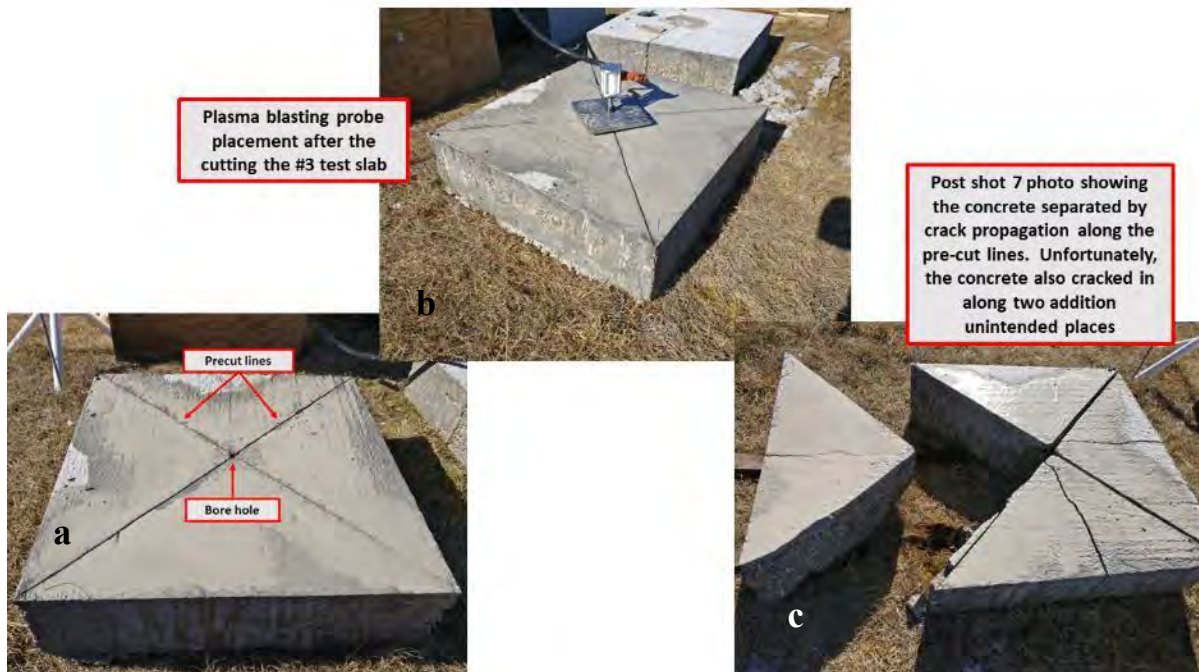


Figure 45. Lines Sawed in a Diagonal Pattern Intersecting the Borehole Centered in Test Slab 3 (a) prior to, (b) preparing for and (c) after Shot 7

Two different concrete saws were used to pre-cut the concrete and control the crack propagation path through the concrete test slabs from the EHF plasma blasting probe shot. Their cutting depths were 2 in and 4.5 ~ 5 in, respectively. Initially the smaller 2-in-depth cutting saw was used in the concrete. Shot 7 was the first test of this methodology as in Figure 45. A concrete saw cut lines 2 in deep in a diagonal pattern intersecting the borehole in the center of test slab 3 prior to shot 7. This method worked well to control the crack propagation path during shot 7 to separate the concrete test section along the pre-cut paths. Two additional cracks also formed, splitting the wedge-shaped blocks into two unintended additional pieces.

A second approach to the 2-in-depth pre-cut method was tried. As in Figure 46, for shot 8, lines were cut to set the desired lines of separation in test slab 4, and the borehole for the probe was drilled in the center of the concrete section to be separated. The goal of this setup was to use the pre-cut lines to control the crack propagation path, and to prevent unintended cracks from forming in the remaining portion of the test slab that was left intact.

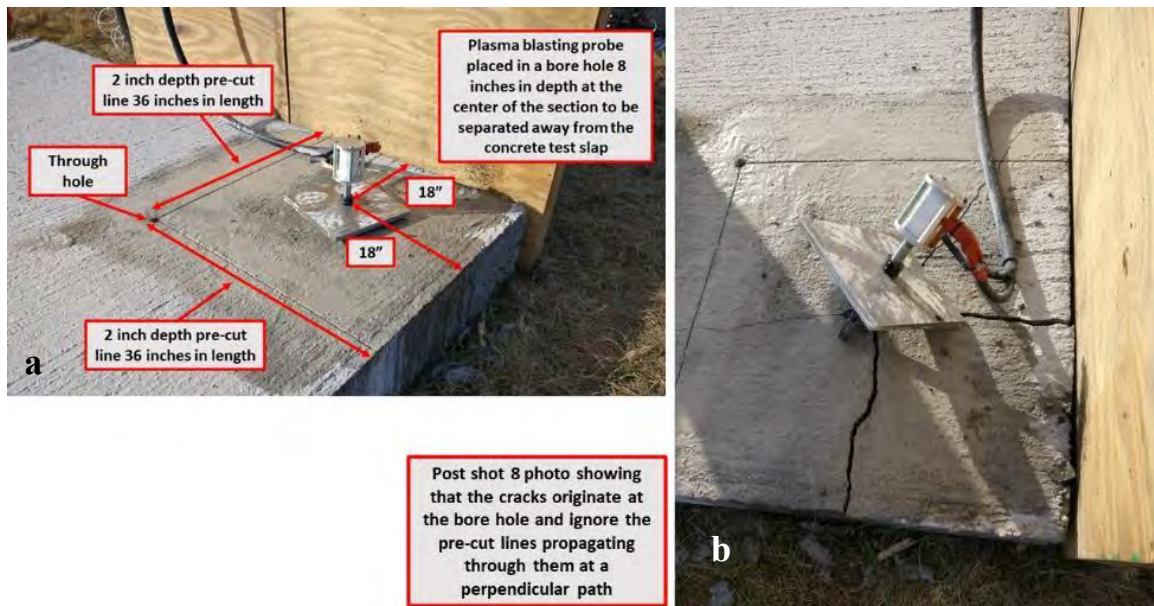


Figure 46. Shot 8; Lines Cut to Set the Desired Separation Path in Test Slab 4; Probe Borehole Centered in Section to Be Separated (a) before and (b) after Shot 8

The setup in Figure 46 did not control the crack propagation path. The major cracks formed from the shot always originate from the borehole containing the plasma blasting probe and propagate away from the borehole. When the pre-cut lines do not cross the borehole or end in the vicinity of the borehole, they do not control crack propagation path for the shot. This was verified by repeating the shot 8 setup in shot 17, which produced the same outcome.

Testing pre-cut setups continued on the second day; a larger concrete saw was used to create deeper 4.5~5-in pre-cuts in the concrete. In Figure 145, Shot 13 in test slab 4 successfully separated off a 36-in-by-36-in section of concrete along the deeper pre-cut lines terminating at the borehole containing the probe. However, an additional crack also propagated back into the larger remaining test slab section meant to be left fully undamaged and intact. More details about shot 13 appear below in the detailed test shot 13 descriptions.

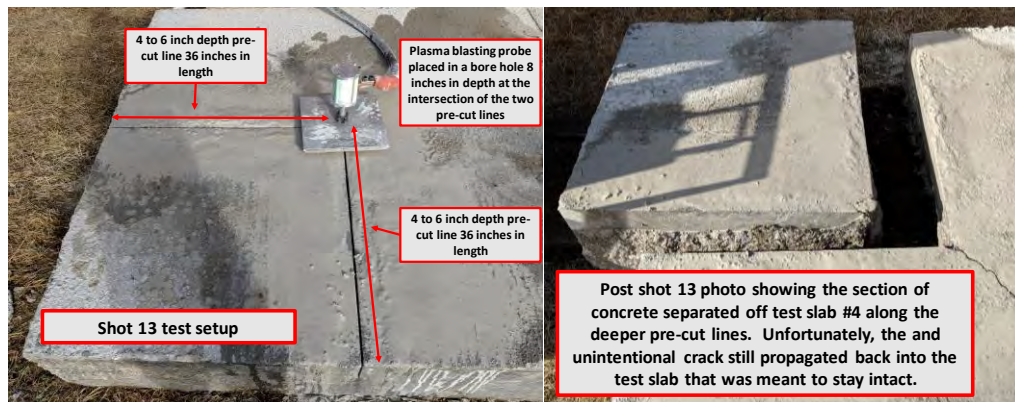


Figure 47. Shot 13 in Test Slab 4

In addition to testing the EHF system with the plasma blasting probe, Hyperion also tested the system using an exploding wire approach. This was not initially planned and was an in-the-field decision. In this test the plasma blasting probe was replaced with a strand of very thin copper wire. In Figure 48, for shot 13, the exploding wire was placed in a 2-in pre-cut and the cut is filled with water. This method failed to crack the concrete slab. It was tried again in shot 18 with the deeper pre-cut and with a section of concrete placed over the wire flat side down to keep the pressure inside the cut holding the exploding wire, and also failed to crack the test slab. Both shots created considerable acoustic (in air) shockwaves that could be physically felt roughly 100 ft from the test slab when fired.

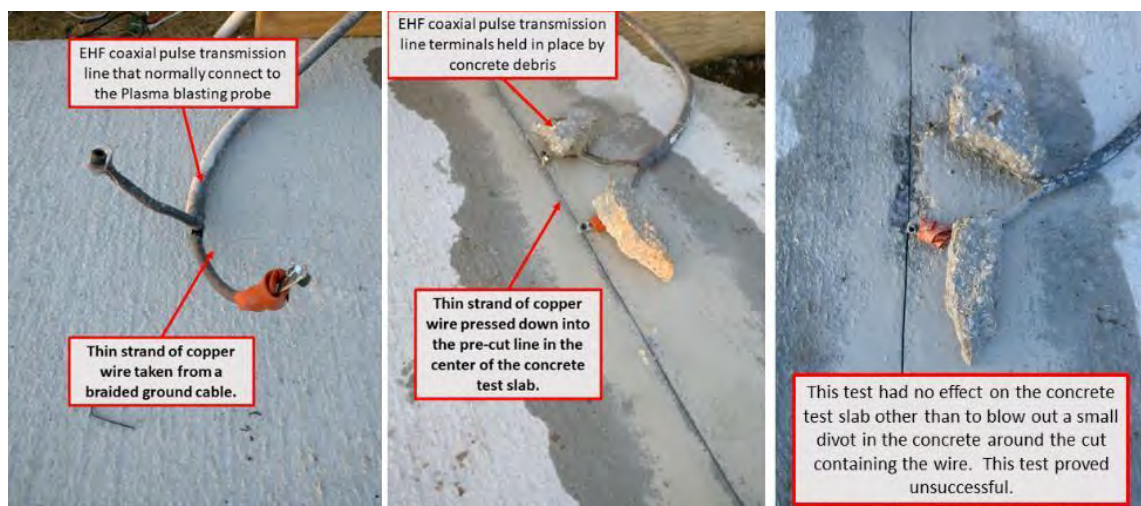


Figure 48. Exploding Wire Test Conducted for Shot 12

This method failed to crack the concrete because: 1.) the unconfined portion of thin wire above the slot (in air) attached to the coaxial cable leads vaporizes extremely quickly creating the highest impedance region, slowing the discharge rate and dissipating the majority of the energy, and 2.) the pressure pulse was not contained inside the confined cut long enough to crack the concrete. This method merits further investigation, using higher-gauge, larger-cross-section, flattened “feeder-leads” inserted into the slots and then connected to the much thinner exploding wire filaments. In addition, some method of containing the pressure in the cut holding the

exploding wire may improve the effectiveness. It is also possible that placing the wire in a borehole instead of a cut may be effective. In any future tests of the exploding wire method, aluminum foil or wire should be used as it will yield more energy in the blast due to the mass and electrical characteristics combined with the chemical interaction of aluminum with water.

Overall, testing the EHF system proved very successful. The system works very well at cracking and breaking up the test concrete slabs at charge energy levels 30% of the maximum capability of the system. A preliminary method for using the system to separate sections of the concrete along pre-cut lines was proven to work effectively with the caveat that unintentional cracks are still occurring in the section of concrete to be retained intact. However, we believe that with a design modification to the plasma blasting probe, this issue can be remedied.

System Assembly Description

The EHF system was assembled at Hyperion's facility in Tupelo, MS. The capacitor charge bank consists of four 176- μF Maxwell 32328 capacitors connected in parallel for a total of 704 μF . Figure 49 shows the assembly of the EHF main HV system. The four Maxwell 32328 capacitors are mounted in a modular MiniTec frame with solid stiffening plates. The capacitor ground terminals are connected in common by the ground return bus plate. Risers are installed on the positive terminals of the capacitors. Spherical washer pairs were also used to correct for capacitor bushing misalignment due to the original capacitor manufacturer's capacitor case top bulkhead bulging.

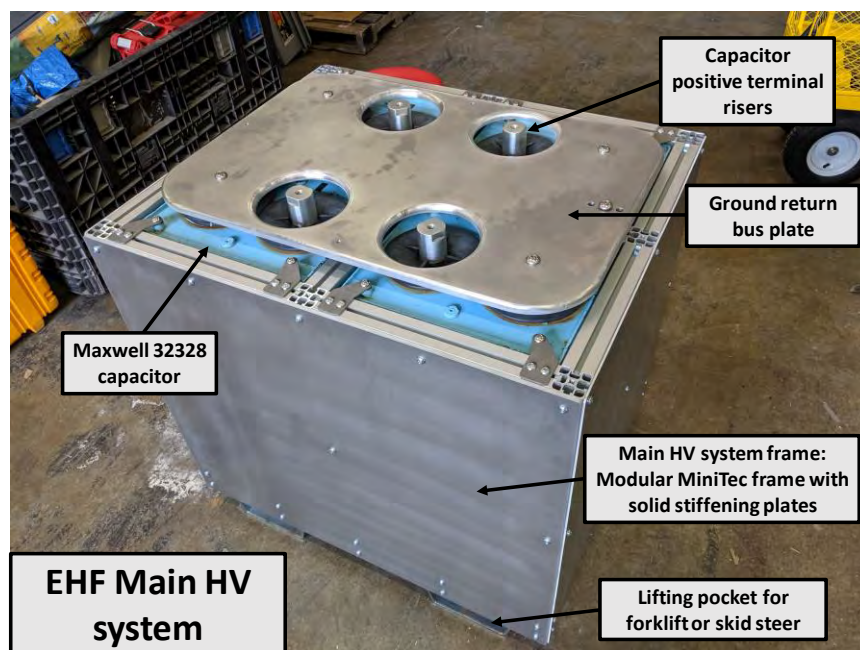


Figure 49. EHF Main HV System Assembly

A dielectric plate is placed over the ground bus plate to electrically insulate the positive bus plate from ground, as in Figure 50. The dielectric plate has cutouts for ground connections and the positive terminal risers. The positive terminal risers so connect to the positive bus plate that the capacitors will be connected in parallel.

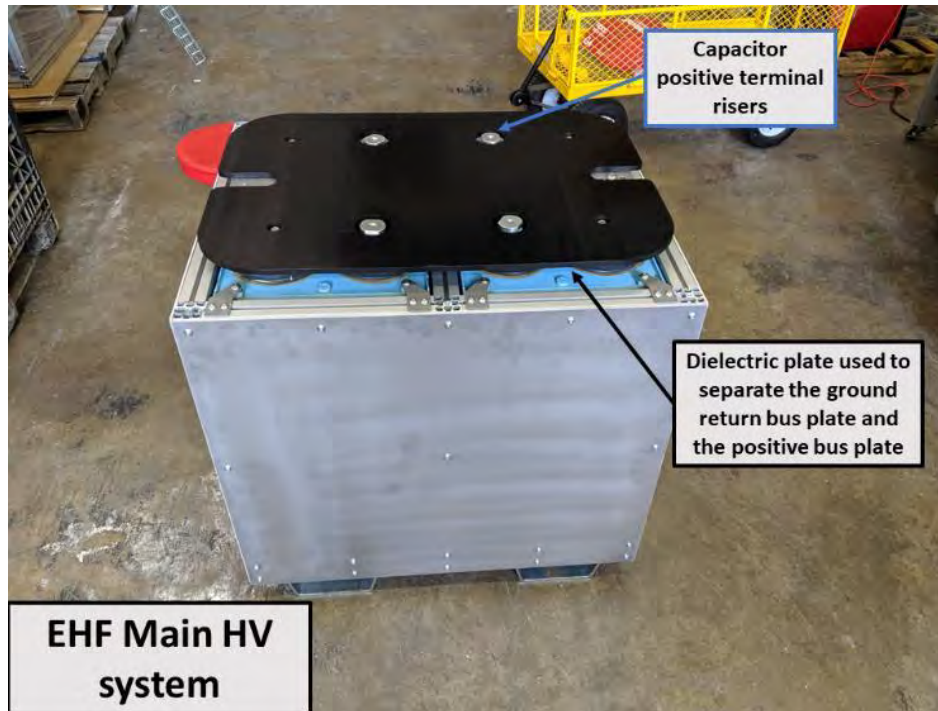


Figure 50. Dielectric Plate over Ground Bus Plate Insulates Positive Bus Plate from Ground

In Figure 51, the positive bus plate connects the positive terminals of the capacitors in parallel through the positive terminal risers. The spark gap bolts flush to the top of the positive bus plate. The spark gap is pressurized with 20 psig nitrogen and then depressurized using a vacuum pump to trigger the electrical pulse from the EHF main HV system. The spark gap trigger voltage was characterized prior to mounting it in the system.

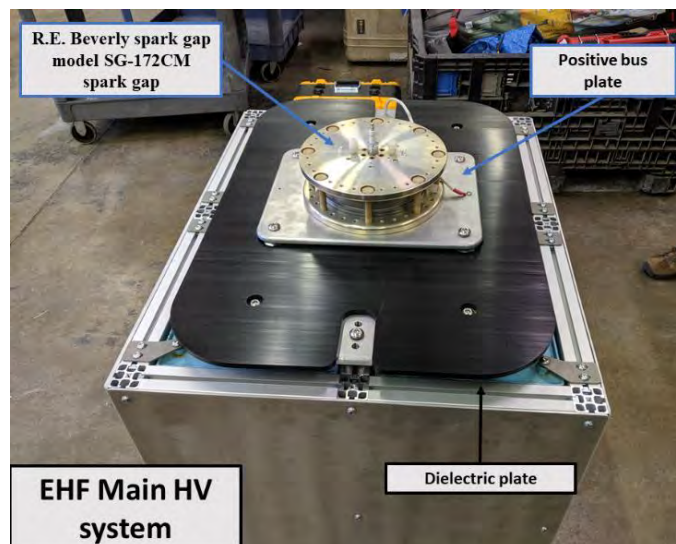


Figure 51. Positive Bus Plate Connects Positive Terminals of Capacitors in Parallel through Positive Terminal Risers

Shown in Figure 52, the output bus plate bolts flush to the top of the spark gap. The positive lead of the EHF coaxial pulse transmission line bolts to the output bus plate and the outside braided line of the EHF coaxial pulse transmission line bolts to the ground return bus plate.

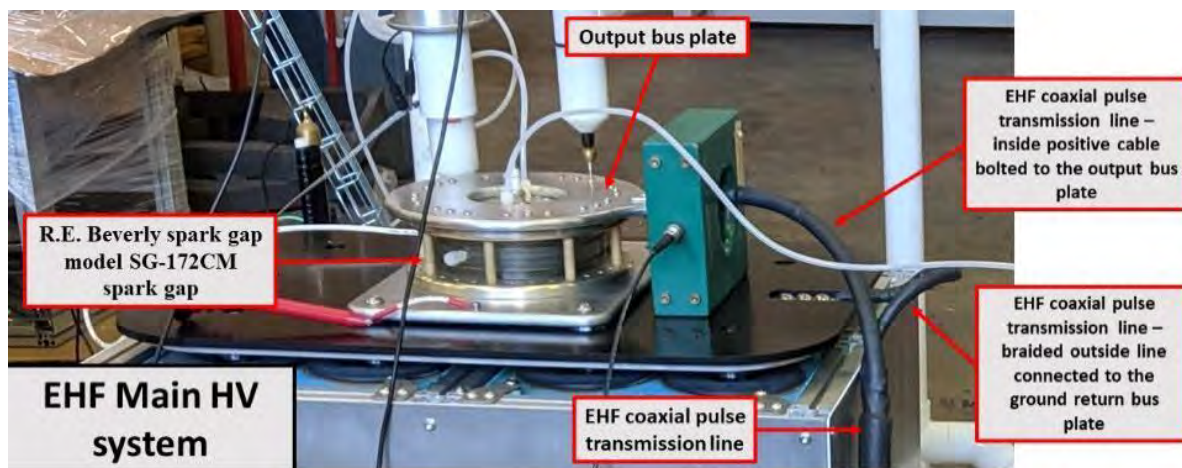


Figure 52. Connection of EHF Coaxial Pulse Transmission Line to EHF Pulser

Figure 53 shows connection of the plasma blasting probe to the EHF Main HV system through the coaxial pulse transmission line. The plasma blasting probe was set into a 5-gal bucket of copper sulfate solution for low-voltage operational testing at less than 4 kV charge prior to moving the EHF system to the field for full system testing.

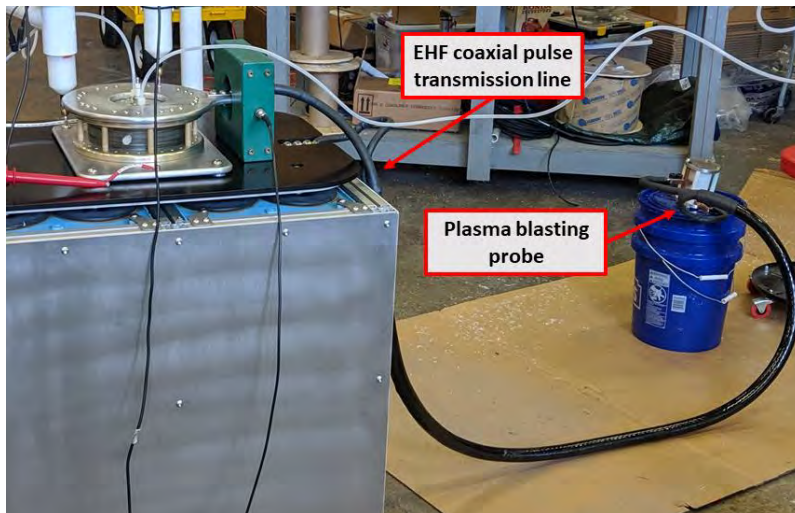


Figure 53. Plasma Blasting Probe Connection to EHF Main HV System

Figure 54 shows the plasma blasting probe 4 just prior to use in field testing. Four plasma blasting probes were assembled for the field testing. However, the probe designs proved to be very rugged and only two probes were used during the testing.

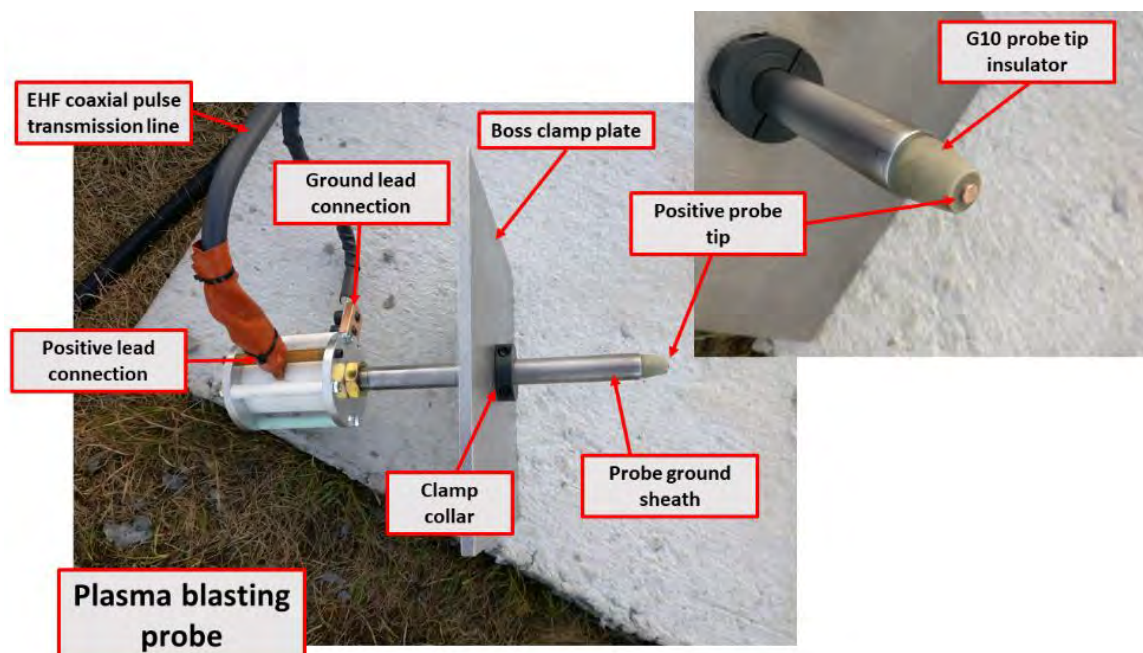


Figure 54. Plasma Blasting Probe 4 Shown Just prior to Use in Field Testing

Field Testing Setup

Testing was conducted in a field where a series of test 4000-lb/in² concrete slabs had been prepared in advance. For this testing series, three 4-ft x 4-ft slabs and one 6-ft x 12-ft slab were used. Test slabs were 12 to 13 in thick. Figure 55 displays a photo of the field-testing setup in progress. The EHF main HV system was positioned next to the test slab such that the coaxial pulse transmission line had sufficient length to position the plasma blasting probe in a prepared borehole in the concrete slab. An instrumentation trailer housed an oscilloscope, HV power supply used to charge the capacitor bank, and pressurized nitrogen supply bottle with a regulator used to pressurize the spark gap. This provided protection for this sensitive equipment in close proximity to the test.

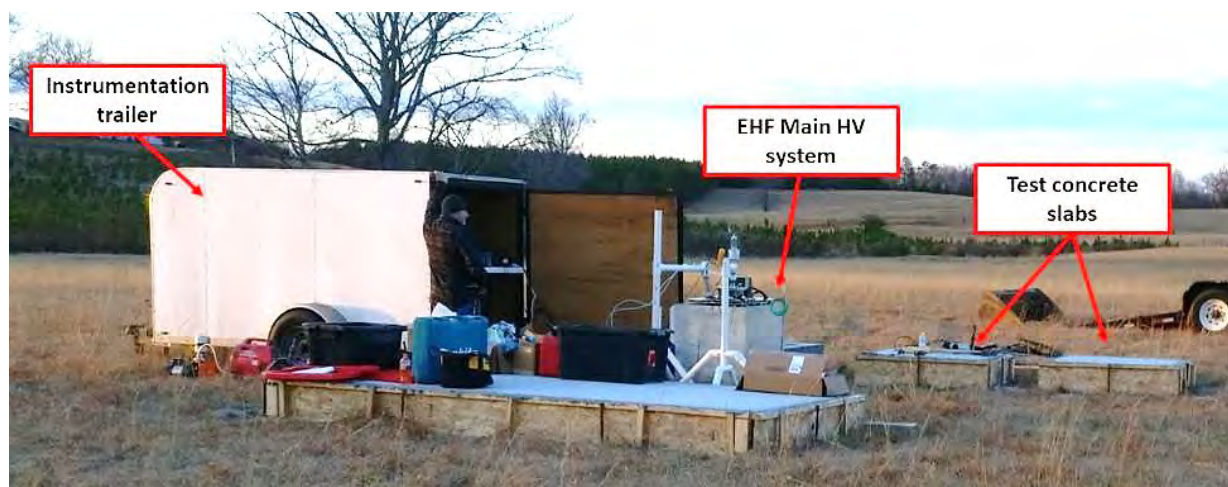


Figure 55. Field Test Setup

Figure 56 shows the debris barrier to shield the EHF main HV system and instrumentation from the blast generated by the plasma blasting probe when triggered. Test personnel cleared away from the test setup prior to firing. The debris barrier is used only to shield the EHF system and instrumentation.

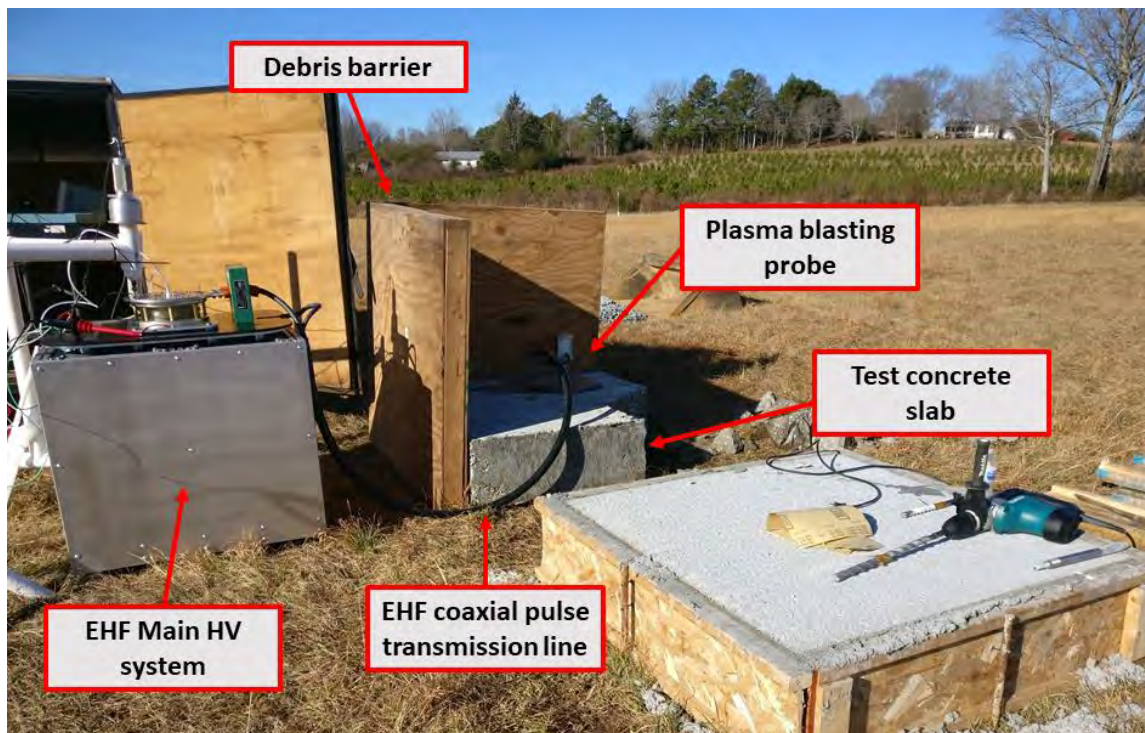


Figure 56. Debris Barrier to Shield EHF Main HV System and Instrumentation

Figure 57 shows the HV instrumentation used to instrument the EHF system test setup. A Tektronix P6015A HV probe was used to monitor the EHF capacitor bank charge voltage. A low-frequency-bandwidth Caltest HVprobe connected to a Fluke DVM was used for local reading of the EHF capacitor bank charge voltage. A North Star PVM-5 HV probe was used for monitoring the output voltage between the spark gap and the positive connection to the EHF coaxial pulse transmission line. A 1-GHz Tektronix oscilloscope was used to collect voltage readings from the Tektronix P6015A HV probe (charge voltage) and the North Star PVM-5 HV probe (output voltage). Figure 58 shows the Pearson 1423 wideband current monitor used to monitor the current pulse to the plasma blasting probe from the output of the spark gap. The 1-GHz Tektronix oscilloscope was also used to collect the signal from the Pearson current probe.

Figure 59 shows a block schematic diagram of the EHF electrical system setup as used during these field tests. A 10-ft earth ground rod at the test site ensured a safe local ground reference. A 1-kW, rack-mount HV power supply was used to charge the EHF capacitor bank both for the testing in the lab and in the field. This power supply was connected to the EHF capacitor bank through a charging N.O. (normally open) 25-kV-rated HV Ross relay and a copper sulfate resistor contained in a 5-gal bucket. An N.C. (normally closed) 25-kV rated Ross relay was used to manually discharge/dump the capacitor bank residual charge to ground through the same copper sulfate resistor once the shot was complete. The charge and discharge/dump Ross relays were mounted in an electrically insulated “suitcase” for portability. Both relays are manually

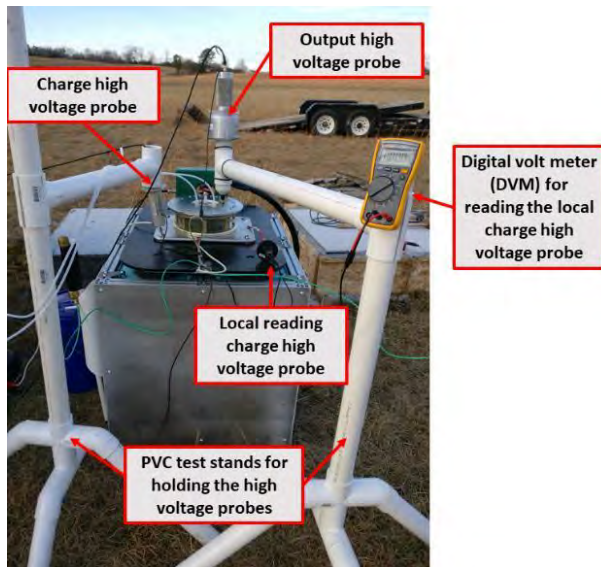


Figure 57. The EHF System Included Three HV Probes

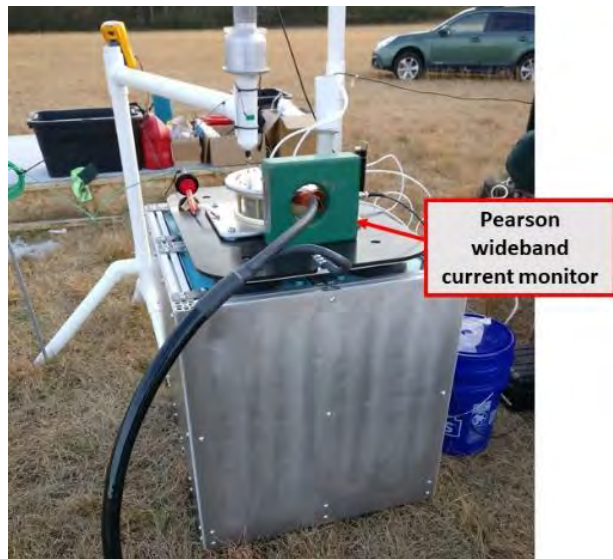


Figure 58. Pearson 1423 Wideband Current Monitor Installed on Output Lead of Coaxial Pulse Transmission Line

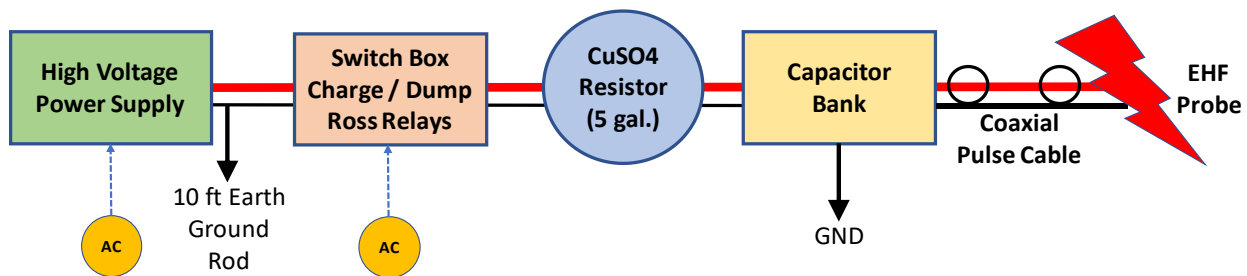


Figure 59. Block Schematic Diagram of EHF Electrical System Setup for Field Tests

operated via toggle switches mounted on the front side of the suitcase. These connections are in Figure 60 and Figure 61. This system provides safety connection for the charging power supply. In addition, the copper sulfate sink is sized such that the capacitor bank can be discharged even when fully charged.

In addition to the 10-ft earth ground rod, Figure 62, additional electrical safety features for the test setup included a shorting stick for manually verifying the capacitors discharged after triggering the EHF system and a shorting clamp to ensure the capacitors remained discharged while not in use.

Figure 63 shows the four 4000-PSI concrete test slabs poured for the testing set. The concrete test slab numbering sequence shown in Figure 63 is used for identifying the concrete test slab used for each shot in the testing descriptions contained in this report.

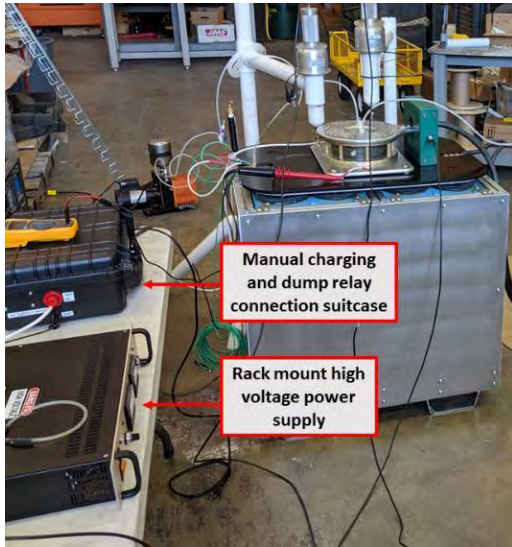


Figure 60. HV Power Supply and Connection to the EHF Capacitor

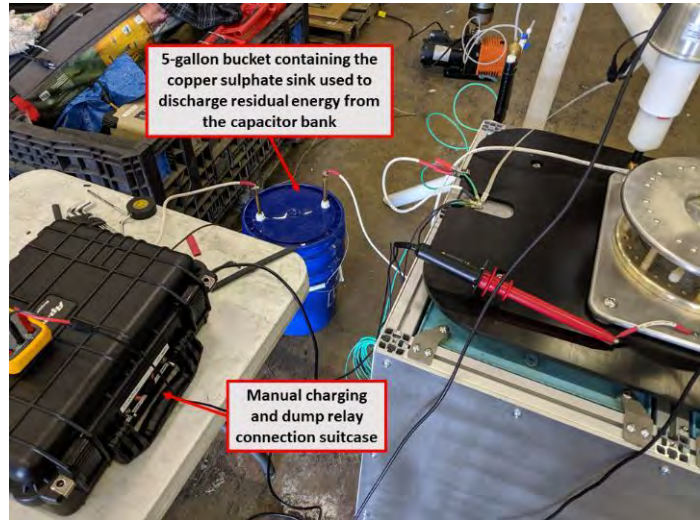


Figure 61. Copper Sulfate Sink Contained in a 5-gal Bucket

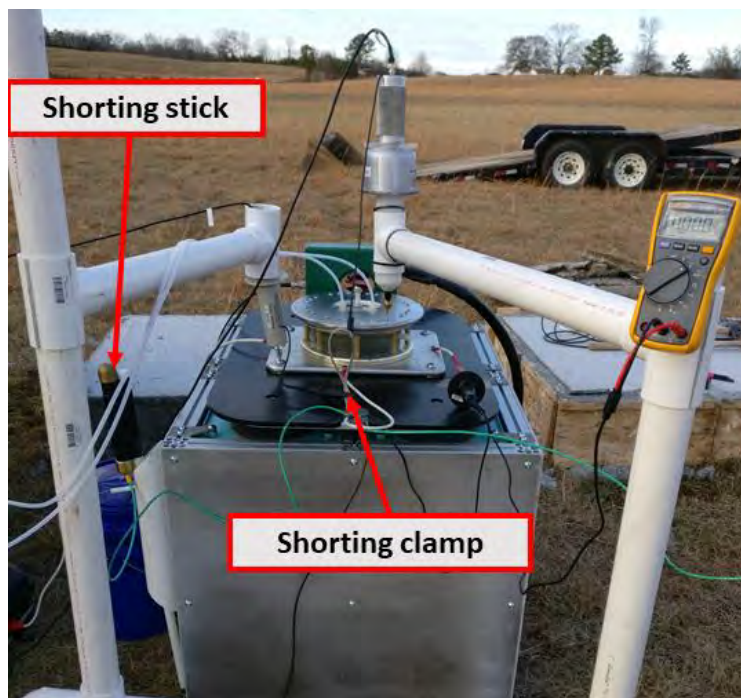


Figure 62. Electrical Safety Features

In Figure 64, to install the plasma blasting probe into the test concrete slab, a Makita hammer drill drilled a 1-in-diameter borehole in the concrete test slab. For initial test shots, a bore hole 6-in deep and then one 7-in deep were tried. These depths were found to be too shallow for effective cracking of the concrete test samples and for the majority of the test shots an 8-in-deep borehole was used.

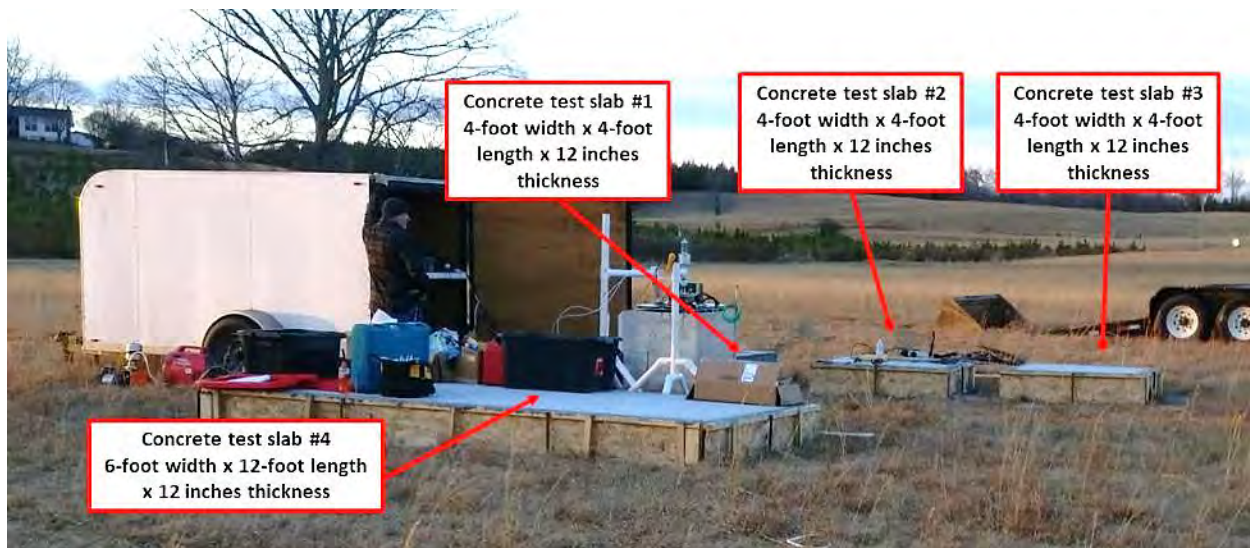


Figure 63. Four 4000-PSI Concrete Test Slabs Poured for the Test Set

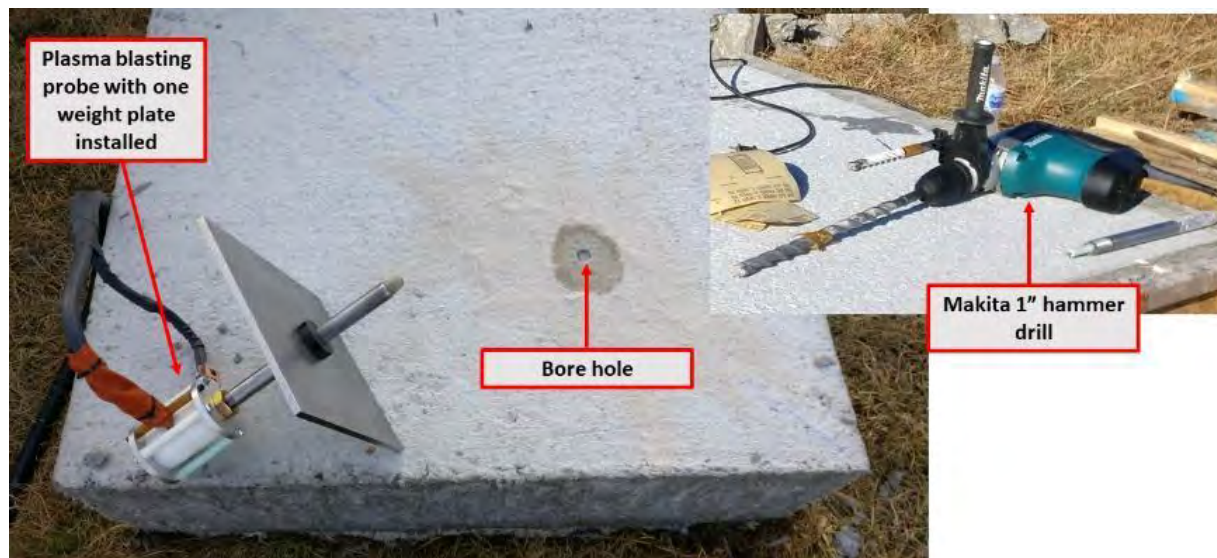


Figure 64. Makita Hammer Drill and 1-in-diameter Borehole in Concrete Slab

Weight plates were installed onto the shaft of the plasma blasting probe and held in place with clamping collars above and below the weight plate as in Figure 65. The first shot used a single weight plate, which was of insufficient mass to keep the probe in the borehole long enough. All subsequent test shots used two weight plates. The position of the weight plates and their locking collars on the shaft of the plasma blasting probe set the insertion depth of the plasma blasting probe into the borehole is shown in Figure 65. In general, the plasma blasting probe depth was set such that the probe was roughly an inch above the bottom of the borehole. For a selection of the test shots, the concrete test slabs were precut using diamond cutting saws. The depth of these setup precuts varied from 2 to 5 in. Figure 66 shows an example of setup precuts. Specifics of the setup precuts are detailed in the test report shot descriptions below.

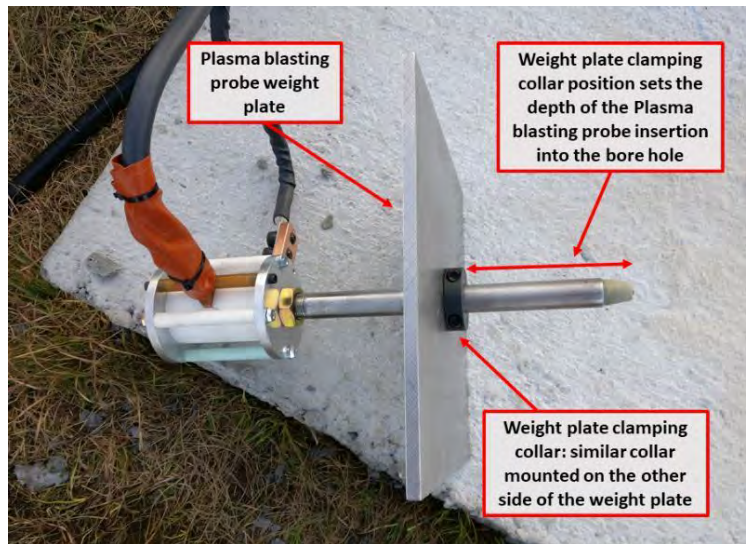


Figure 65. Plasma Blasting Probe Weight Plate

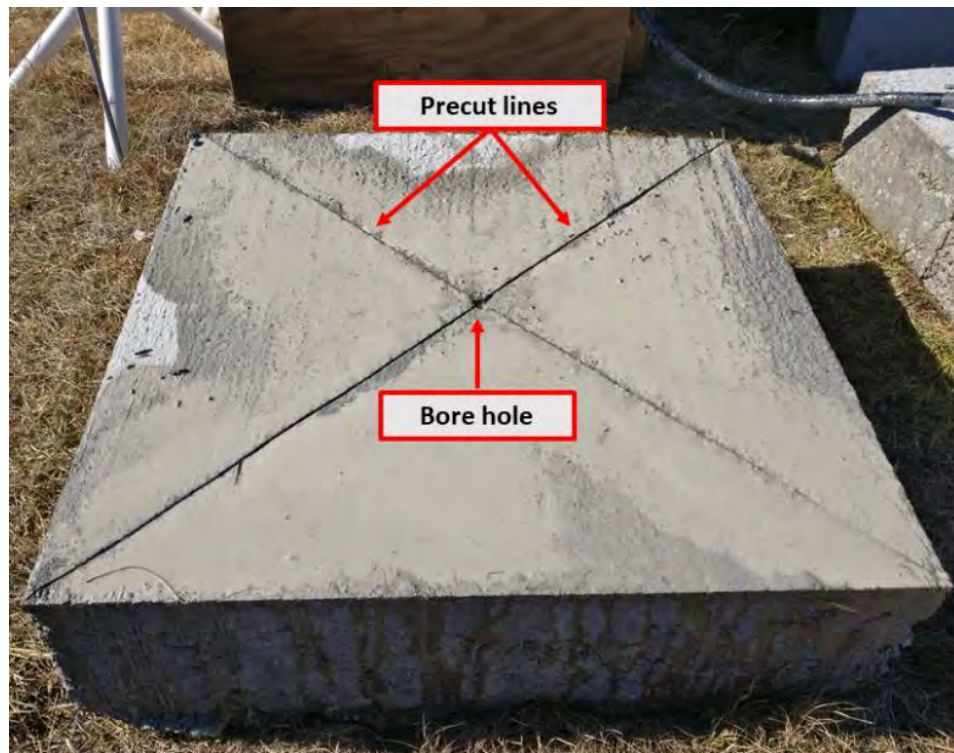


Figure 66. Precut Lines in Concrete Test Slab

Testing Procedure

Each test shot began with the setup of the concrete test slab and plasma blasting probe. First the borehole was drilled; if precuts were to be used, they were measured out and cut with the diamond saw. The plasma blasting probe was cleaned up from the last shot using sandpaper and a Scotch Brite heavy-duty scouring pad. Plasma blasting probe weight plate clamping collars were adjusted for shaft position as necessary and reclamped to set the desired plasma blasting probe depth.

With the plasma blasting probe in place, the spark gap was purged with pressurized nitrogen and the spark gap pressure was set to approximately 20 psig. The regulator on the pressurized nitrogen was backed off such that when the vacuum pump depressurized the gap, the pressurized nitrogen supply did not attempt to regulate the pressure drop.

The grounding clamp from the EHF system capacitor bank was removed. Manual toggle switches for the charging and discharging Ross relays were activated to align the EHF main system capacitor bank to the rack-mounted HV power supply and isolated the capacitor bank from the copper sulfate sink. The HV power supply was turned on and EHF system capacitor bank was charged. While charging, the capacitor bank voltage was monitored on both the local Caltest voltage probe via the DVM and the Tektronix HV probe via the oscilloscope. During charging, the operator stood by the HV power supply to secure power should the charging process of the capacitor bank have any problems. If any issue arose, the operator would shut off the HV power supply, open the charging Ross relay and close the discharging Ross relay to discharge the capacitor bank to the copper sulfate sink.

Once the capacitor bank reached planned charge voltage for the test shot, the operator isolated the HV power supply by opening the charging Ross relay and set the oscilloscope to record voltage and current data from instrumentation installed on the EHF system. The operator and all other personnel moved clear of the EHF system.

For the test setup, one operator moved a safe distance to video the plasma blasting probe and test slab of concrete for the shot. When in place, the operator taking the video signaled a second operator to trigger the EHF system to fire by depressurizing the spark gap. This second operator stood behind the instrumentation trailer with the vacuum pump. This position put the instrumentation trailer between the vacuum pump operator and the test shot and EHF system, shielding the operator from any debris generated from the test shot.

When the EHF system had fired, the operators first safed the EHF system by closing the discharging Ross relay shorting the EHF system capacitor bank into the copper sulfate sink and then using the shorting stick to verify that the capacitor bank discharged. The operator used the local voltage probe reading on the digital volt meter to verify the capacitor bank had no remaining charge and then clamped the capacitor bank shorted to prevent any charge buildup. With the EHF system safe, the spark gap was purged with nitrogen to clear out the gap volume, and photos and test data were taken to record the results of the test shot.

Testing Results

Testing results are recorded in detail for each shot. Table 5 and Table 6 contain the data summary for the testing sequence by shot number. Video was collected for each of these shots as well.

A cursory review of the 20 shot test series was conducted looking at different parameters and associative trends. Two examples of this analysis shown in Figure 67 and Figure 68 examine how the EHF pulse current peak compared to the corresponding capacitor bank charge voltage and energy. To help better to understand the scatter of the data points, each point is identified by data labels with the shot number, sometimes the concrete slab Sample, and a short descriptor. One rationale applied to better understand the scatter and identify a trend was to identify EHF

Table 5. Test Shot Summary Table by Test Shot Number

Shot number	Test slab number	Probe number	Bore hole depth (in)	Probe depth (in)	Charge voltage (kV)	Charge energy (kJ)	Peak current (kA)
1	1	4	6	6	5.33	10	9.8
2	1	4	6	6	7.4	19.3	NR
3	1	4	7	6	7.2	18.2	28.9
4	1	4	7	6	7.5	19.8	31
5	1	4	7	6	7.6	20.3	36.2
6	2	4	7	6	10.5	38.8	75.4
7	3	4	8	7	12	50.7	80
8	4	4	8	7	10.6	39.6	53.2
9	4	4	8	7	10.5	38.8	56.2
10	4	4	8	7	10.5	38.8	72.7
11	4	4	8	7	15.78	87.6	132
12	4	wire	N/A	N/A	15.06	79.8	76.4
13	4	4	8	7	10.61	39.6	69.4
14	4	4	8	7	15.8	87.9	130.1
15	4	4	8	7	10.5	38.8	101.5
16	4	4	8	7	10.5	38.8	134.8
17	4	3	8	7	10.5	38.8	70.1
18	4	wire	N/A	N/A	16.55	96.4	40.1
19	4	3	8	7	10.5	38.8	77.4
20	4	3	8	7	15.7	86.8	153.6

Table 6. Test Shot Summary by Test Shot Number

Shot	Pre-cut used? (Y/N)	Pre-cut intersect bore hole (Y/N)	Shot summary notes
1	N	N/A	Instrumentation shot at lower voltage, did not crack test slab.
2	N	N/A	Same borehole as shot 1, corner of test slab 1 sectioned off
3	N	N/A	Corner of test slab 1 sectioned off in shot 2 broke-up
4	N	N/A	Similar to shot 2, opposite corner of test slab 1 sectioned off
5	N	N/A	Probe in borehole between the two corners sectioned off in shots 2 and 4. Sectioned off concrete sliver along relatively straight crack line. Cracked remaining section of test slab 1 into two pieces.
6	N	N/A	To look at natural crack propagation from the shot. Charge energy for this shot was double that used for shots 2–5.
7	Y	Y	First test of pre-cut lines. Test slab 3 pre-cut along diagonals from corner to corner. Slab sectioned along pre-cut line. Two unintended crack lines left test slab in six large chunks.

8	Y	N	Borehole in center of the section to be separated. Pre-cut lines not intersecting borehole to create a 36-ft by 36-ft section. Shot did not control the crack propagation along pre-cut lines
9	Y	Y	Dry-fire (no water in borehole)
10	Y	Y	Placed borehole along a pre-cut line from shot 8. Crack lines did not follow pre-cut line. Cracks from shots 8 & 9 may be factor.
11	Y	Y	Charge energy increased to break up/remove shot 8–10 slab.
12	Y	Y	Exploding wire test, unsuccessful
13	Y	Y	Set up 36-in x 36-in section with deeper pre-cut; successfully separated from test slab
14	N	N/A	Broke up 36-in x 36-in section separated in shot 13
15	Y	N	Dry-fire (no water in borehole), nose cone surface carbonized, slightly bent, some interior exposure, possible damage to center conductor dielectric tube
16	Y	N	Repeat of shot 15, probe 4 failed
17	Y	N	Pre-cuts offset from borehole. Crack propagation not controlled
18	N	N/A	Exploding wire test, unsuccessful
19	Y	Y	Deeper pre-cut 36-in x 36-in section separated from test slab
20	N	N/A	Breakup of 36-in x 36-in section separated in shot 19

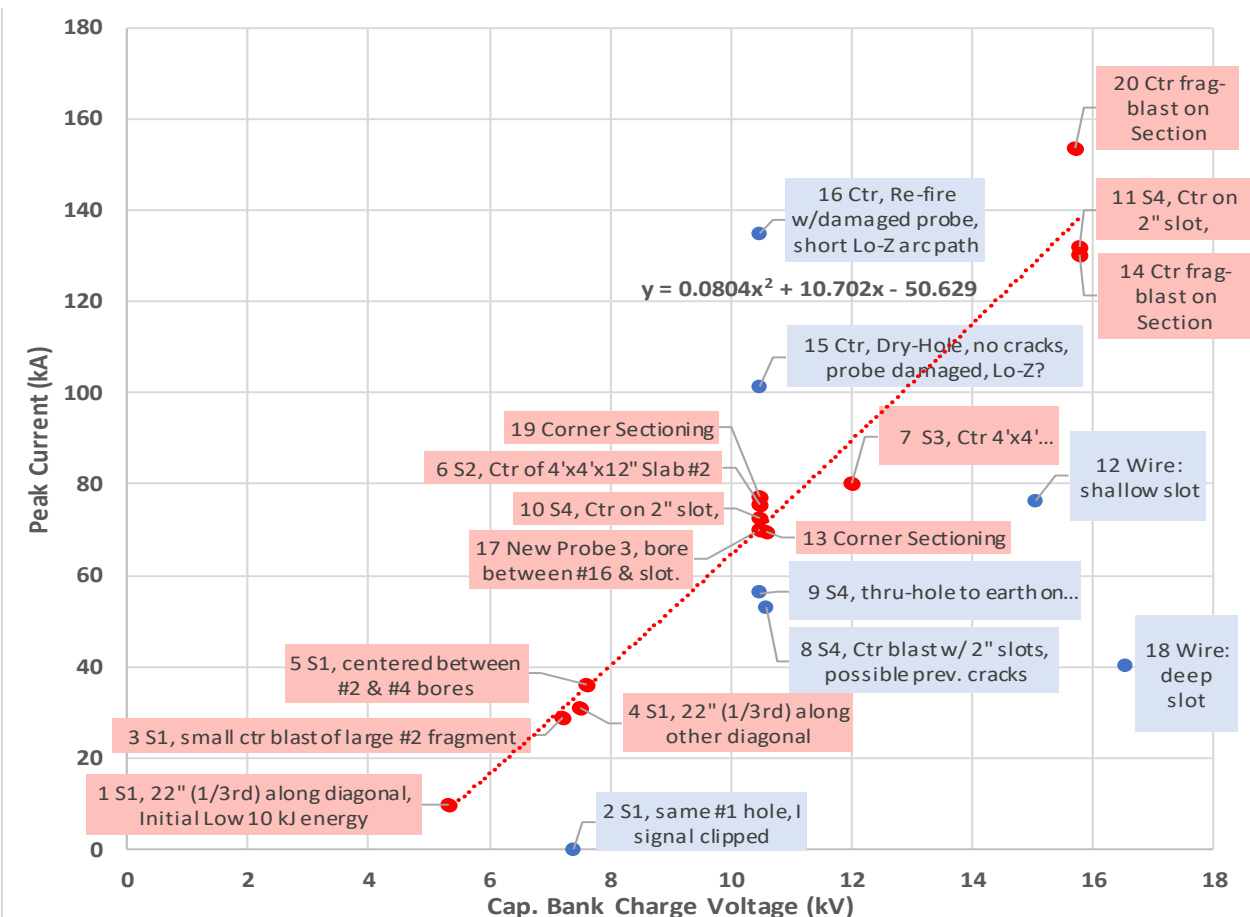


Figure 67. Plot of Peak Current as a Function of Capacitor Bank Charge Voltage for EHF Shots 1–20; Presumed Outlier Points Are Plotted in Blue

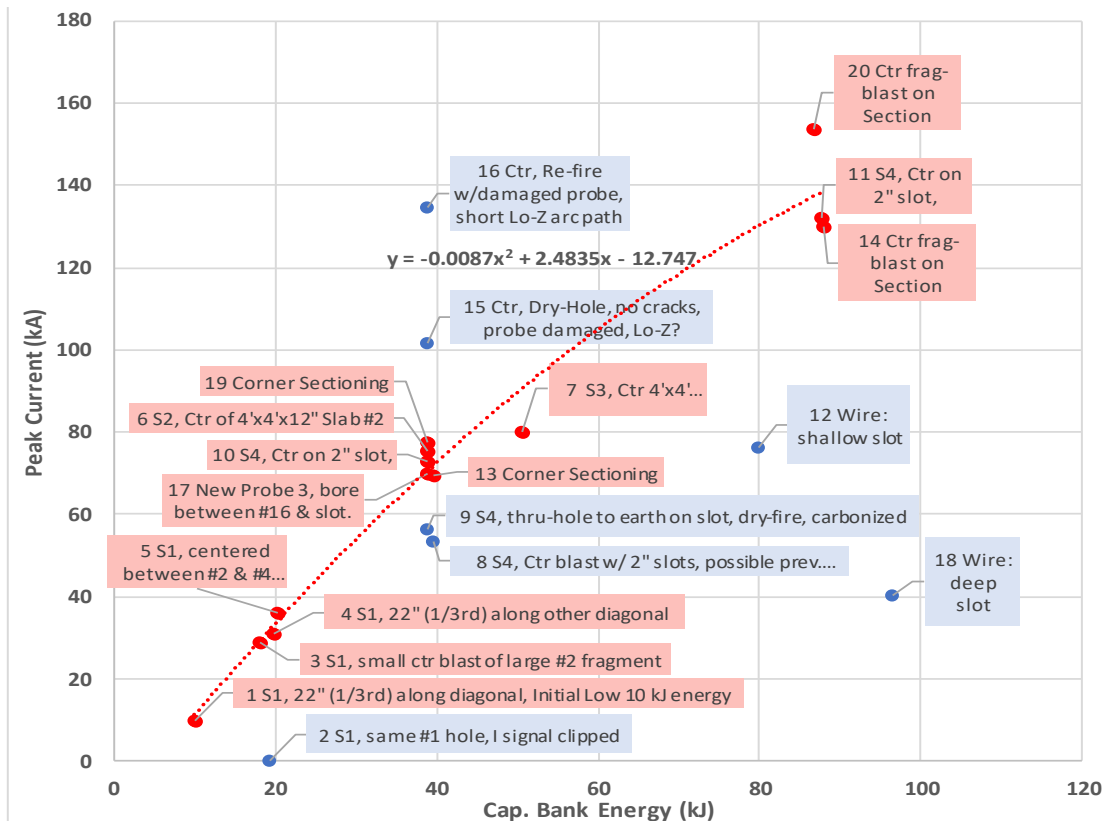


Figure 68. Plot of Peak Current as a Function of Capacitor Bank Charge Energy for EHF Shots 1–20; Presumed Outlier Points Plotted in Blue

test shots that were likely non-ideal due to relatively unconfined blasts, or abnormal test conditions. Examples of these outlier test shots are: “dry-fire” shots (no water in borehole, shots 9 and 15), abnormal low probe impedance due to damage-induced internal short path arcing (shot 16), possibly reduced confinement due to previous blast cracking thru or nearby (shot 8), and relatively unconfined wire shots (shots 12 and 18). These outlier points are colored Blue. Test shots that occurred normally, under nominal conditions, and therefore expected to have developed reasonable confined EHF pressures are colored Red. In Figure 67 and Figure 68, a red dotted trend line using a polynomial fit based only on the high-pressure, red points were added to show possibly charge voltage and energy trends.

Although 20 shots are not enough to establish statistical trends, the trend line’s decreasing slope at higher energy in Figure 68 implies that the energy used was sufficient to fragment these relatively thin concrete samples, i.e. the concrete breaks quickly at higher energies, cracks open and vents pressure early. This is validated in the shot photographic records shown below. Shots in the 20-40 kJ range often cause 1–3 cracks and 60–90 kJ shots cause substantially more fragmentation into small pieces.

Detailed Descriptions of Shots 1–20:

The graphic in Figure 69 depicts the Shot 1–20 Positions in Concrete Samples S1, S2, S3 (4 ft x 4 ft), and Sample S4 (6 ft x 12 ft).

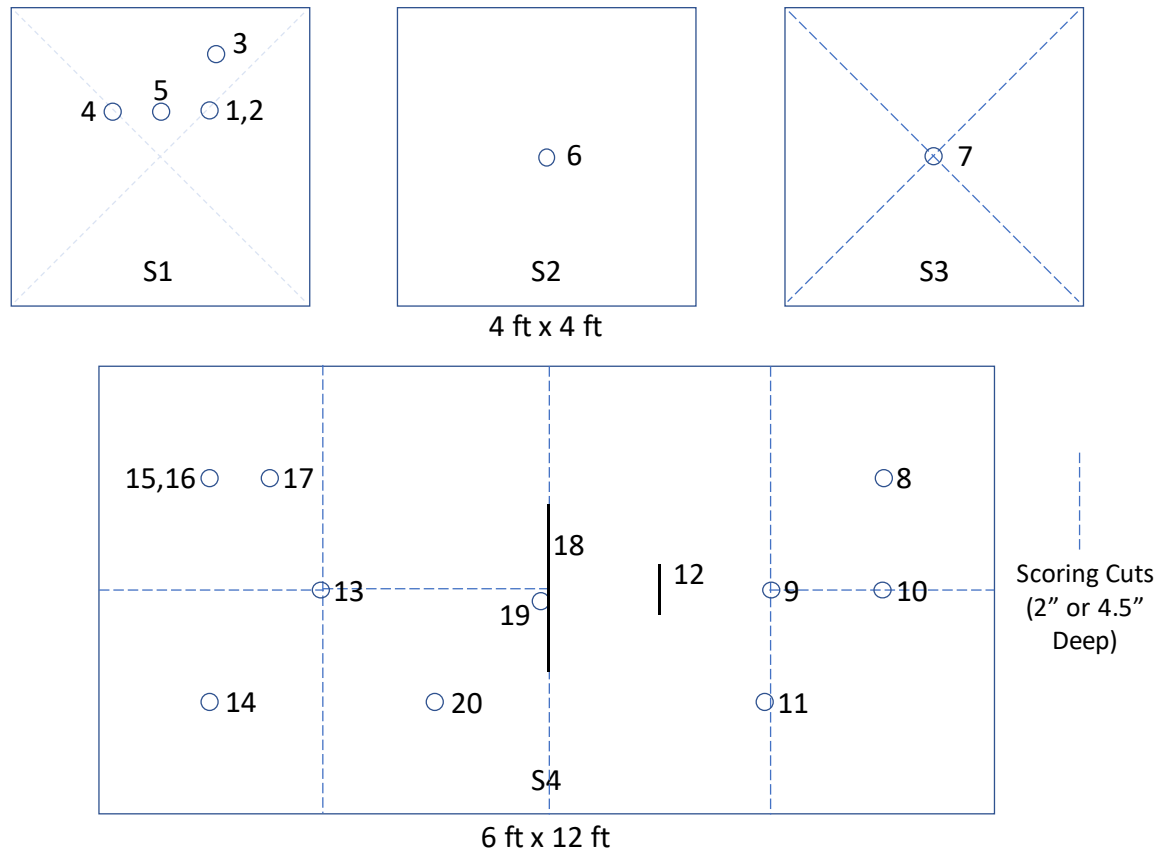


Figure 69. Test Shot 1–20 Positions in Concrete Samples S1–S4

Shot 1

The plasma blasting probe was placed in a 6-in-deep borehole 22 in in on a diagonal line across the square concrete test slab from corner to opposite corner. Length of the diagonal line from corner to corner is 66 in. This placed the probe 16 in from test slab edges on either side. Figure 70 shows the borehole and plasma blasting probe setup; results for shot 1 are shown in Figure 70 and Table 7. Oscilloscope traces of voltage and current collected from the capacitor, output HV probes and output current probe are in Figure 71 and Figure 72. Voltage signals were incorrectly scaled at the oscilloscope and were adjusted in post processing by a factor of 1.6.

Shot 1 served as an initial low-voltage/energy shot primarily to check diagnostic instrumentation setups and did not visibly damage the concrete slab. As in Figure 73, shot 1 did not damage or wear the plasma blasting probe. The probe rapidly shot out of the borehole. From shot 1, we concluded that higher energy (higher charge voltage) was needed to crack the concrete test slab, and that also a second weight plate should be added to the plasma blasting probe.



Figure 70. Shot 1: Concrete Test Slab and Plasma Blasting Probe Setup
Table 7. Data for Shot 1: Test Setup and Results

Shot 1	3-Dec-19
Plasma blasting probe used	Probe 4 -new stepped G10 probe
EHF pulse transmission line used	Coaxial design
Number of weight plates installed on the plasma blasting probe	1
Test concrete slab	4000 lb/in ² - 4-ft x 4-ft x 12 in thick block 1
Borehole location	22 in diagonally from the corner (66 in is total diagonal length of the test slab)
Borehole depth (in)	6
Borehole diameter (in)	1
Water used in borehole	Yes, bottled water, nothing added to the water
Setup precuts used for this shot	No
First test shot on this concrete slab?	Yes
Plasma blasting probe insertion depth (in)	6
Probe intact after shot	Yes
Charge voltage (VDC)	5330
EHF system capacitance (μF)	704
Charge energy (kJ)	10.0
Peak current (kA)	9.8
Notes	Instrumentation test; Did not visibly crack test concrete slab

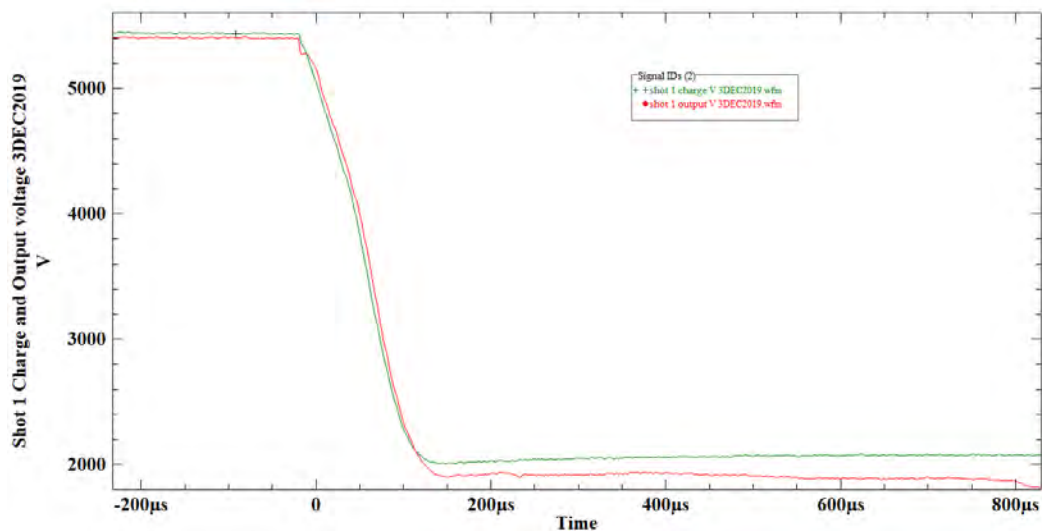


Figure 71. Shot 1: Charge and Output Voltage for Time of Trigger of EHF System

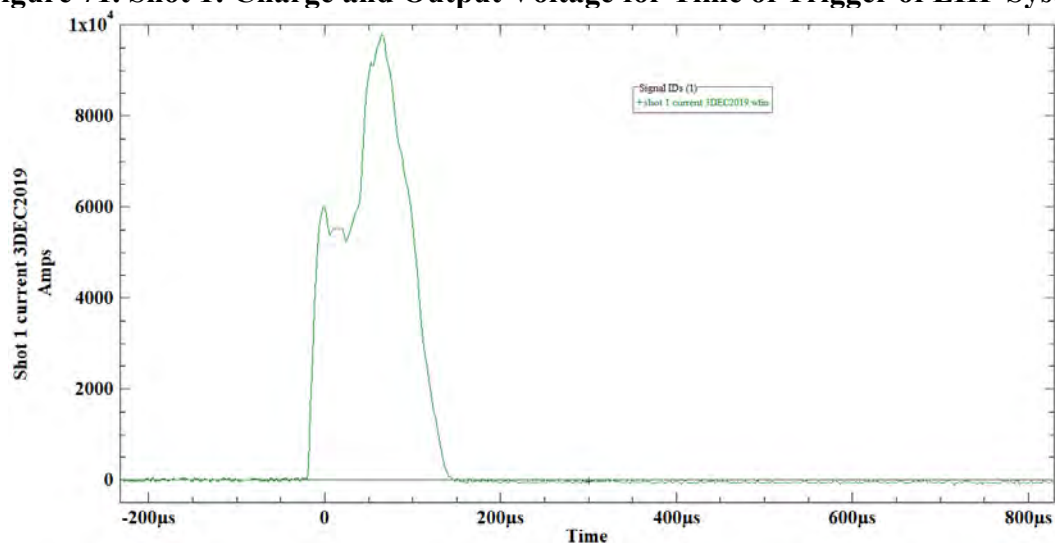


Figure 72. Shot 1: Current Reading for Time of Trigger from Output of EHF System to Plasma Blasting Probe



Figure 73. Plasma Blasting Probe Tip post Fire on Shot 1 (after Clean-up); No Visible Damage to Probe from the Shot

Shot 2

Shot 2 used the test borehole from shot 1. An additional weight plate was added to the plasma blasting probe. The charge energy was doubled to 20 kJ. See shot 1 test setup description for placement of the plasma blasting probe in the concrete test slab. Test setup and results for shot 2 are shown in Table 8. Voltage and current traces collected by the oscilloscope from the capacitor and output HV probes and output current probe are shown in Figure 74 and Figure 75. Voltage signals were incorrectly scaled at the oscilloscope and were adjusted in post processing by a factor of 2.1.

Table 8. Data for Shot 2: Test Setup and Results

Shot 2	3-Dec-19
Plasma blasting probe used	Probe 4: cleaned and re-used
EHF pulse transmission line used	Coaxial design
Number of weight plates installed on the plasma blasting probe	2
Test concrete slab	4000 lb/in ² – 4-ft x 4-ft x 12-in-thick block 1
Borehole location	22 in diagonally from the corner (66-in total diagonal length of test slab) *same borehole used for shot 1
Borehole depth (in)	6
Borehole diameter (in)	1
Water used in borehole	Yes, bottled water, nothing added to the water
Setup precuts used for this shot	No
First test shot on this concrete slab?	No, second shot on this test slab, reused shot 1 borehole
Plasma blasting probe insertion depth (in)	6
Probe intact after shot	Yes
Charge voltage (VDC)	7400
EHF system capacitance (μF)	704
Charge energy (kJ)	19.3
Peak current (kA)	Current off scale due to incorrect oscilloscope settings -.
Notes	Successful shot, separated corner off test concrete slab along two main cracks.

Shot 2 successfully fractured the concrete test slab. Two main fracture lines formed separating a side corner from the concrete test slab. The plasma blasting probe popped up from shot 2 but stayed in the borehole. Photos of the concrete test slab after shot 2 appear in Figure 76 through Figure 80. A photo of the plasma blasting test probe after shot 2 is shown in Figure 81. No damage noted to the probe. The probe was cleaned up and used again for shot 3.

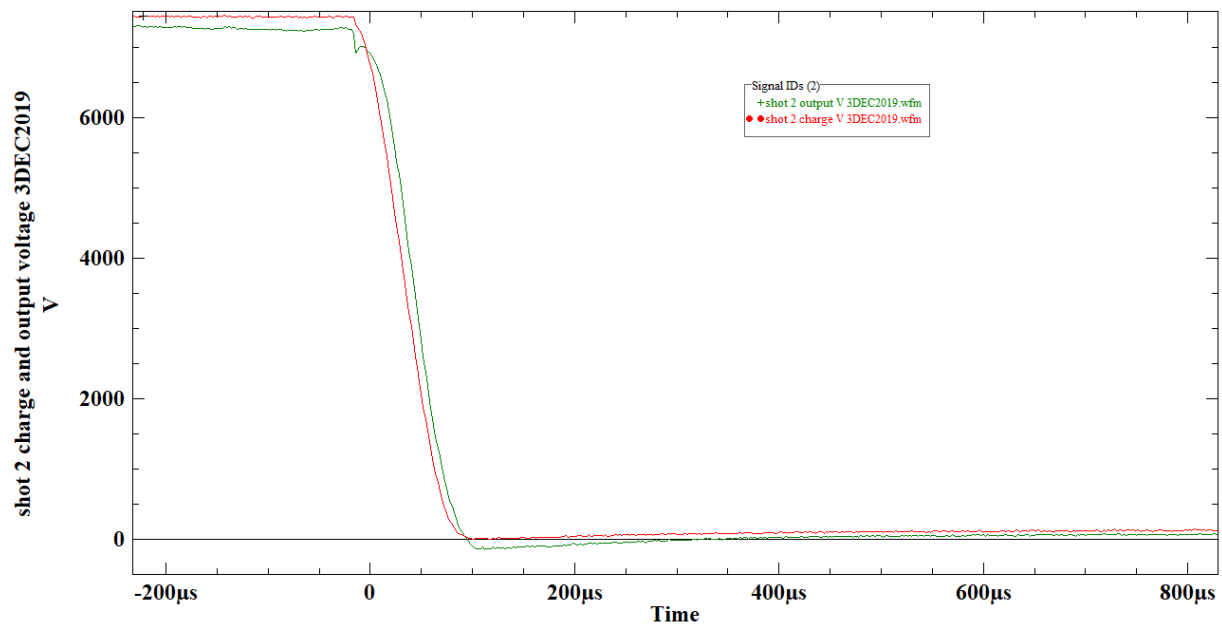


Figure 74. Shot 2: Charge and Output Voltage for Time of Trigger of the EHF System

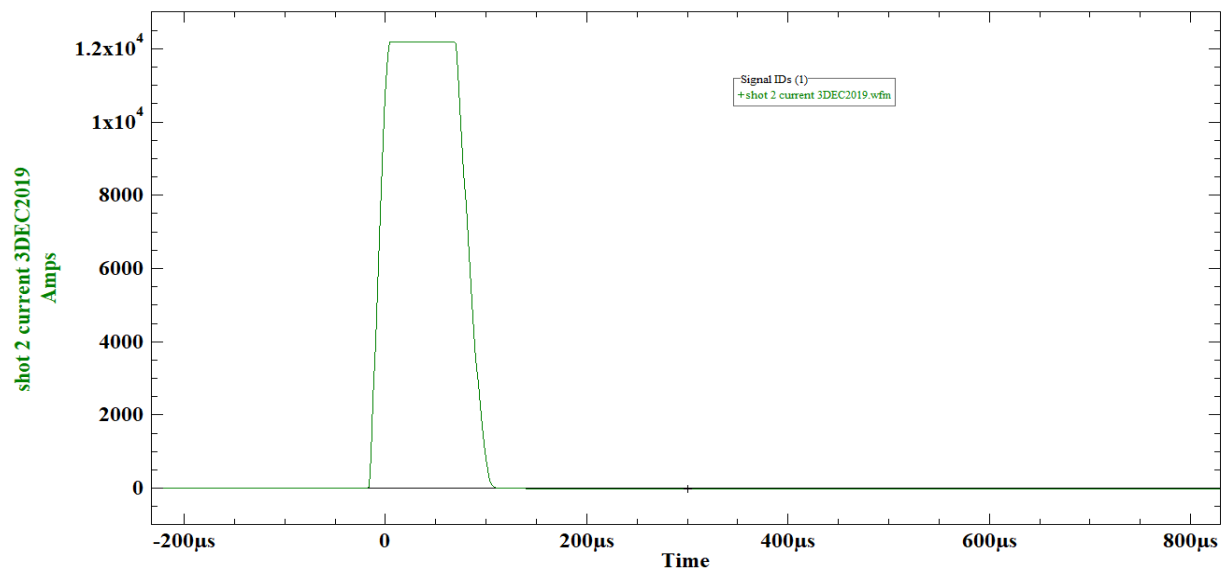


Figure 75. Shot 2: Current Reading (Clipped) for Time of Trigger from EHF System Output to Plasma Blasting Probe



Figure 76. Shot 2: Concrete Test Slab Successfully Fractured

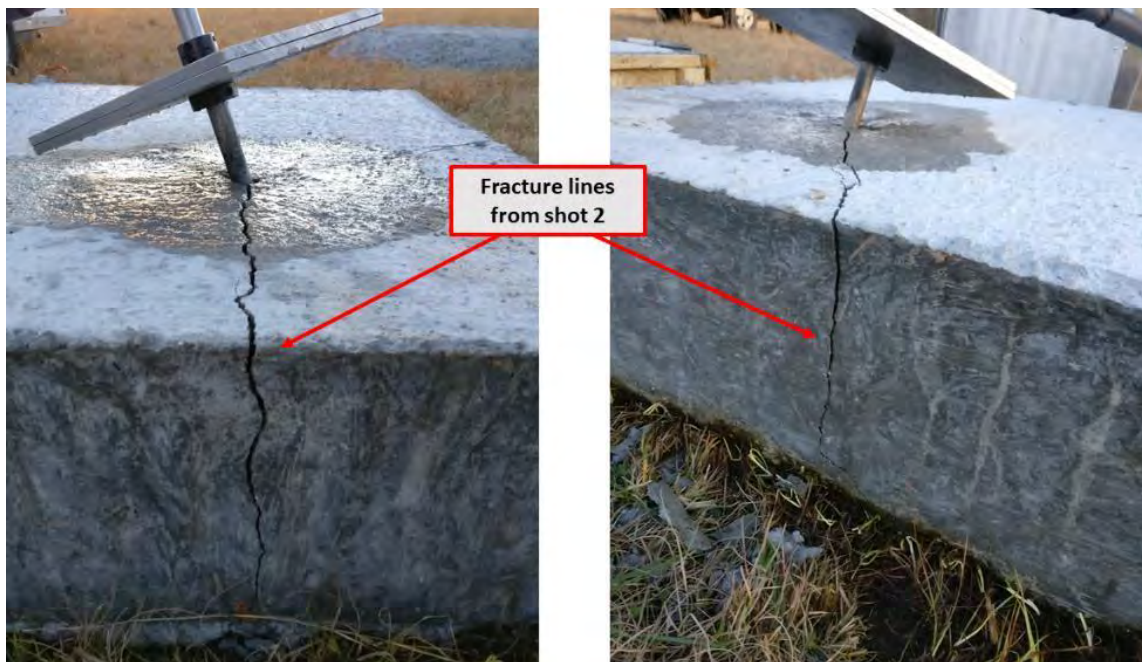


Figure 77. Shot 2: Fracture Lines



Figure 78. Shot 2: Fractured Section after Separated Concrete Section Pulled Back



Figure 79. Shot 2: Closeup Image of Separated Borehole Section



Figure 80. Shot 2: Test Concrete Slab Showing Separation of Corner Section



Figure 81. Photo of Plasma Blasting Test Probe after Shot 2; No Damage Noted to Probe

Shot 3

Shot 3 was used to break up the chunk of concrete separated from test concrete Slab 1 by shot 2. A borehole was drilled into roughly the center of this chunk of concrete. Figure 82 shows the plasma blasting probe set up in the separated chunk of concrete. The borehole depth with increased to 7 in from the 6-in depth used for shots 1 and 2. The plasma blasting probe depth was maintained at 6 in. This created a 1-in volume of water under the tip of the plasma blasting probe. Test setup and results for shot 3 are shown in Table 9. Voltage and current traces collected by the oscilloscope from the capacitor and output HV probes and output current probe are shown in Figure 83 and Figure 84, respectively. Voltage signals were incorrectly scaled at the oscilloscope and adjusted in post processing by a factor of 1.6.



Figure 82. Shot 3: Plasma Blasting Probe Set up in Chunk of Concrete Separated by Shot 2

Table 9. Data for Shot 3: Test Setup and Results

Shot 3	4-Dec-19
Plasma blasting probe used	Probe 4: cleaned and re-used
EHF pulse transmission line used	Coaxial design
Number of weight plates installed on plasma blasting probe	2
Test concrete slab	Section separated from test concrete slab 1
Borehole location	Borehole roughly centered on separated chunk
Borehole depth (in)	7
Borehole diameter (in)	1
Water used in borehole	Yes, bottled water, nothing added to the water
Setup precuts used for this shot	No
First test shot on this concrete slab?	No, section of concrete separated off test slab 1 by shot 2
Plasma blasting probe insertion depth (in)	6
Probe intact after shot	Yes
Charge voltage (VDC)	7200
EHF system capacitance (μF)	704
Charge energy (kJ)	18.2
Peak current (kA)	28.9
Notes	Successful shot, broke separated concrete section. 7-in borehole depth added 1-in water volume under probe tip

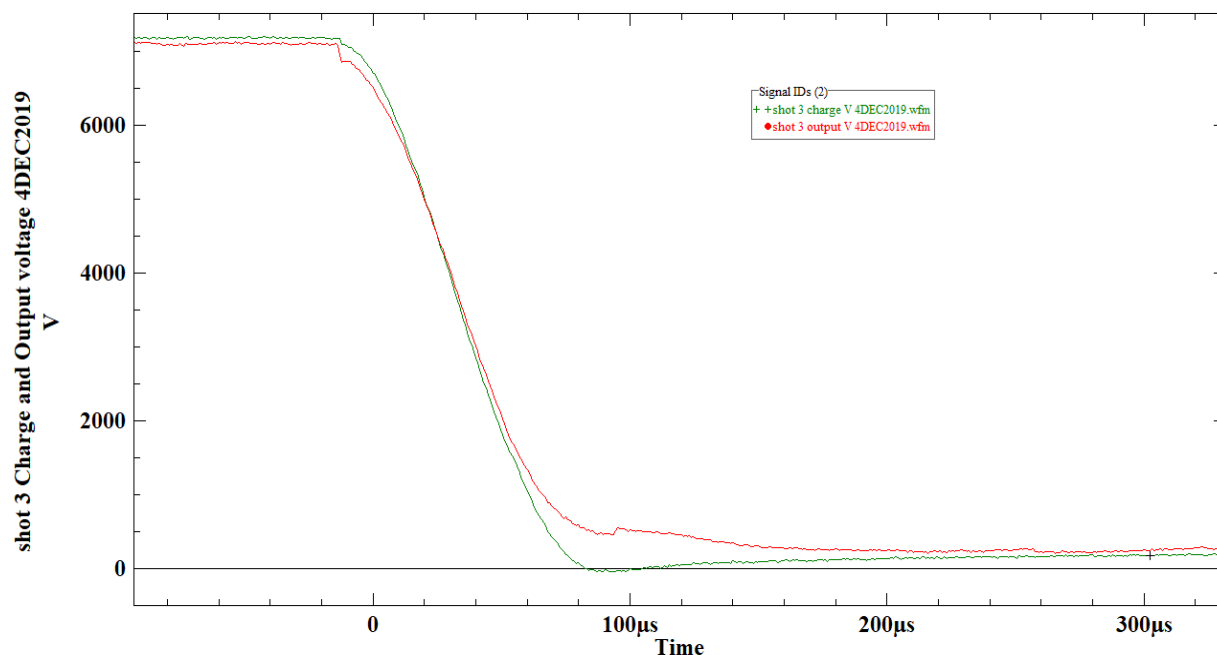


Figure 83. Shot 3: Charge and Output Voltage for Time of Trigger of the EHF System

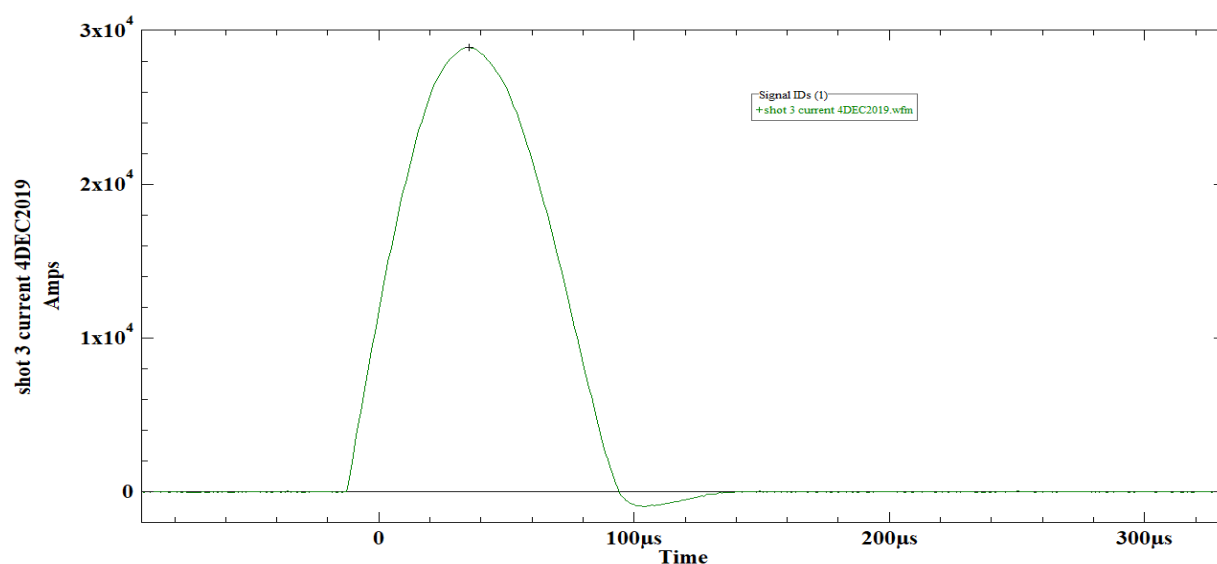


Figure 84. Shot 3: Time of Trigger from EHF System Output to Plasma Blasting Probe

The separated chunk of concrete from shot 2 was successfully broken up by shot 3 into several smaller fragments. Post shot photos are shown in Figure 85 and Figure 86. Photo of the plasma blasting test probe after shot 3 is shown in Figure 87. No damage was noted to the probe, which was cleaned up and used again for shot 4.



Figure 85. Shot 3: Completely Fractured Debris from Chunk of Concrete from Shot 2



Figure 86. Shot 3: Debris; Fragments of Chunk of Concrete Separated by Shot 2



Figure 87. Plasma Blasting Test Probe after Shot 3

Shot 4

Shot 4 repeated the shot 2 setup on the concrete test slab used in shots 1 and 2. Plasma blasting probe placement is similar to the setup for shot 1, 22 in on the second diagonal line across the square slab—the opposite diagonal used for probe placement in shot 1. On the 66-in diagonal the probe was 16 in from edges on either side of the concrete test slab. Figure 88 shows the borehole and plasma blasting probe setup. Table 10 describes the test setup and results. Voltage and current traces collected by the oscilloscope from the capacitor and output HV probes and output current probe are shown in Figure 89 and Figure 90.



Figure 88. Shot 4: Setup in Concrete Test Slab 1

Table 10. Data for Shot 4: Test Setup and Results

Shot 4	4-Dec-19
Plasma blasting probe	Probe 4: cleaned and re-used
EHF pulse transmission line	Coaxial design
Number of weight plates installed on plasma blasting probe	2
Test concrete slab	concrete slab 1 missing corner section after shot 2
Borehole location	22 in along diagonal off adjacent corner to Shot 1/2
Borehole depth (in)	7
Borehole diameter (in)	1
Water used in borehole	Yes, bottled water, nothing added to the water
Setup precuts used for this shot	No
First test shot on this concrete slab?	No, this test slab was shot used in shots 1&2
Plasma blasting probe insertion depth (in)	6
Probe intact after shot	Yes
Charge voltage (VDC)	7500
EHF system capacitance (μF)	704
Charge energy (kJ)	19.8
Peak current (kA)	31.0
Notes	Successful shot, repeated shot 2 result. Corner of slab separated from the larger concrete slab successfully.

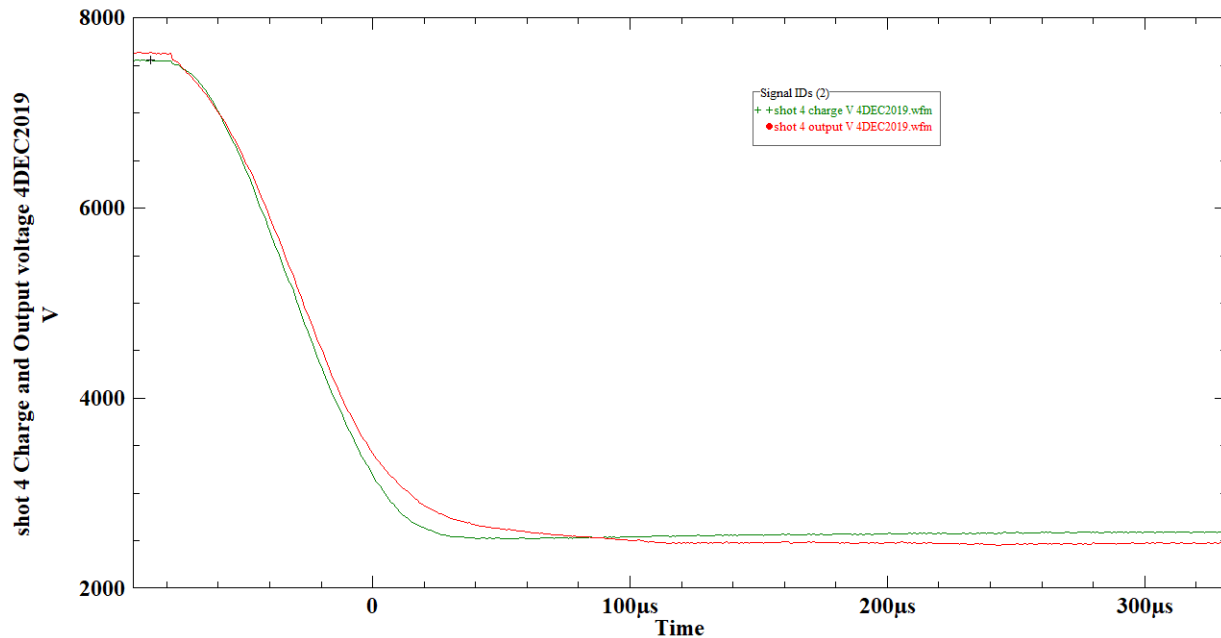


Figure 89. Shot 4: Charge and Output Voltage for Time of Trigger of EHF System

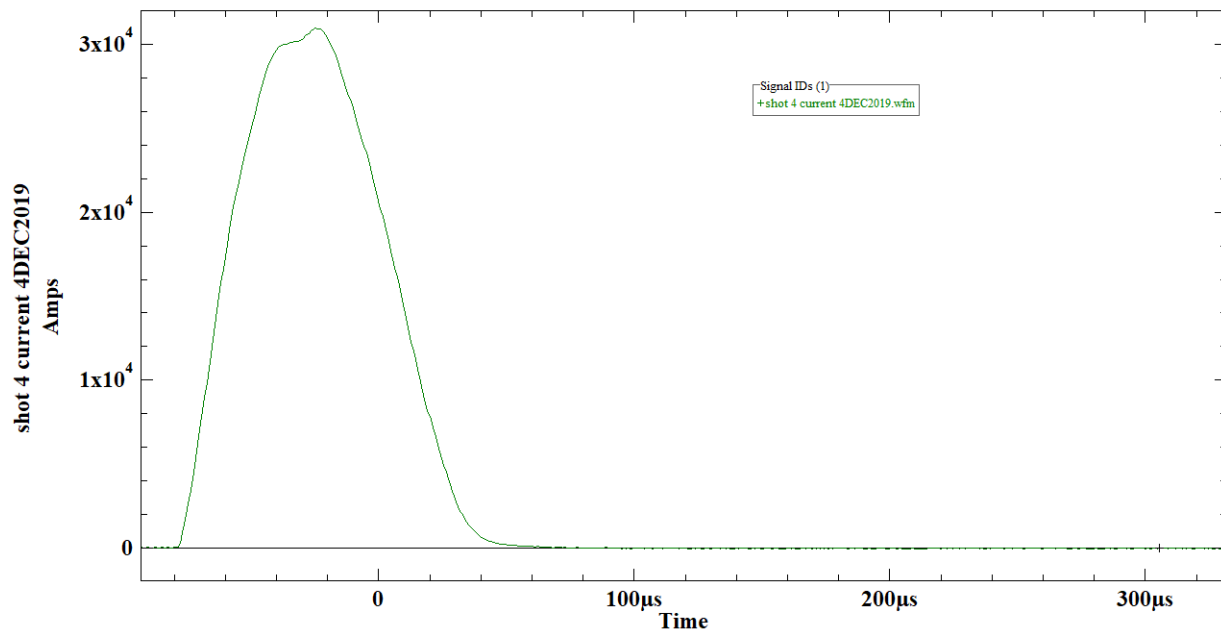


Figure 90. Shot 4: Current–Time Plot of Trigger from EHF System to Plasma Probe

Shot 4 successfully recreated the results of shot 2 with the same setup. The corner section of the test slab was fractured free from the larger test slab. The results of this test shot are shown in Figure 91 and Figure 92. A photo of the plasma blasting test probe is shown in Figure 93. No damage was noted to the probe other than some ablation of the probe tip. The probe was cleaned up and used again for shot 5.



Figure 91. Shot 4: Separated Corner of Test Slab; Repeats Shot 2 Result



Figure 92. Shot 4: Fracture Lines in Concrete Test Slab 1



Figure 93. Plasma Blasting Test Probe after Shot 4

Shot 5

Shot 5 was set up in concrete test slab 1 with the borehole located halfway in between the boreholes for shots 2 and 4. This was an attempt to separate off the remaining sliver of concrete in-between the sections separated in shots 2 and 4. The borehole and plasma blasting probe setup for shot 5 is shown in Figure 96. Test setup and results for shot 5 are in Table 11. Voltage and current traces collected by the Oscilloscope from the capacitor and output high voltage probes and output current probe are shown in Figure 94 and Figure 95.

Table 11. Data for Shot 5: Test Setup and Results

Shot 5	4-Dec-19
Plasma blasting probe	Probe 4: cleaned and reused
EHF pulse transmission line	Coaxial design
Number of weight plates installed on plasma blasting probe	2
Test concrete slab	Slab 1 with corner section missing after shot 2 and separated section from shot 4 still in place
Borehole location	Centered in line with boreholes for shots 2 and 4
Borehole depth (in)	7
Borehole diameter (in)	1
Water used in borehole?	Yes, bottled water, nothing added to the water
Setup precuts used for this shot	No
First test shot on this concrete slab?	No, test slab was used in shots 1, 2, and 4
Plasma blasting probe insertion depth (in)	6
Probe intact after shot	Yes
Charge voltage (VDC)	7600
EHF system capacitance (μF)	704
Charge energy (kJ)	20.3
Peak current (kA)	36.2
Notes	Separated off remaining section between sections removed by shots 2 and 4, but large crack split slab into two large sections

Shot 5 results are shown in Figure 97 through Figure 100. The chunk between the sections separated in shots 2 and 4 was successfully separated from the test slab. However, shot 5 also generated an additional crack into the test slab that fractured the remaining section of test slab into two large pieces. No damage noted to the probe other than some ablation of the probe tip. The probe was cleaned up and used again for shot 6.

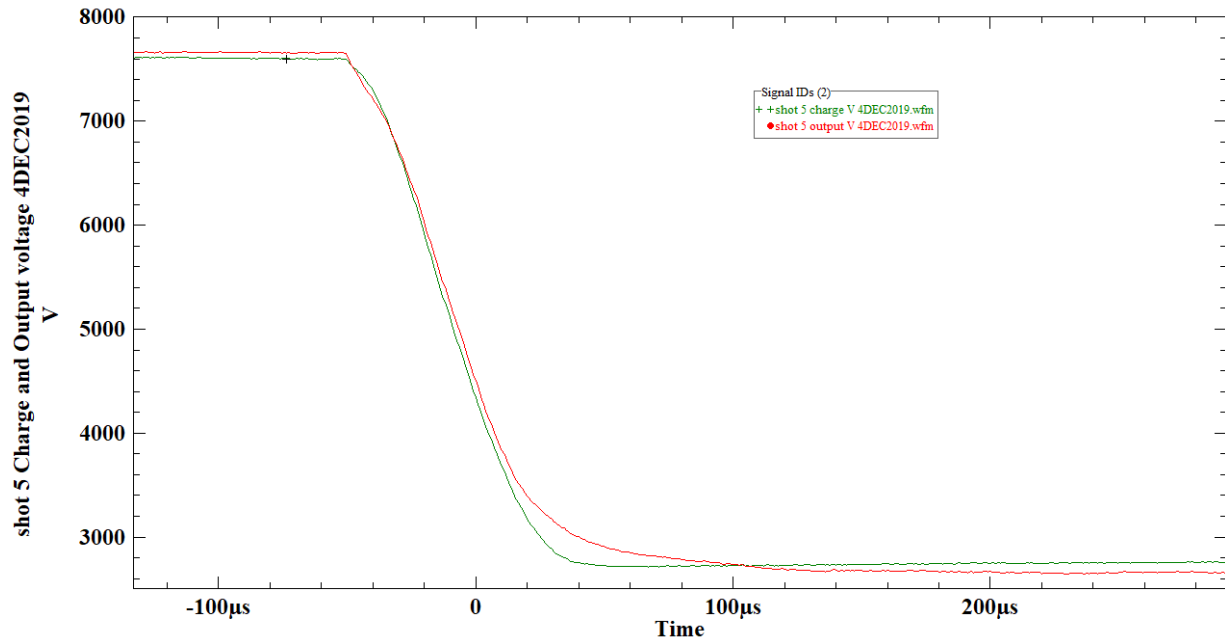


Figure 94. Shot 5: Charge and Output Voltage for Time of Trigger of the EHF System

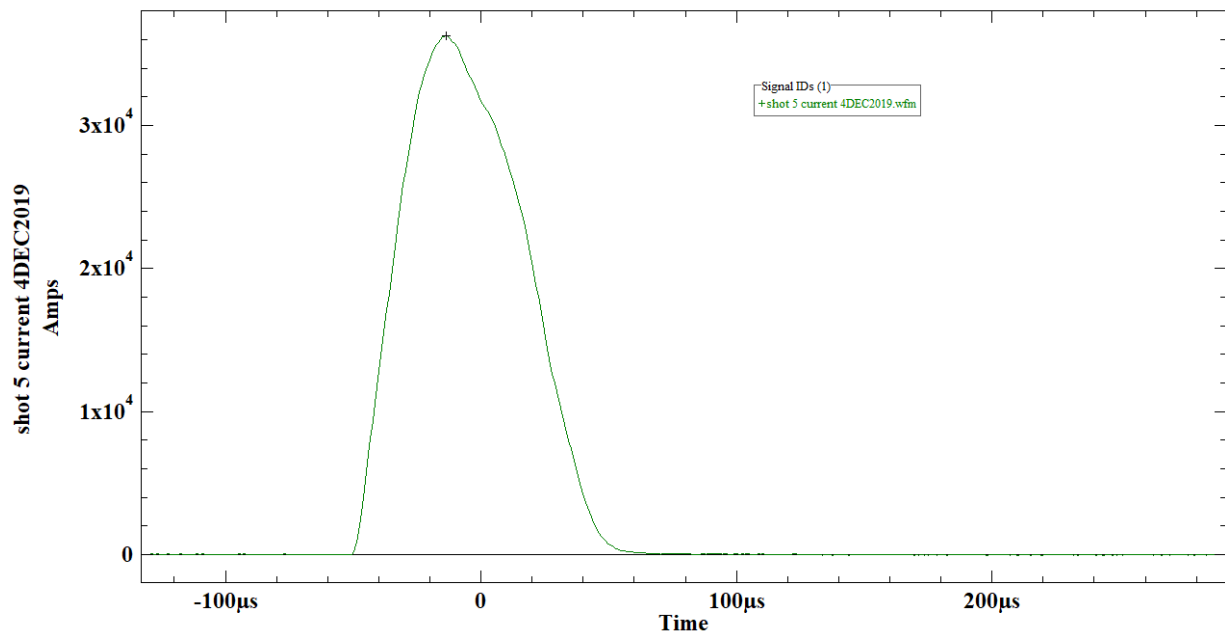


Figure 95. Shot 5: Time–Current Plot of Trigger from EHF System to Plasma Probe



Figure 96. Shot 5: Borehole for Plasma Blasting Probe Located between Shot 2 and 4 Boreholes

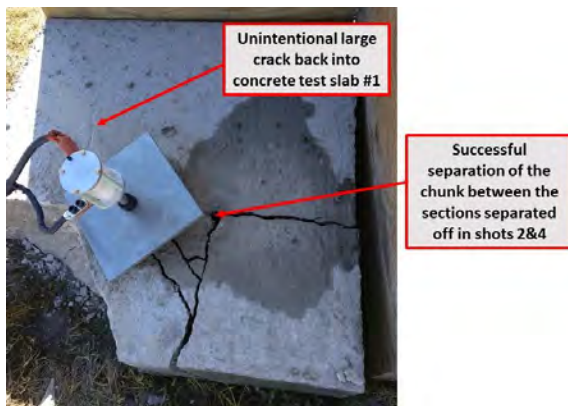


Figure 97. Shot 5: Sliver between Sections Separated from Test Slab by Shots 2 and 4



Figure 98. Shot 5: Remaining Section of Concrete Test Slab 1 after Debris Removal



Figure 99. Shot 5: Conical Section Separated below Borehole



Figure 100. Remaining Pieces of Test Slab 1 Shown with Fault Line up

Shot 6

The Plasma blasting probe was placed in a borehole drilled in the center of a new concrete slab 4 ft x 4 ft x 12 in thick (concrete test Slab 2). The borehole was 2 ft from all sides of the slab, hole depth was increased to 8 in, and the plasma blasting probe was inserted to 7 in. This placed the probe an inch deeper in the concrete but retains the 1-in water volume below the probe. Charge energy for this shot was double that used for shots 2–5. Figure 101 shows the borehole and plasma blasting probe setup for shot 6. Test setup and results for shot 6 are in Table 12. Voltage and current traces collected by the oscilloscope from the capacitor and output HV probes and output current probe are shown in Figure 102 and Figure 103.



Figure 101. Shot 6: Setup; Borehole Drilled in Center of 4-ft x 4-ft Concrete Test Slab 2

Table 12. Data for Shot 6: Test Setup and Results

Shot 6	4-Dec-19
Plasma blasting probe	Probe 4: cleaned and re-used
EHF pulse transmission line	Coaxial design
Number of weight plates installed on plasma blasting probe	2
Test concrete slab	Concrete test slab 2: 4 ft x 4 ft x 12 in thick
Borehole location	Placed in center of the, 2 ft from the edge on all sides.
Borehole depth (in)	8
Borehole diameter (in)	1
Water used in borehole	Yes, bottled water, nothing added to the water
Setup precuts used for this shot	No
First test shot on this concrete slab?	Yes
Plasma blasting probe insertion depth (in)	7
Probe intact after shot	Yes
Charge voltage (VDC)	10500
EHF system capacitance (μF)	704
Charge energy (kJ)	38.8
Peak current (kA)	75.4
Notes	Charge energy was double that used shots 2–5 to look at natural crack propagation from the shot

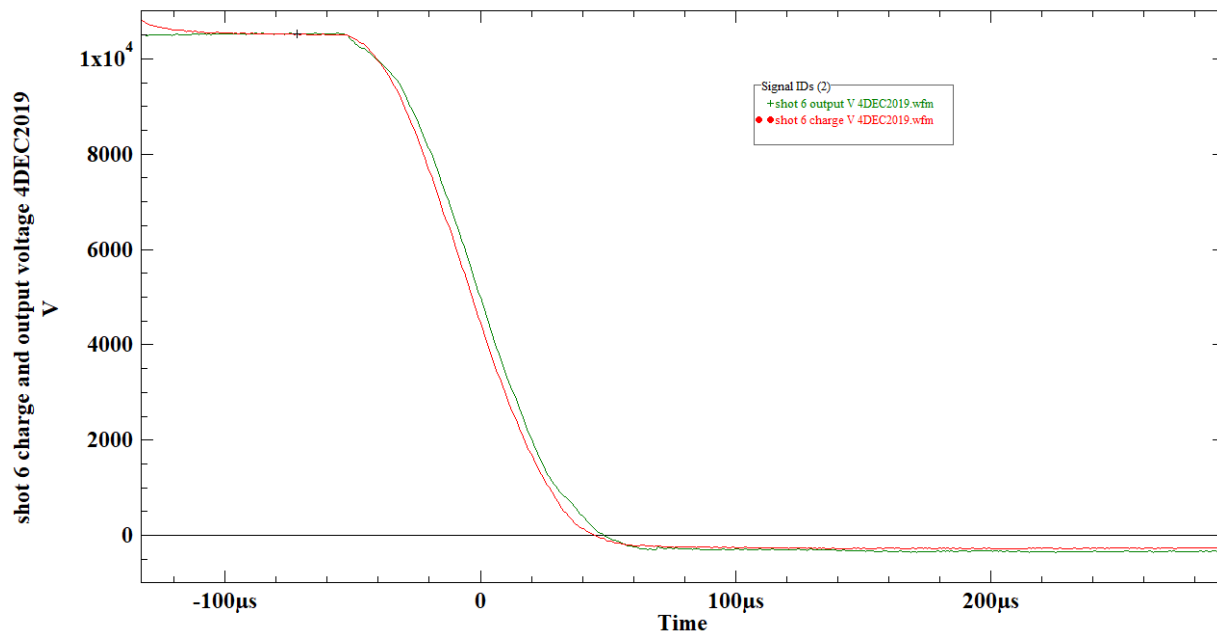


Figure 102. Shot 6: Charge and Output Voltage for Time of Trigger of the EHF System

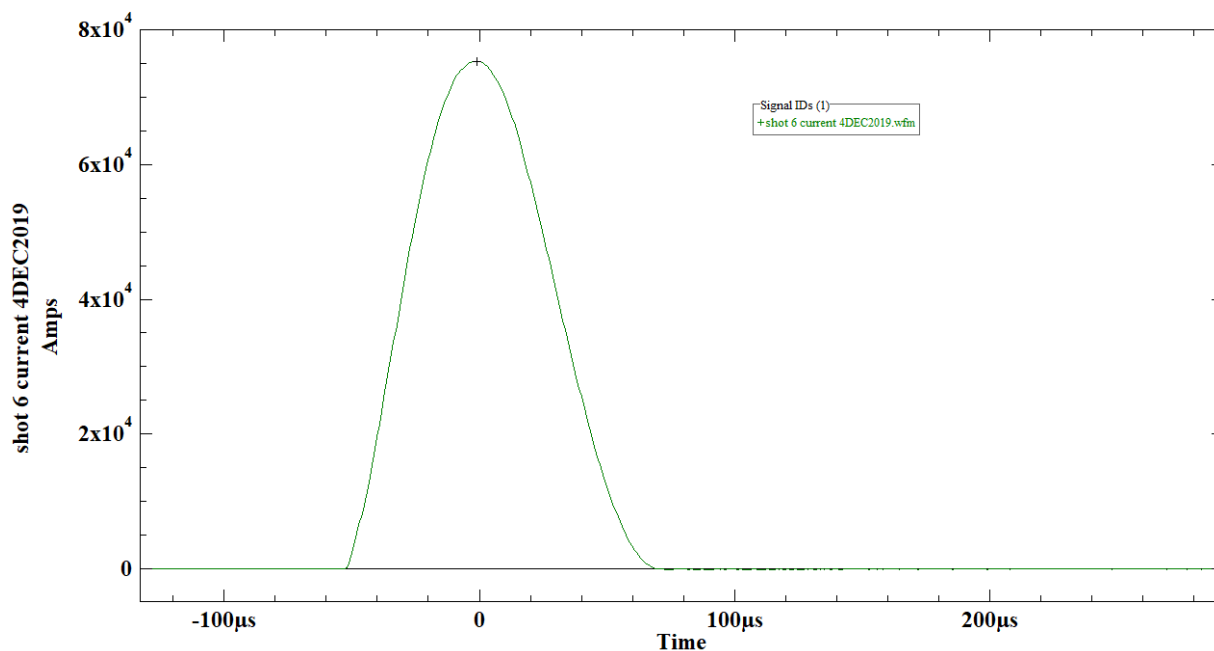


Figure 103. Shot 6: Time-Current Plot for Trigger from EHF System to Plasma Probe

Figure 104 shows the shot 6 result. Shot 6 had sufficient energy to crack the 4-ft by 4-ft test slab into three separate sections. Some of the energy in the shot was lost to spall cracking around the top of the borehole. A photo of the plasma blasting test probe after shot 6 is shown in Figure 105. No damage noted to the probe other than some ablation of the probe tip, even with doubling the energy of the prior shots (2–5). Probe was cleaned up and used again for shot 7.



Figure 104. Shot 6: Concrete Test Slab Cracked into Three Sections



Figure 105. Plasma Blasting Test Probe after Shot 6.

Shot 7

The plasma blasting probe was placed in a borehole drilled in the center of another new concrete test slab 4 ft x 4 ft x 12-in thick (concrete test slab 3) 2 ft from all sides of the slab. The concrete was pre-cut to a depth of 2 in with a diamond concrete saw. Pre-cuts ran along both diagonals from corner to corner and extended through the borehole. Pre-cuts are shown in Figure 106 and the plasma blasting probe placement in Figure 107. Charge energy for this shot was increased from 39 kJ used in shot 6 to 50 kJ. Test setup and results for shot 7 are shown in Table 13. Voltage and current traces collected by the oscilloscope from the capacitor and output HV probes and output current probe are shown in Figure 108 and Figure 109.

Results of shot 7 are shown in Figure 110 through Figure 115. Concrete test slab 3 separated along the pre-cut 2-in-deep diagonal lines. However, two additional crack lines did occur in the separated sections. This was clearly a successful demonstration of ability to separate concrete along pre-cut lines, but will require methodological refinement to prevent unintentional cracking along with the desired segment separation cracks. These additional cracks may have been due to using too much charge energy for the EHF system or it is possible that the pre-cut lines are too shallow to control the separation cracking completely. Both of these hypotheses were explored in subsequent shots.

No damage was noted to the probe from shot 7. It was cleaned up and used again for shot 8.

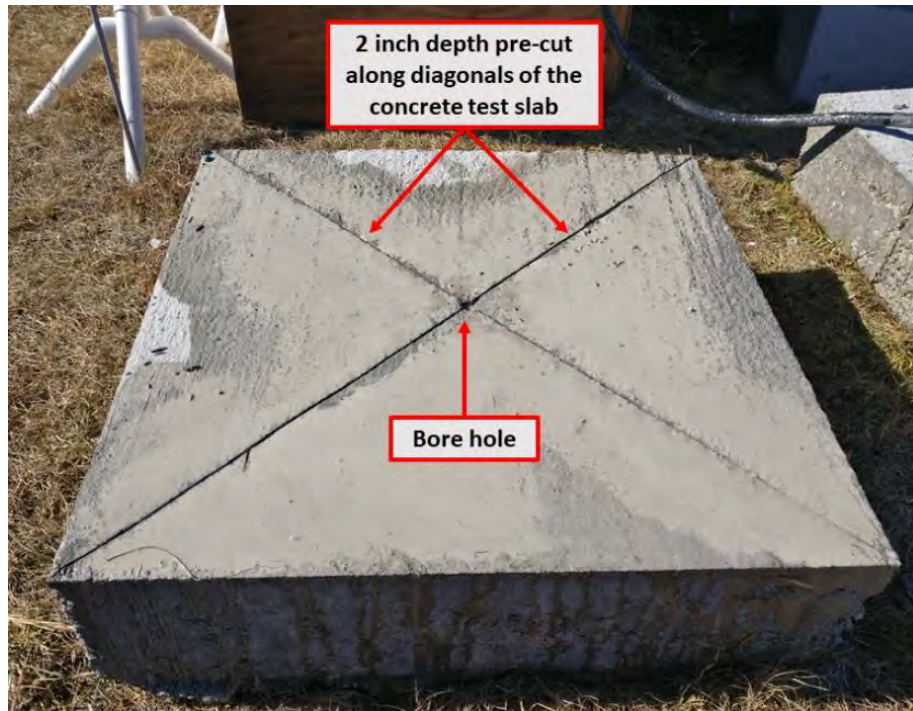


Figure 106. Shot 7: 2-in-deep Diagonal Pre-cuts in Concrete Test Section 3



Figure 107. Shot 7: Plasma Blasting Probe Set into Concrete Test Slab 3 with 2-in-deep Pre-cuts along the Diagonals

Table 13. Data for Shot 7: Test Setup and Results

Shot 7	4-Dec-19
Plasma blasting probe	Probe 4: cleaned and re-used
EHF pulse transmission line	Coaxial design
Number of weight plates installed on plasma blasting probe	2
Test concrete slab	Concrete slab 3: 4 ft x 4 ft x 12 in thick
Borehole location	In center of slab, 2 ft from the edge on all sides
Borehole depth (in)	8
Borehole diameter (in)	1
Water used in borehole?	Yes, bottled water, nothing added to the water
Setup precuts used for this shot	Yes, 2-in-deep diagonal pre-cuts across full surface of test slab, extending through borehole
First test shot on this concrete slab?	Yes
Plasma blasting probe insertion depth (in)	7
Probe intact after shot	Yes
Charge voltage (VDC)	12000
EHF system capacitance (μF)	704
Charge energy (kJ)	50.7
Peak current (kA)	80.0
Notes	First look at controlling crack propagation by pre-cutting slab with a diamond concrete saw, showed that cracking can be directed using this method, but test slab had additional cracks. Further testing will look at improving crack control.

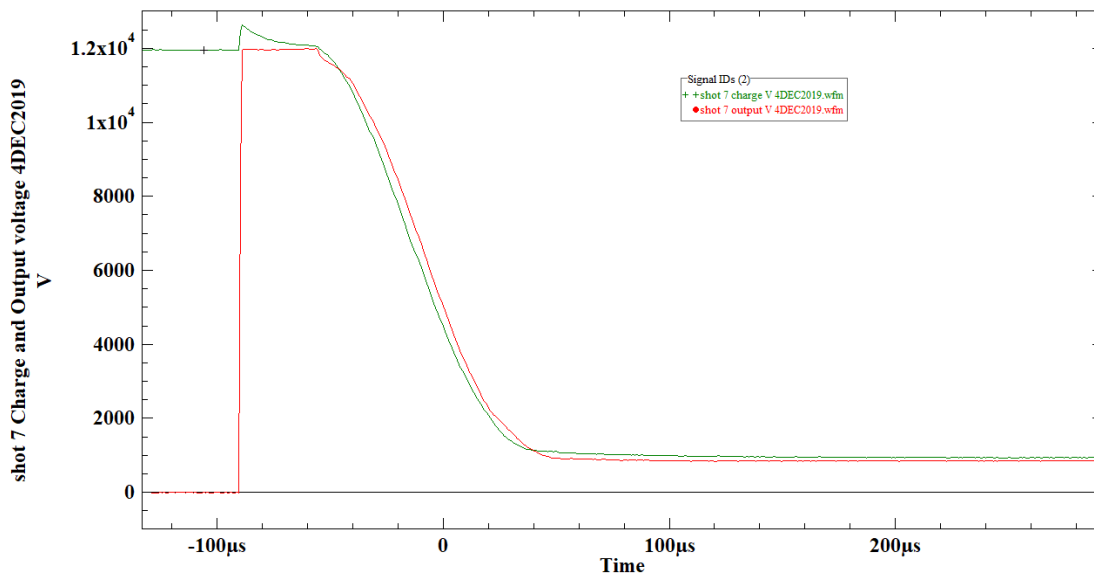


Figure 108. Shot 7: Charge and Output Voltage for Time of Trigger of the EHF System

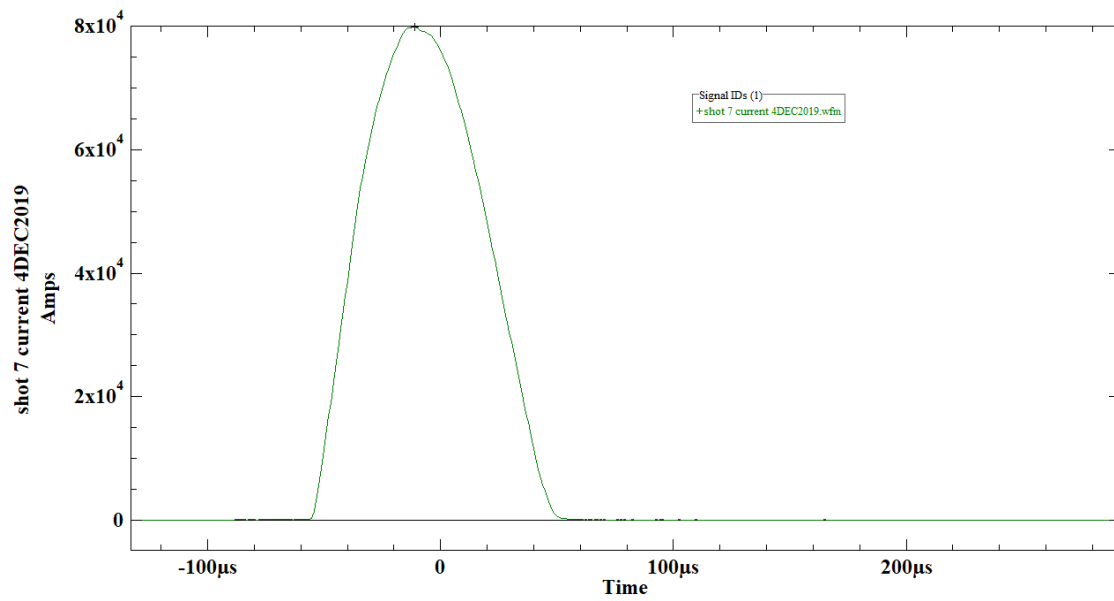


Figure 109. Shot 7: Time-Current Plot for Trigger from EHF System to Plasma Probe



Figure 110. Shot 7: Crack Separation along the Pre-cuts of Test Slab 3



Figure 111. Shot 7: Close-up of an Unintended Transverse Crack in Test Slab 3



Figure 112. Shot 7: Corner Crack along the 2-in-deep Pre-cut Lines in Test Slab 3



Figure 113. Shot 7: Test Concrete Slab 3 Section Separated by Shot along Pre-cut Lines



Figure 114. Shot 7: Crack Cross-section of Chunk Separated along Pre-cut Diagonal Lines



Figure 115. Shot 7: Unintended Cracks in Two Other Chunks Separated along Pre-cuts

Shot 8

Shot 8 attempted to section off a chunk 36 in by 36 in from 6-ft-wide by 12-ft-long concrete test slab 4. Two boreholes were drilled, One all the way through the 12-in-thick test slab at a point 36 in in from intersecting sides of the concrete test slab. Precuts 2-in deep were made from the edges of the test slab to the through hole. The plasma blasting probe was placed in the second, an 8-in-deep borehole in the center of the section to separate from the test concrete slab (18 in from the same edges (Figure 116). Charge energy for this shot was lowered to 39.6 kJ from the 50 kJ used in shot 7. Test setup and results for shot 8 are shown in Table 14. Voltage and current traces collected by the oscilloscope from the capacitor and output HV probes and output current probe are shown in Figure 117 and Figure 118.

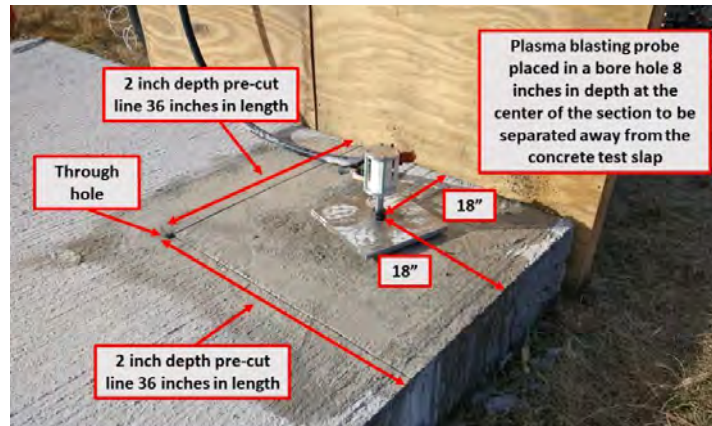


Figure 116. Shot 8: Placement of 2-in-deep Pre-cuts and Plasma Blasting Probe

Table 14. Data for Shot 8: Test Setup and Results

Shot 8	4-Dec-19
Plasma blasting probe	Probe 4: cleaned and re-used
EHF pulse transmission line	Coaxial design
Number of weight plates installed on plasma blasting probe	2
Test concrete slab	Concrete slab 4: 6 ft x 12 ft x 12 in thick
Borehole location	Placed 36 in in from two corner sides.
Borehole depth (in)	8
Borehole diameter (in)	1
Water in borehole?	Yes, bottled water, nothing added to the water
Setup precuts used for this shot	Yes, 2-in-deep intersecting pre-cuts intersecting edges of the concrete test slab sectioned off a 36-in by 36-in area of test. Through hole was drilled at the intersection of the pre-cuts.
First test shot on this concrete slab?	Yes
Plasma blasting probe insertion depth (in)	7
Probe intact after shot	Yes
Charge voltage (VDC)	10600
EHF system capacitance (μF)	704
Charge energy (kJ)	39.6
Peak current (kA)	53.2
Notes	2-in-deep pre-cuts to section off 36-in by 36-in area of concrete test slab with probe in center of the chunk to be cut off. Main cracks started at borehole containing probe, ran outward ignoring pre-cuts distant from plasma blasting probe site.

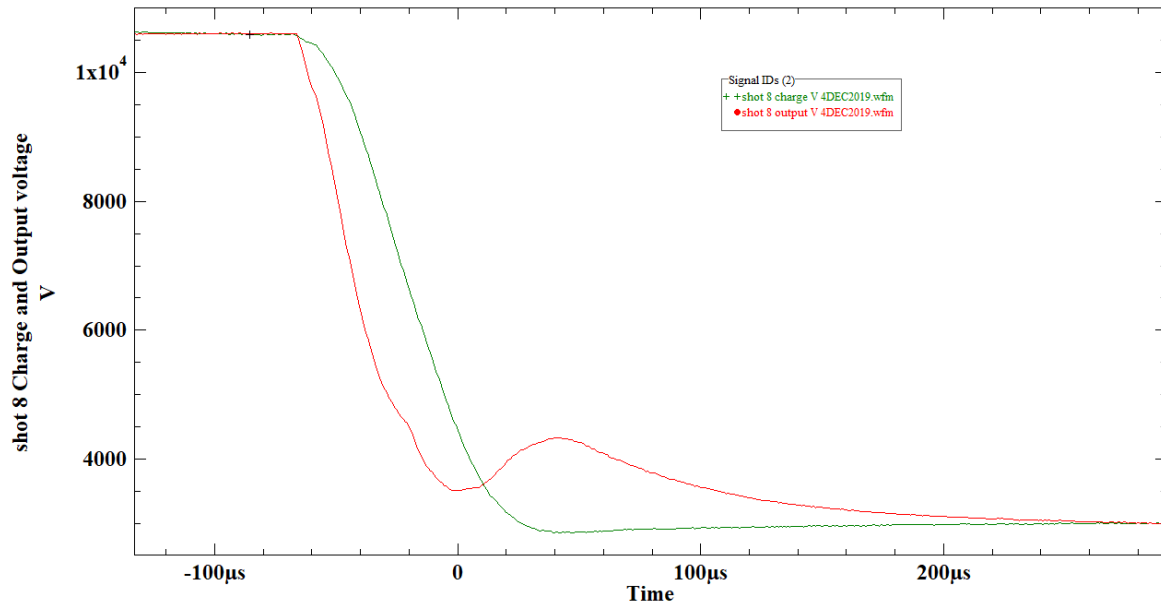


Figure 117. Shot 8: Charge and Output Voltage for Time of Trigger of EHF System

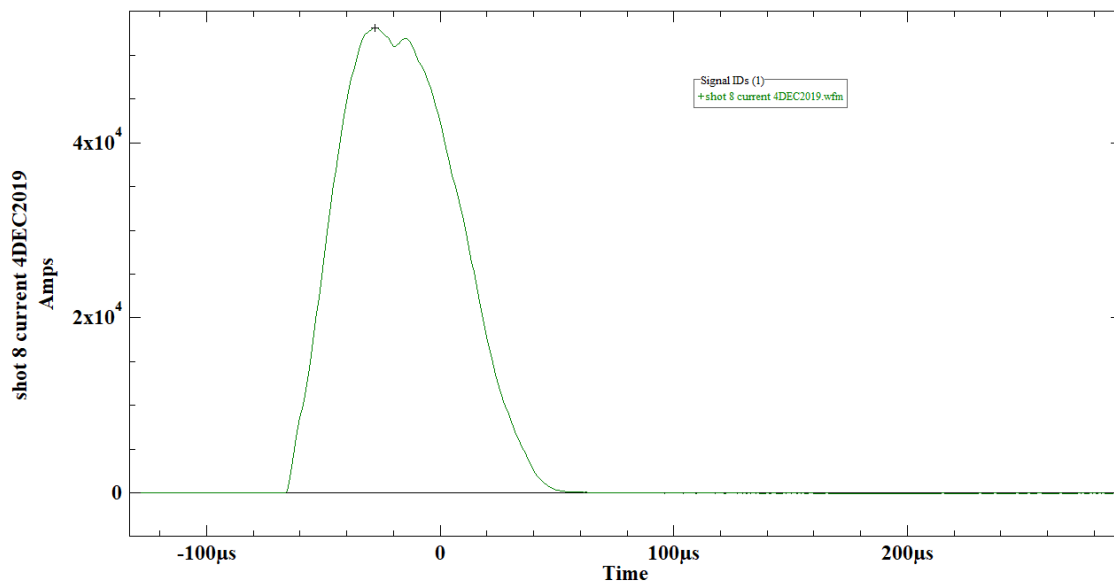


Figure 118. Shot 8: Time–Current Plot for Trigger from EHF System to Plasma Probe

Figure 119 and Figure 120 show results of shot 8. This setup failed to control the path of propagation by the cracks. Main cracks formed from this shot start at the borehole containing the probe and propagate outward, ignoring pre-cuts made at a distance from the plasma blasting probe location. Overall, this test reinforces that pre-cuts must start at and/or intersect the plasma blasting probe location to affect the crack propagation path. No damage noted to probe from shot 8. It was cleaned up and used again for shot 9.

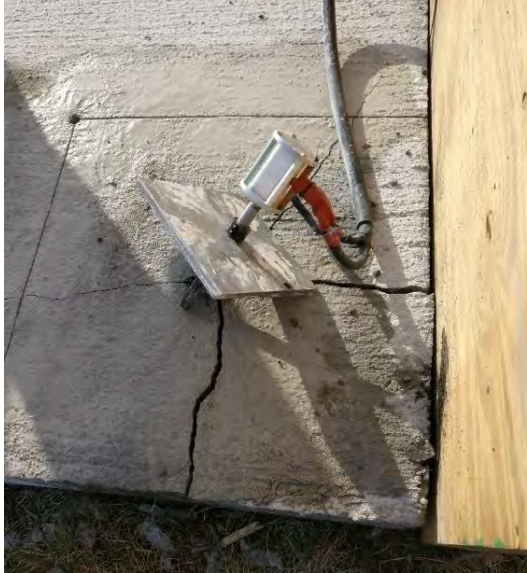


Figure 119. Shot 8: Central EHF Blast Location Setup and Pre-cuts Failed to Control Path of Crack Propagation



Figure 120. Shot 8: Crack Propagating Perpendicularly through Pre-cut Line

Shot 9

Shot 9 built upon the setup for shot 8. A 2-in-deep pre-cut was added to section off the end of the concrete test slab. The Plasma blasting probe was placed in the *through hole* drilled for shot 8 (completely through 12-in concrete slab to earth). Figure 121 shows pre-cuts and plasma blasting probe placement. Table 15 lists the test setup and results for shot 9. Voltage and current traces collected by the oscilloscope from the capacitor and output HV probes and output current probe are shown in Figure 122 and Figure 123.

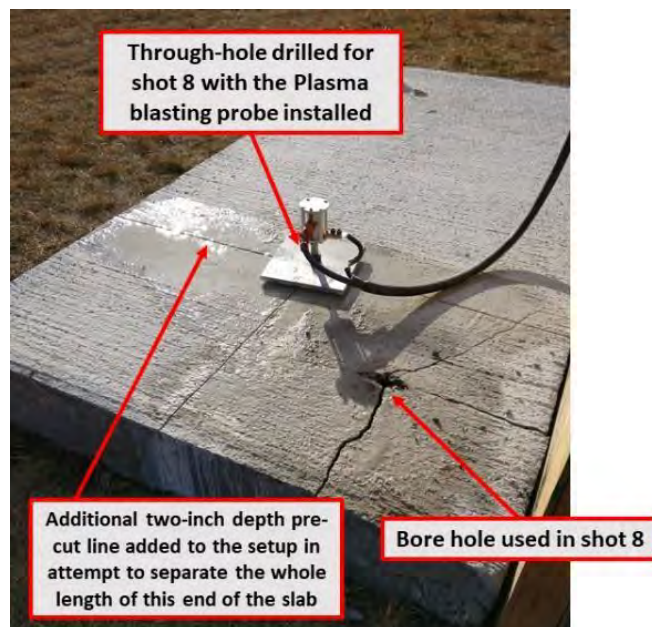


Figure 121. Shot 9: Setup Building on Shot 8 Setup

Table 15. Data for Shot 9: Test Setup and Results

Shot 9	4-Dec-19
Plasma blasting probe	Probe 4: cleaned and re-used
EHF pulse transmission line	Coaxial design
Number of weight plates installed on plasma blasting probe	2
Test concrete slab	Concrete slab 4: 6-ft x 12-ft x 12-in thick
Borehole location	Placed in the through hole from shot 9.
Borehole depth (in)	Borehole extends all the way through the slab
Borehole diameter (in)	1
Water used in borehole	Yes, bottled water, nothing added to the water
Setup precuts used for this shot	Yes, after shot 8, added 2-in-deep cut to section off end of concrete test slab.
First test shot on this concrete slab?	No, second shot on this concrete test slab
Plasma blasting probe insertion depth (inches)	7
Probe intact after shot	Yes
Charge voltage (VDC)	10500
EHF system capacitance (μF)	704
Charge energy (kJ)	38.8
Peak current (kA)	56.2
Notes	2-in-deep pre-cut added to shot 8 test setup, to section off end of concrete test slab. Plasma blasting probe in shot 8 through hole

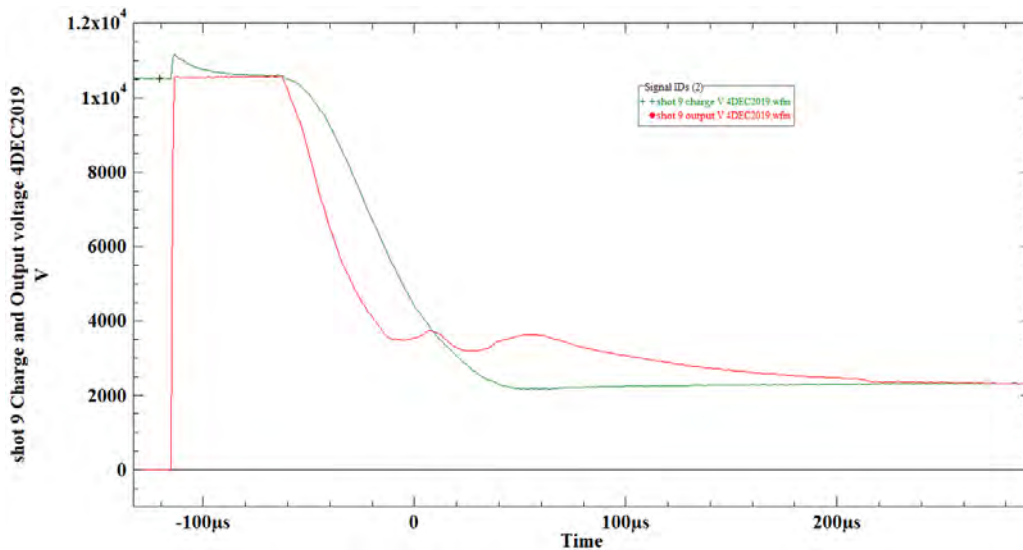


Figure 122. Shot 9: Charge and Output Voltage for Time of Trigger of EHF System

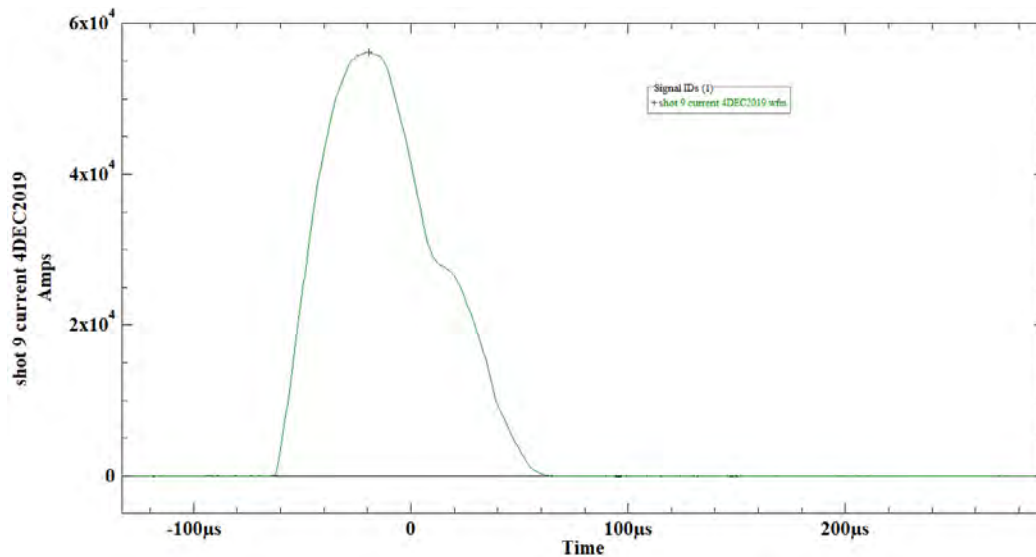


Figure 123. Shot 9: Time-Current Plot for Trigger from EHF System to Plasma Probe

Shot 9 had no observed effect on the concrete test slab. As the borehole used was drilled all the way through (from shot 8), the shot was not able to build up a pressure pulse and therefore no cracking visibly occurred in the concrete test slab. Figure 124 shows the plasma blasting test probe after shot 9. No damage is visible, but considerably more carbon deposited on the probe after shot 9 than other shots. The water may have leaked out of the borehole prior to triggering the EHF system, and the system “dry fired” in the borehole. This would account for the additional carbon the probe, which was cleaned up and used again for shot 10.



Figure 124. Plasma Blasting Test Probe after Shot 9

Shot 10

Starting with the test setup after shot 9, a new borehole was drilled in the center of the slab width (36 in in from either side) and 18 in in from the edge of the length of the slab along one of the 2-in-deep lines pre-cut for shot 8. Placement of the plasma blasting probe for shot 10 is shown in Figure 125. Table 16 summarizes test setup and results for shot 10. Voltage and current traces collected by the oscilloscope from the capacitor and output HV probes and output current probe appear in Figure 126 and Figure 127.



Figure 125. Shot 10: Setup Built on Shot 9 Setup.

Table 16 Data for Shot 10: Test Setup and Results

Shot 10	4-Dec-19
Plasma blasting probe used	Probe 4: cleaned and re-used
EHF pulse transmission line used	Coaxial design
Number of weight plates installed on the plasma blasting probe	2
Test concrete slab	Concrete slab 4: 6 foot x 12 foot x 12 inch thick
Borehole location	Centered in the slab width (36 in from each side), 18 in from end of the slab
Borehole depth (in)	8
Borehole diameter (in)	1
Water used in borehole	Yes, bottled water, nothing added to the water
Setup precuts used for this shot	Yes, this test used the existing setup from shot 9.
First test shot on this concrete slab?	No, third shot on this concrete test slab
Plasma blasting probe insertion depth (in)	7
Probe intact after shot	Yes
Charge voltage (VDC)	10500
EHF system capacitance (μF)	704
Charge energy (kJ)	38.8
Peak current (kA)	72.7
Notes	Borehole drilled in the center of shot 9 slab 18 in from the end along one of the 2-in-deep lines cut for shot 8. Cracks did not follow the pre-cut line intersecting the borehole.

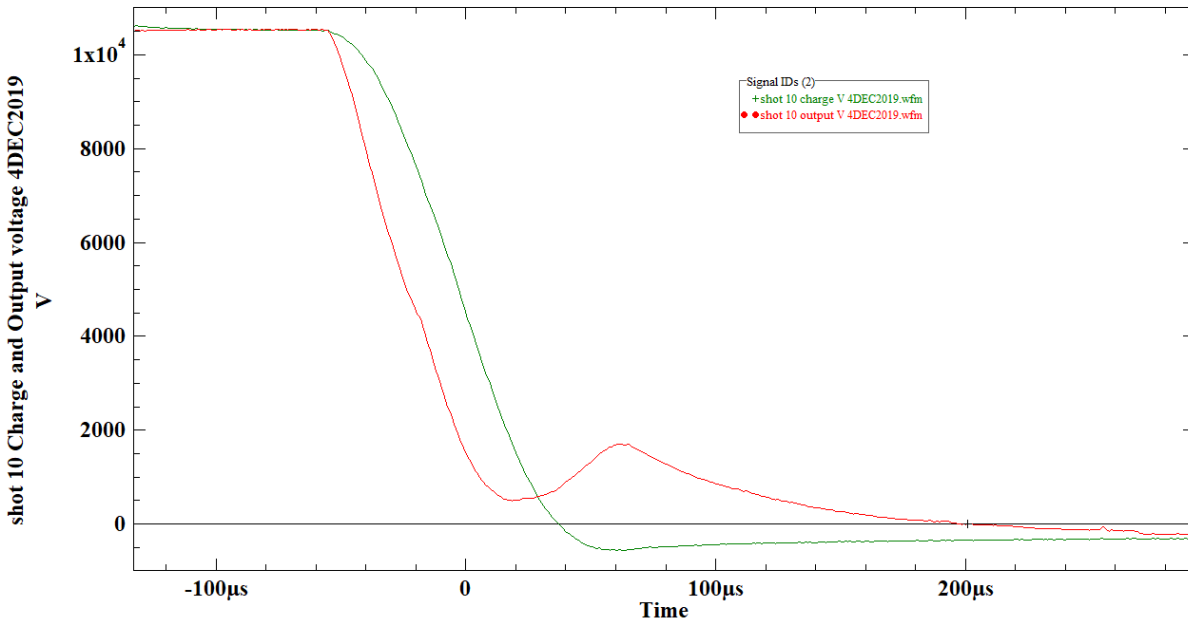


Figure 126. Shot 10: Charge and Output Voltage for Time of Trigger of EHF System

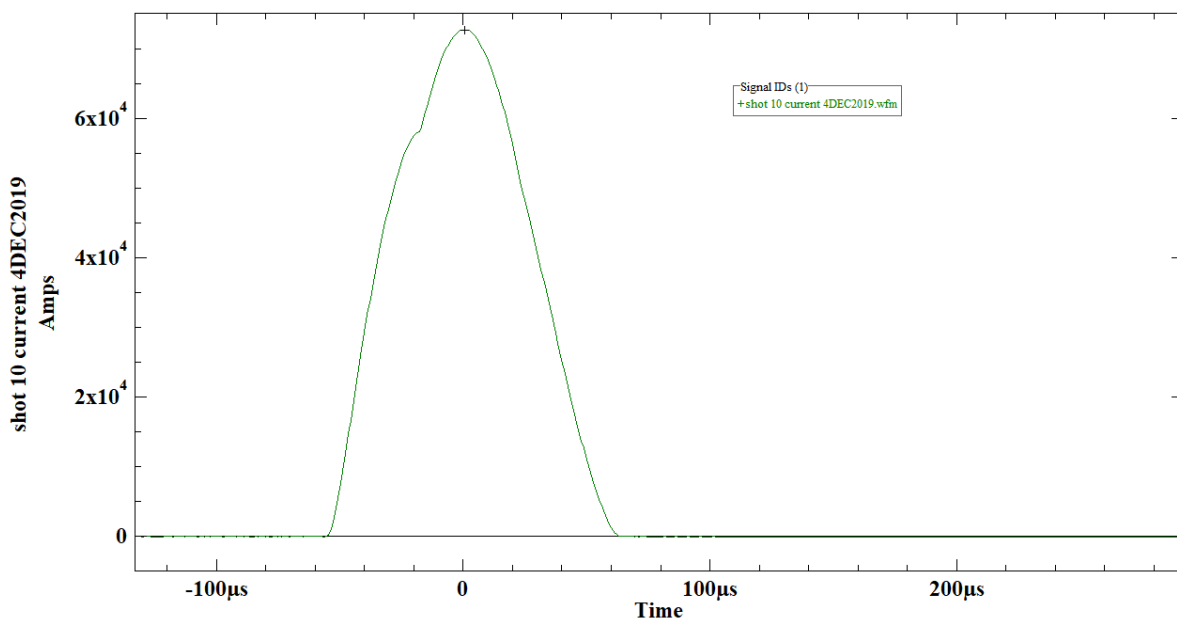


Figure 127. Shot 10: Time–Current Plot for Trigger from EHF System to Plasma Probe

Figure 128 shows the results of shot 10. Large cracks propagated across the width of the concrete test slab, but did not follow the 2-in-deep pre-cut lines. This was the third shot on this area of the concrete test slab and there was no available means in the field to know what unseen cracks had formed in the concrete during shots 8 and 9. Due to the likely buildup of damage to the concrete test slab over consecutive shots, no conclusions were drawn from this test shot. No damage to the probe was seen from shot 10. It was cleaned and used again for shot 11.



Figure 128. Shot 10: Large Cracks Did Not Follow Pre-cut Lines.

Shot 11

This test shot was intended to break up and remove the concrete test slab used for shots 8,9, and 10. Charge energy was increased significantly, to 87.6 kJ, to observe the effect of using a higher-energy pulse. Placement of the plasma blasting probe for shot 11 is shown in Figure 129. Table 17 describes the test setup and results for shot 11. Voltage and current traces collected by the oscilloscope from the capacitor and output HV probes and output current probe are presented in Figure 130 and Figure 131.



Figure 129. Shot 11: Placement of Plasma Blasting Probe in Borehole

Table 17. Data for Shot 11: Test Setup and Results

Shot 11	4-Dec-19
Plasma blasting probe	Probe 4: cleaned and re-used
EHF pulse transmission line	Coaxial design
Number of weight plates installed on plasma blasting probe	2
Test concrete slab	Concrete slab 4: Initially 6 ft x 12 ft x 12 in
Borehole location	Centered 18 in from edge of the slab on shot 9 pre-cut line
Borehole depth (in)	8
Borehole diameter (in)	1
Water used in borehole	Yes, bottled water, nothing added to the water
Setup precuts used for this shot?	Yes, this test used the existing setup from shot 9.
First test shot on this concrete slab?	No, fourth shot on this concrete test slab.
Plasma blasting probe insertion depth (in)	7
Probe intact after shot	Yes
Charge voltage (VDC)	15775
EHF system capacitance (μF)	704
Charge energy (kJ)	87.6
Peak current (kA)	132.0
Notes	Mainly to break up and remove concrete test slab used for shots 8,9, and 10. Charge energy increased to observe effect

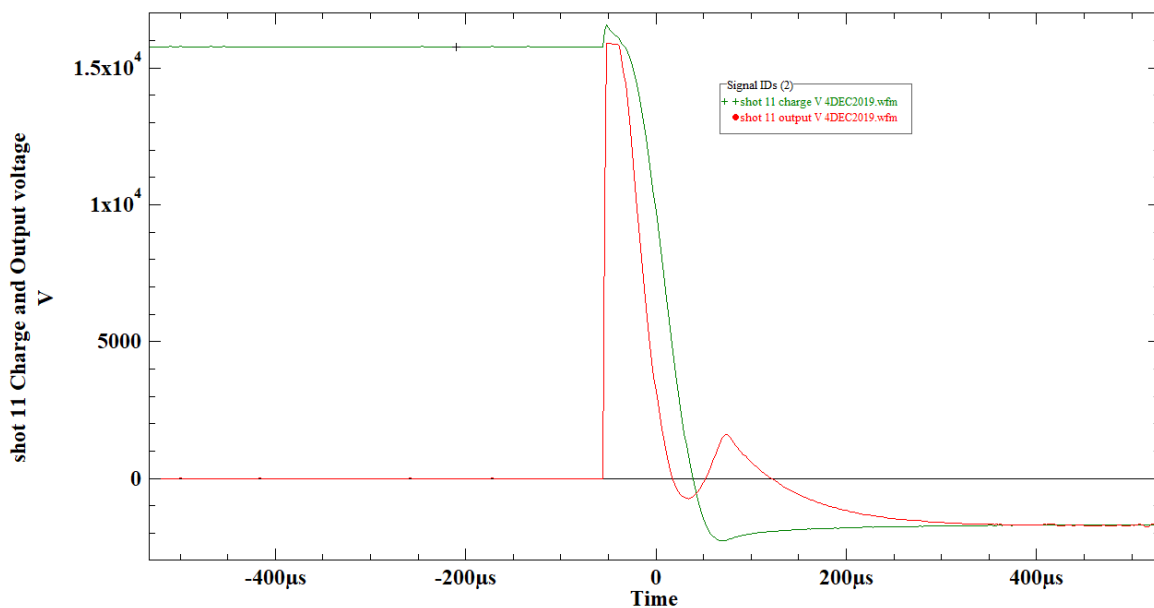


Figure 130. Shot 11: Charge and Output Voltage for Time of Trigger of EHF System

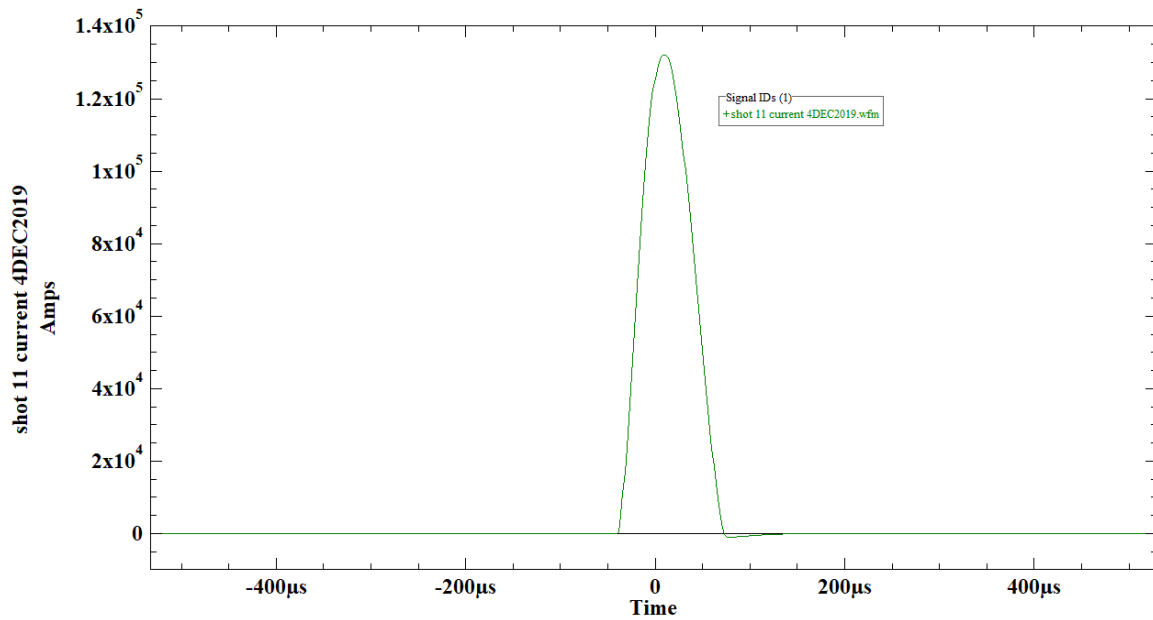


Figure 131. Shot 11: Time-Current Plot for Trigger from EHF System to Plasma Probe

Figure 132 shows cracks and chunk separation from the concrete test slab resulting from shot 11. Crack propagation from this shot was a mixture of new crack lines and some crack following pre-cut lines. After shot 11, the separated concrete chunks that resulted from the combination of shots 8 through 11 were removed from the end of the concrete test slab. The resultant edge shown in Figure 133 is what remains of one end of test slab 4 after removal of the larger separated chunks. Figure 134 shows probe 4 after shot 11. Signs of wear are evident but the probe is still useable. It was cleaned up and used again for shot 13.



Figure 132. Shot 11: Cracks and Chunk Separation from Concrete Test Slab



Figure 133. Shot 11: Slab after Removal of Large Concrete Chunks Separated by Shots 8–11



Figure 134. Shot 11: Probe 4 Shows Signs of Wear, but Is Still Useable

Shot 12

This test was conducted to see if an exploding wire could be used to fracture the concrete test slab. For this test setup a 2-in-deep pre-cut was made the length of the test slab as shown in

Figure 136. The two leads of the EHF coaxial pulse transmission line that normally connect to the plasma blasting probe were connected to the length of copper wire as shown in Figure 135. The wire was pressed down to the bottom of the pre-cut in the center of the slab as shown in Figure 137. When the current pulse was transmitted to the thin wire, it vaporized the wire and create a plasma and a pressure pulse.



Figure 136. Shot 12: 2-in-deep Pre-cut Line for Exploding Wire Test

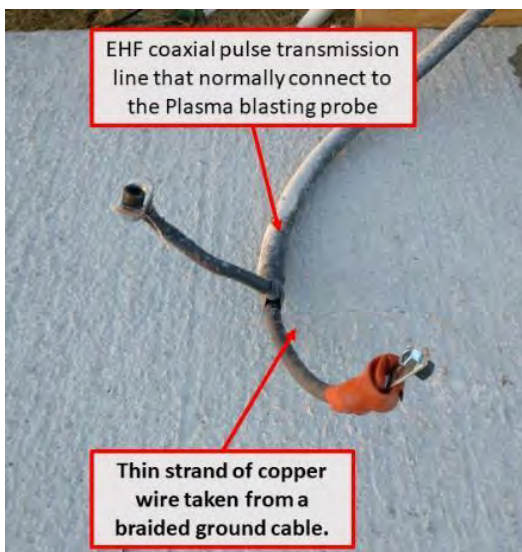


Figure 135. Copper Wire Connected across Terminals of EHF Coaxial Pulse Transmission Line to EHF Main HV System

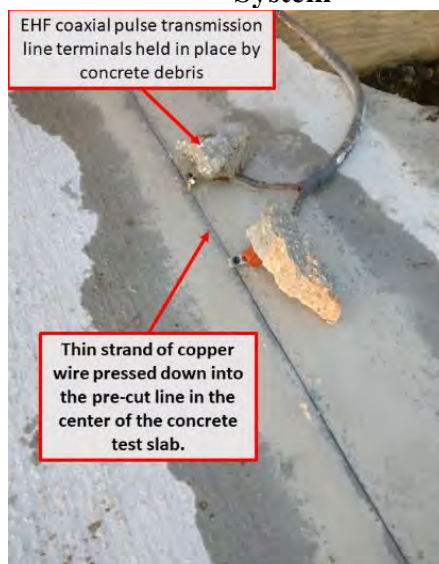


Figure 137. Shot 12: Copper Wire in Slit Line for Exploding Wire Test

Table 18 lists test setup and results for shot 12. Voltage and current traces collected by the oscilloscope from the capacitor and output HV probes and output current probe are shown in Figure 135 and Figure 137.

Table 18. Data for Shot 12: Test Setup and Results

Shot 12	4-Dec-19
Plasma blasting probe	Exploding wire test (cooper wire used)
EHF pulse transmission line	Coaxial design
Number of weight plates installed on plasma blasting probe	2
Test concrete slab	Concrete slab 4: Initially 6 ft x 12 ft x 12 in thick
Borehole location	N/A; exploding wire inserted into slit cut into concrete slab
Borehole depth (in)	N/A
Borehole diameter (in)	N/A
Water used in borehole	N/A
Setup precuts used for this shot?	2-in-deep slit across full 6-ft length of the concrete test slab.
First test shot on this concrete slab?	No, this is the fifth shot on this concrete test slab.
Plasma blasting probe insertion depth (in)	N/A
Probe intact after shot	Yes
Charge voltage (VDC)	15060
EHF system capacitance (μF)	704
Charge energy (kJ)	79.8
Peak current (kA)	76.4
Notes	Test to see if an exploding wire could fracture concrete test slab. Wire pressed to bottom of pre-cut slit 2-in deep down center of length of test slab. Leads of the EHF coaxial pulse transmission line connected to the length of copper wire. Exploding wire had no appreciable effect on concrete test slab blasted out a shallow divot along the section of pre-cut line that contained the wire.

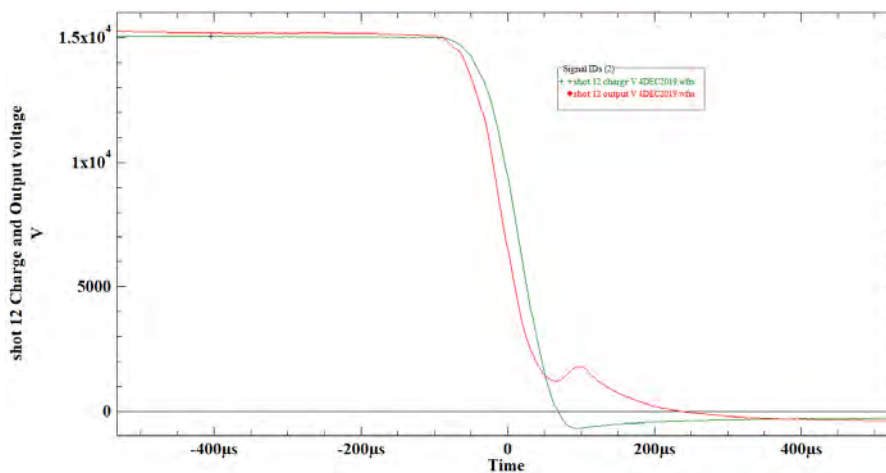


Figure 138. Shot 12: Charge and Output Voltage for Time of Trigger of EHF System

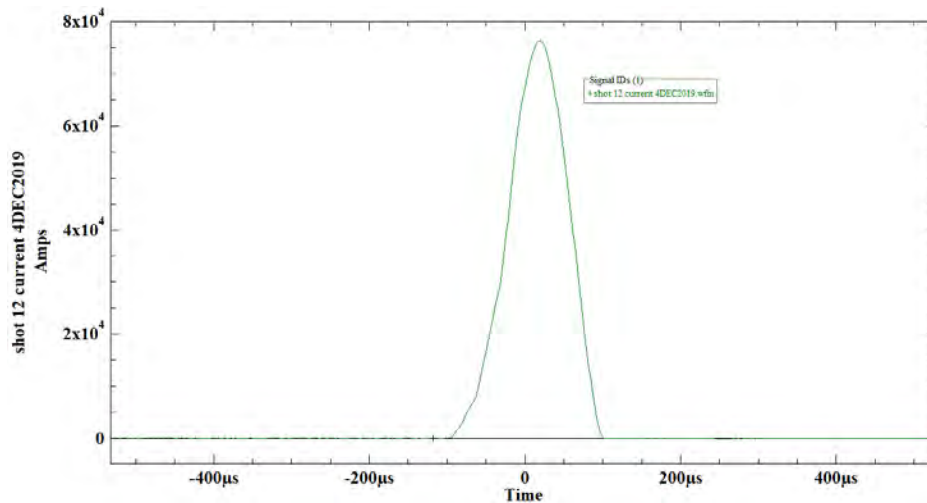


Figure 139. Shot 12: Time-Current Plot for Trigger from EHF System to Plasma Probe

Figure 140 shows results of shot 12 exploding wire test. The exploding wire had no appreciable effect on the concrete test slab other than blasting out a shallow divot in the section of pre-cut line that contained the wire. The exploding wire test created a significant pressure spike that could be physically felt moving through the air roughly 100 ft away from the test setup. The wire possibly failed to crack the concrete because the pressure pulse created was not contained and could escape out the top of the cut in the concrete that contained it. This concept for cracking concrete could have potential, but due to time constraints, it was not pursued in detail. Shot 18 was an additional unsuccessful attempt of the exploding wire method, discussed later in this report



Figure 140. Shot 12: Exploding Wire Blasted out Shallow Divot along Wire in Pre-cut Line

Shot 13

Shot 13 used a deeper (~4.5 in) pre-cut line in a 36-in by 36-in section of concrete test slab 4. The borehole was placed at the intersection of the pre-cut lines. The pre-cut lines terminated close to, but not touching the borehole as shown in Figure 141. Figure 142 shows the test setup for shot 13. The charge energy of shot 13 was 39.6 kV, as higher energies were shown in previous shots to cause unintentional cracks in the concrete in areas away from pre-cut lines.

Table 19 displays test setup and results for shot 13. Voltage and current traces collected by the oscilloscope from the capacitor and output HV probes and output current probe are shown in Figure 143 and Figure 144.



Figure 141. Shot 13: Pre-cut Lines End Close to (~0.5 in), but Do Not Connect to Borehole

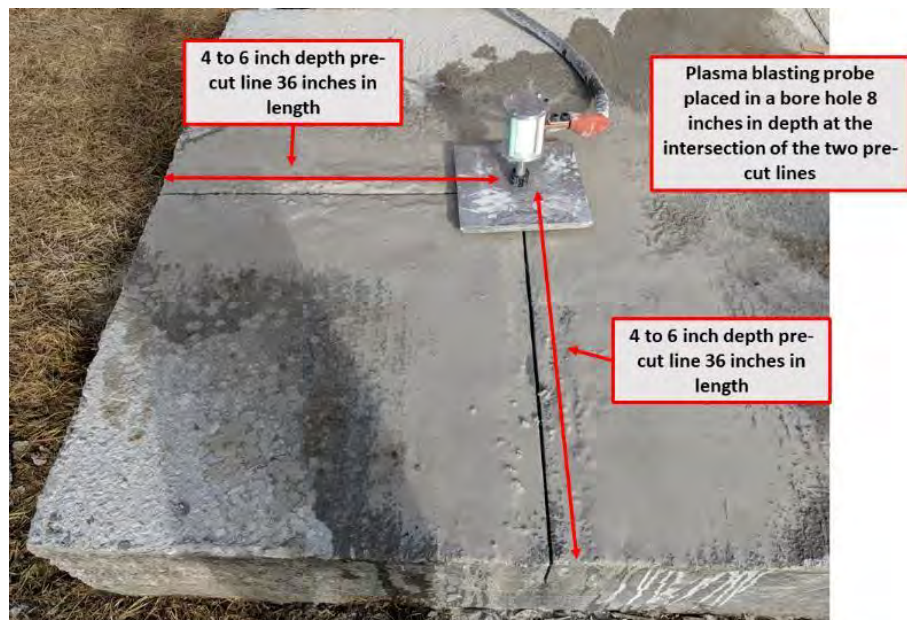


Figure 142. Shot 13: Plasma Blasting Probe Borehole at Intersection of Pre-cut Lines

Table 19. Data for Shot 13: Test Setup and Results

Shot 13	5-Dec-19
Plasma blasting probe	Probe 4: cleaned and re-used
EHF pulse transmission line	Coaxial design
Number of weight plates installed on the plasma blasting probe	2
Test concrete slab	Concrete slab 4: Initially 6 ft x 12 ft x 12 in thick
Borehole location	36 in from edges of slab at intersection of pre-cut lines.
Borehole depth (in)	8
Borehole diameter (in)	1
Water used in borehole?	Yes, bottled water, nothing added to the water
Setup precuts used for this shot	Yes, Pre-cut lines were ~4.5 in deep, ended ~0.5 in from borehole, 36 in from end and side of 4 concrete test slab
First test shot on this concrete slab?	No, fifth shot on this concrete test slab.
Plasma blasting probe insertion depth (in)	7
Probe intact after shot	Yes
Charge voltage (VDC)	10610
EHF system capacitance (μF)	704
Charge energy (kJ)	39.6
Peak current (kA)	69.4
Notes	Used deeper (4~6 in) pre-cut line to separate 36-in by 36-in section of concrete from the slab. Charge energy of shot down to 39.6 kJ to limit unintentional cracks away from pre-cut lines. Sectioned off 36-in by 36-in section but small unintentional crack formed away from pre-cut section.

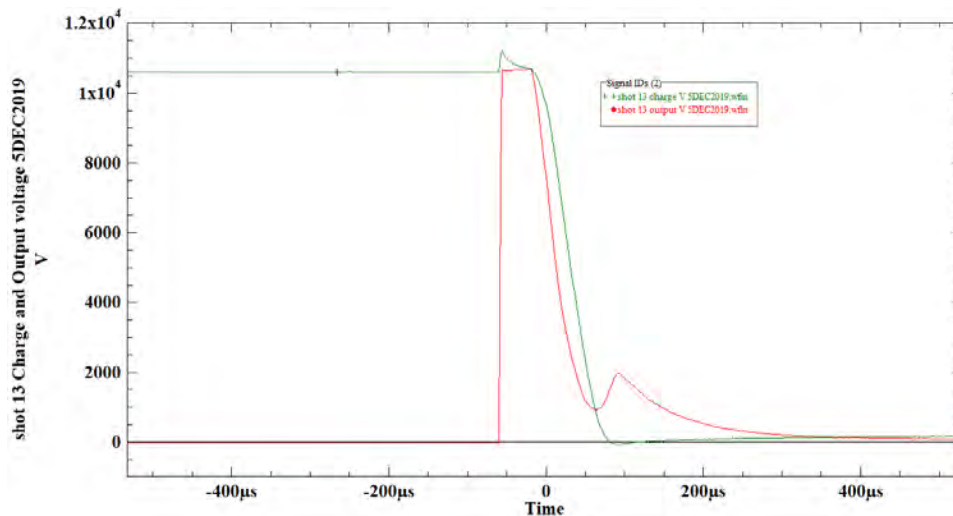


Figure 143. Shot 13: Charge and Output Voltage for Time of Trigger of EHF System

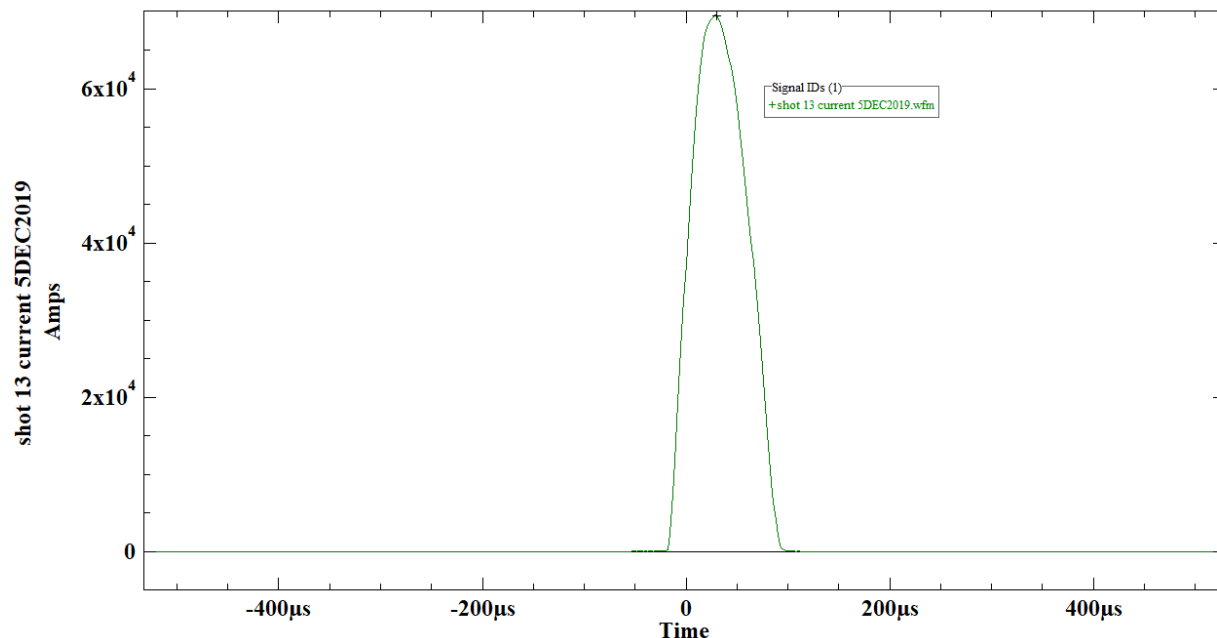


Figure 144. Shot 13: Time-Current Plot for Trigger from EHF System to Plasma Probe

Shot 13 proved very successful at sectioning off a chunk of concrete bounded by the deeper pre-cut lines (Figure 145 through Figure 148). The 36-in by 36-in section of concrete separated off along the pre-cut lines. However, an unintentional crack did form in the test slab and propagated away from the intended separation section. The results of this shot prove that a section of concrete can be separated off using the EHF system in conjunction with pre-cuts of sufficient cut depth. However, future experiments should look at improving the methodology to prevent unintentional cracking in the section of concrete to be retained.

After shot 13 probe 4 showed signs of wear, but was cleaned up and used again for shot 14.



Figure 145. Shot 13: Cracked along Both Pre-cut Lines on 4 Concrete Test Slab



Figure 146. Shot 13: Fracture Lines from Borehole to Edge of Concrete Test Slab



Figure 147. Shot 13: Separated Section of Concrete with Crack



Figure 148. Shot 13: Unintentional Crack from Borehole into Concrete Test Slab

Shot 14

A borehole was drilled at the center of the 36-in by 36-in section separated from 4 concrete test slab in shot 13. The test setup for shot 14 is shown in Figure 149. The goal of this shot was to break-up the section separated in shot 13 into smaller, more manageable chunks. A higher charge energy of 87.9 kJ was used for this shot to get more fragmentation of the concrete section. Test setup and results for shot 14 are shown in Figure 149 and Table 20. Voltage and current traces collected by the oscilloscope from the capacitor and output HV probes and output current probe are shown in Figure 150 and Figure 151.



Figure 149. Shot 14: Plasma Blasting Probe in Concrete Section Separated by Shot 13

Table 20. Data for Shot 14: Test Setup and Results

Shot 14	5-Dec-19
Plasma blasting probe	Probe 4: cleaned and re-used
EHF pulse transmission line	Coaxial design
Number of weight plates installed on the plasma blasting probe	2
Test concrete slab	36-in by 36-in piece shot 13 separated off 4 concrete test slab
Borehole location	Borehole drilled at the center of the 36-in by 36-in section separated from 4 concrete test slab in shot 13
Borehole depth (in)	8
Borehole diameter (in)	1
Water used in borehole	Yes, bottled water, nothing added to the water
Setup precuts used for this shot	No pre-cuts; goal is to break section separated by shot 13 into smaller, more manageable chunks
First test shot on this concrete slab?	No, breaking up a chunk of concrete separated off on shot 13.
Plasma blasting probe insertion depth (in)	7
Probe intact after shot	Yes
Charge voltage (VDC)	15800
EHF system capacitance (μF)	704
Charge energy (kJ)	87.9
Peak current (kA)	130.1
Notes	Goal is to fragment 36-in by 36-in section separated by shot 13 into smaller more manageable chunks. A higher charge energy of 87.9 kJ successfully broke up the separated section into several more manageable chunks of concrete.

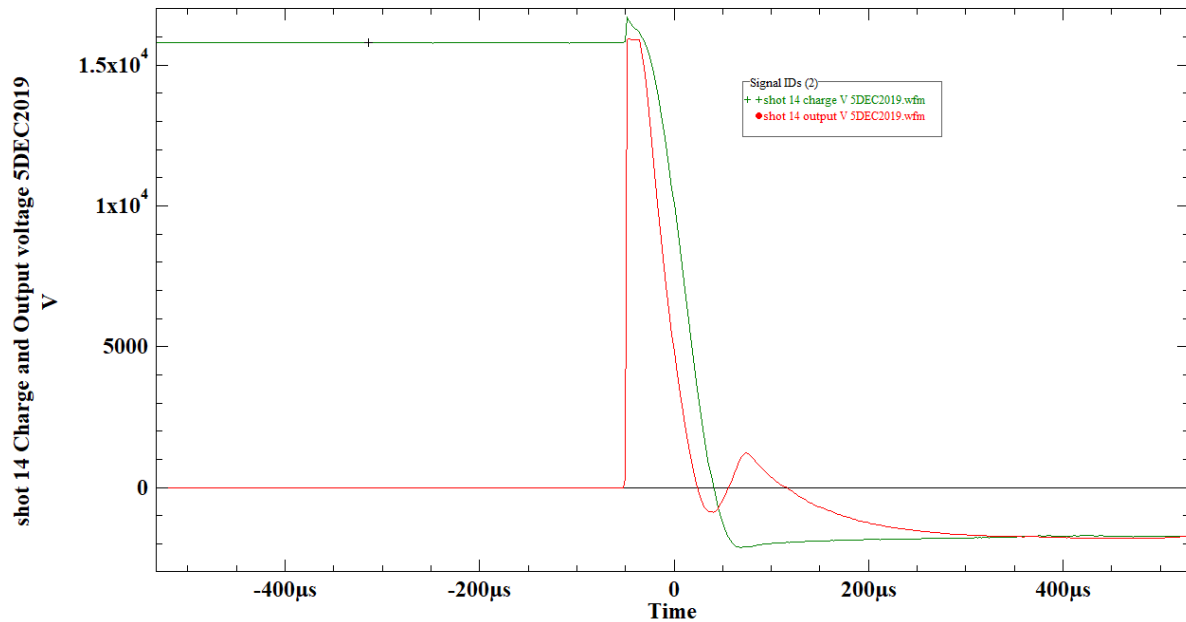


Figure 150. Shot 14: Charge and Output Voltage for Time of Trigger of the EHF System

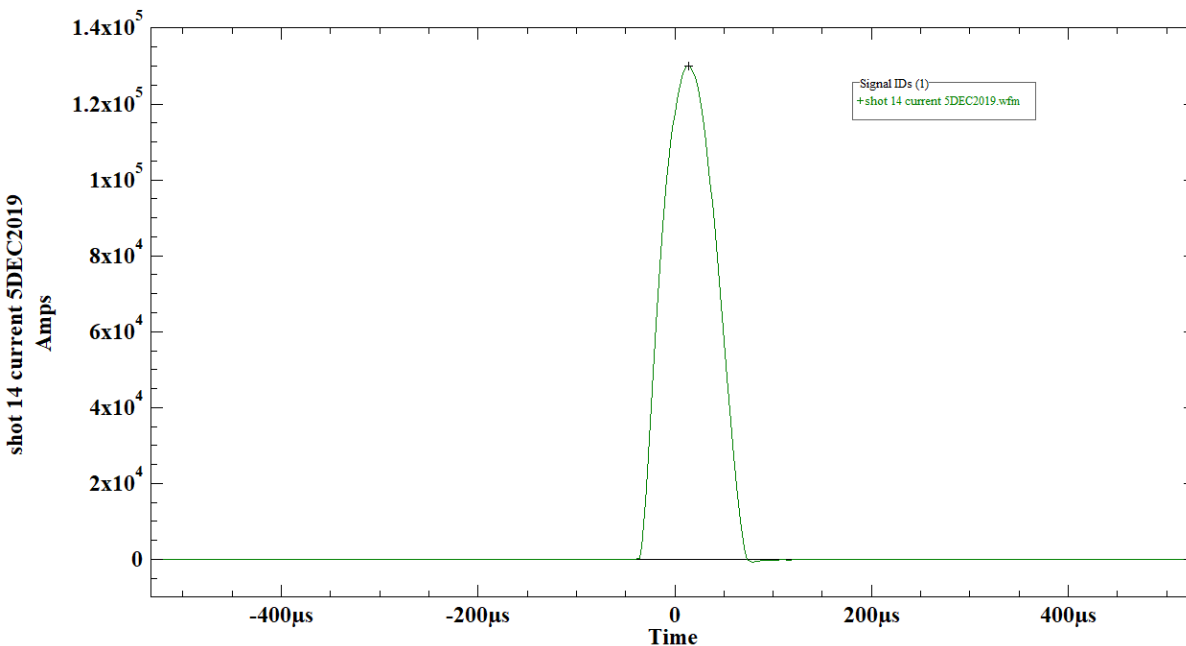


Figure 151. Shot 14: Time–Current Plot for Trigger from EHF System to Plasma Probe

Shot 14 successfully broke the 36-in by 36-in separated concrete section from shot 13 into smaller, more manageable chunks. High charge energy is more useful for this application as it caused further fragmentation. Figure 152 and Figure 153 show results of shot 14. After shot 14 Probe 4 showed signs of wear, but was still useable. It was cleaned up and used again for shot 15.



Figure 152. Shot 14: Debris And Concrete Chunks from Separated Concrete Section



Figure 153. Shot 14: Debris And Concrete Chunks from Separated Concrete Section

Shot 15

Goal of this shot was to separate off a second 36-in by 36-in section still attached to concrete test slab 4 after shot 13. A 4~6 in deep pre-cut set the desired separation line for this shot. The plasma blasting probe was set into a borehole centered on the section to be separated, 18 in from either edge. Figure 154 shows the test setup. Table 21 describes the test setup and results for shot 15. Voltage and current traces collected by the oscilloscope from the capacitor and output HV probes and output current probe are shown in Figure 155 and Figure 156.

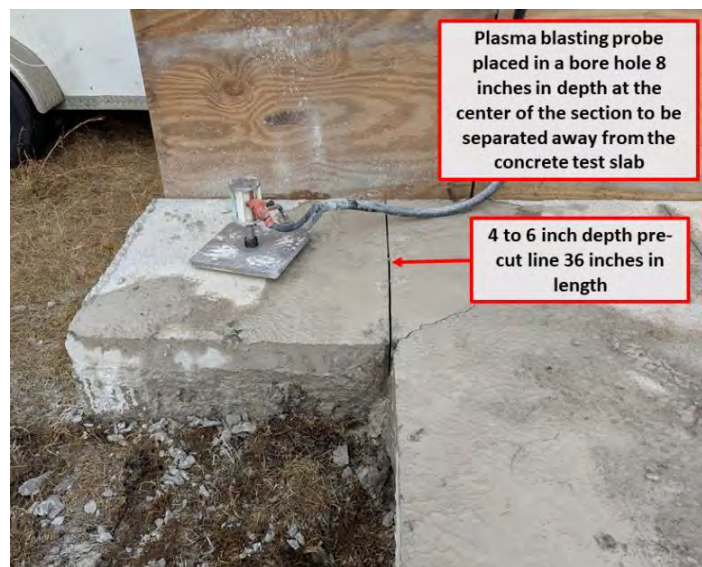
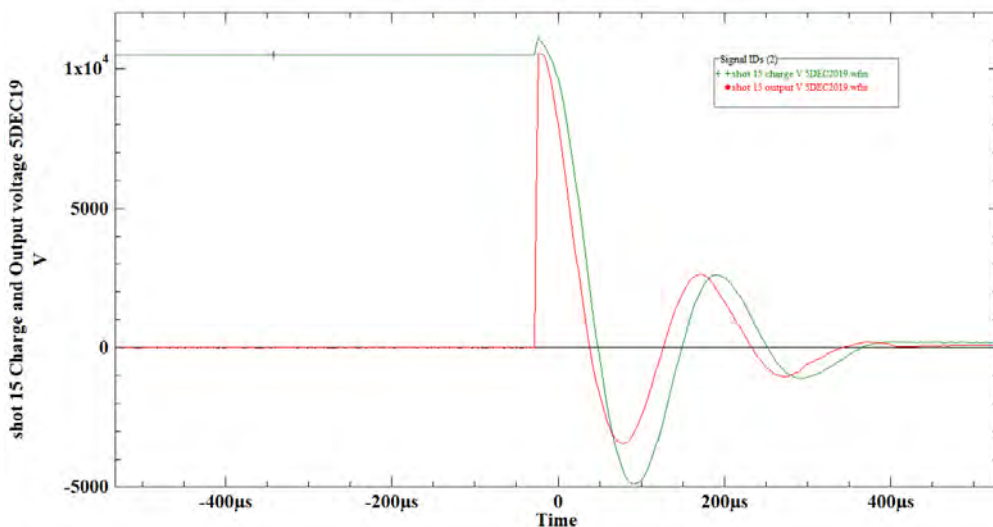


Figure 154. Shot 15: Plasma Blasting Probe in Borehole

Table 21. Data for Shot 15: Test Setup and Results

Shot 15	5-Dec-19
Plasma blasting probe	Probe 4: cleaned and re-used
EHF pulse transmission line	Coaxial design
Number of weight plates installed on the plasma blasting probe	2
Test concrete slab	Concrete slab 4: Initially 6 ft x 12 ft x 12 in thick
Borehole location	Center of second 36-in by 36-in section still attached to 4 concrete test slab after shot 13.
Borehole depth (in)	8
Borehole diameter (in)	1
Water used in borehole	Yes, bottled water, nothing added to the water
Setup precuts used for this shot	Yes, 4~6-in-deep pre-cut along shot 13 fracture line, to separate another 36-in by 36-in section from 4 concrete test slab
First test shot on this concrete slab	No, several shots have been completed on this concrete test slab.
Plasma blasting probe insertion depth (in)	7
Probe intact after shot	Yes
Charge voltage (VDC)	10500
EHF system capacitance (μF)	704
Charge energy (kJ)	38.8
Peak current (kA)	101.5
Notes	Goal to separate a second 36-in by 36-in section from 4 concrete slab. We failed to add water to borehole prior to the shot, which had no visible effect on the concrete test slab.

**Figure 155. Shot 15: Charge and Output Voltage for Time of Trigger of EHF System**

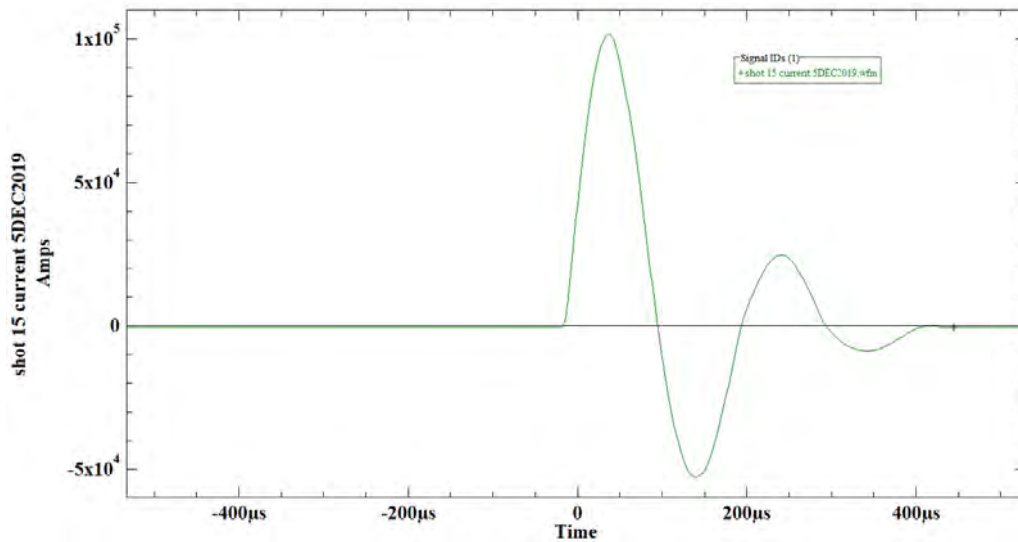


Figure 156. Shot 15: Time-Current Plot for Trigger from EHF System to Plasma Probe

Unfortunately, no water was in the borehole for the shot; as a result the “dry-fire” shot had no visible effect on the concrete test slab. Figure 157 shows the plasma blasting probe after shot 15. The probe had significant carbon buildup and damage around the probe tip. The nose cone tip surface was bent over slightly with partial interior exposure and possible damage to the center conductor dielectric tube. The attempt to use the probe again resulted in failure of the next shot, likely due to damage incurred from the “dry-fire” in this shot.



Figure 157. Shot 15: Plasma Blasting Probe after Dry Fire (Left) Probe Tip Is Slightly Bent, Significant Carbon Buildup. (Right) Cleaned Probe Shows Adhesive Delamination

Shot 16

Shot 16 setup was a repeat of shot 15 after we failed to add water to the borehole prior to triggering shot 15. The same borehole was used as was the goal—to separate off the second 36-in by 36-in section from concrete test slab 4—and the 4~6-in-deep pre-cut along the intended separation line. The plasma blasting probe was set into the borehole centered on the section to be separated. The test setup for shot 16 is shown in Figure 158. Test setup and results for shot 16 are shown in Table 22. Figure 159 and Figure 160 show voltage and current traces collected by the oscilloscope from the capacitor and output HV probes and output current probe.



Figure 158. Shot 16: Same Setup and Borehole as Shot 15

Table 22. Data for Shot 16: Test Setup and Results

Shot 16	5-Dec-19
Plasma blasting probe	Probe 4: cleaned and re-used
EHF pulse transmission line	Coaxial design
Number of weight plates installed on the plasma blasting probe	2
Test concrete slab	Concrete slab 4: Initially 6 ft x 12 ft x 12 in thick
Borehole location	Repeat of shot 15, Borehole in center of 36-in by 36-in section with pre-cut line to steer cracking
Borehole depth (in)	8
Borehole diameter (in)	1
Water used in borehole	Yes, bottled water, nothing added to the water
Setup precuts used for this shot	Yes, repeat of shot 15 with same 4~6-in-deep pre-cut designed to direct crack to separate second 36-in by 36-in section from 4 concrete test slab.
First test shot on this concrete slab?	No, several shots have been completed on this concrete test slab.
Plasma blasting probe insertion depth (in)	7
Probe intact after shot	Yes
Charge voltage (VDC)	10500
EHF system capacitance (μF)	704
Charge energy (kJ)	38.8
Peak current (kA)	134.8
Notes	Repeat of shot 15, to shear off 36-in by 36-in section along 4~6-in-deep line pre-cut in 4 test slab after shot 13. G10 tip blew off plasma blasting probe. Cracks away from offset pre-cut.

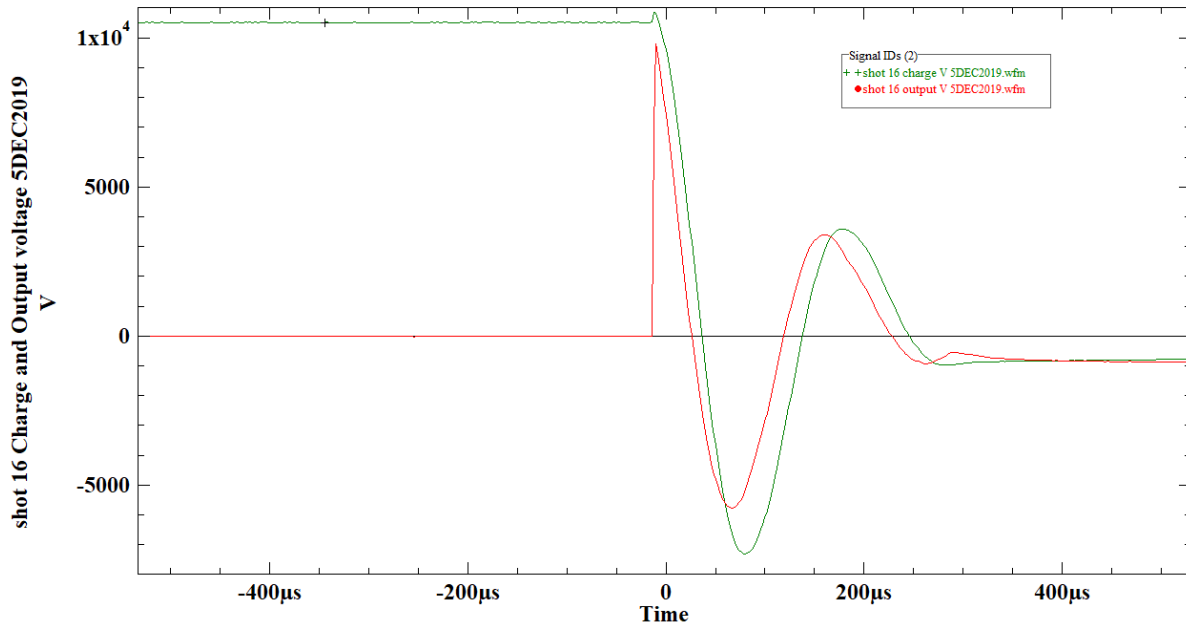


Figure 159. Shot 16: Charge and Output Voltage for Time of Trigger of EHF System

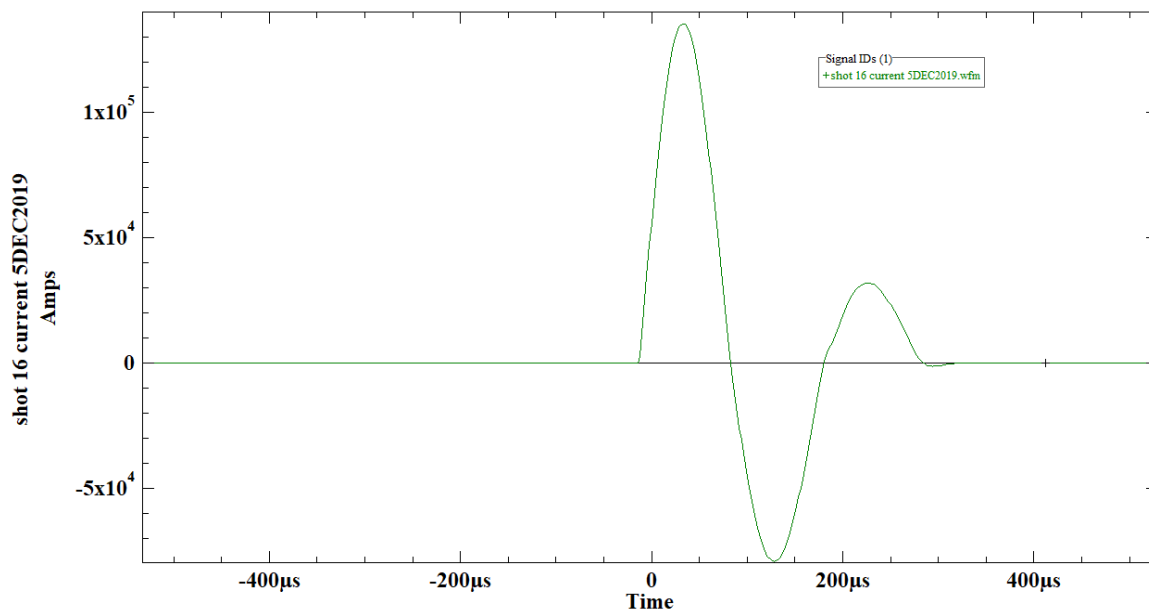


Figure 160. Shot 16: Time–Current Plot for Trigger from EHF System to Plasma Probe

The plasma blasting probe mechanically failed during this shot—the G10 probe tip separated from the center electrode and outer ground sheath and blew off. Figure 161 and Figure 162 show the probe failure, and also that the test concrete slab did crack and separate. This shot replicated the crack propagation behavior observed in shot 8, where the pre-cuts were offset from the borehole and not connected either across or terminating at it. The pre-cut in this configuration did not direct the crack propagation path.



Figure 161. Shot 16: Plasma Blasting Probe Failed; Cracks Did Not Follow Pre-cut Line



Figure 162. Shot 16: Failed Plasma Blasting Probe Tip and Cracks Formed from Borehole

Shot 17

Plasma blasting probe used for Shot 17 is Probe 3, another new stepped G10 probe. The test setup for Shot 17 is shown in Figure 163. The borehole was placed halfway between the pre-cut defining the 36-in by 36-in section still attached to 4 concrete test slab and the borehole used in shots 15 and 16, away from the pre-cut line and borehole. The goal was to separate off the 36-in by 36-in section from 4 concrete test slab, a second attempt to steer crack formation with the 4~6-in-deep pre-cut from shot 15. Test setup and results for shot 17 are listed in Table 23. Voltage and current traces collected by the oscilloscope from the capacitor and output HV probes and output current probe are shown in Figure 164 and Figure 165.



Figure 163. Shot 17: Probe in Hole between Hole for Shots 15 & 16, and Cut in Test Slab 4

Table 23. Data for Shot 17: Test Setup and Results

Shot 17	5-Dec-19
Plasma blasting probe	Probe 3: New stepped G10 probe 3 installed after shot 16
EHF pulse transmission line	Coaxial design
Number of weight plates installed on the plasma blasting probe	2
Test concrete slab	Concrete slab. Initially 6 ft x 12 ft x 12 in thick
Borehole location	Halfway between pre-cut defining 36-in by 36-in section to be sheared off 4 concrete test slab and shot 15 borehole
Borehole depth (in)	8
Borehole diameter (in)	1
Water used in borehole	Yes, bottled water, nothing added to the water
Setup precuts used for this shot	Yes, 4~6-in-deep pre-cut from shot 15 intended to shear 36-in by 36-in section from 4 concrete test slab.
First test shot on this concrete slab?	No, several shots have been completed on this concrete test slab.
Plasma blasting probe insertion depth (in)	7
Probe intact after shot	Yes
Charge voltage (VDC)	10500
EHF system capacitance (μF)	704
Charge energy (kJ)	38.8
Peak current (kA)	70.1
Notes	Borehole halfway (3 in) from 4~6-in-deep pre-cut to shot 15 borehole, hoped to steer crack along pre-cut line in 4 test slab. As for shots 8 and 16, offset pre-cut did not control crack propagation path.

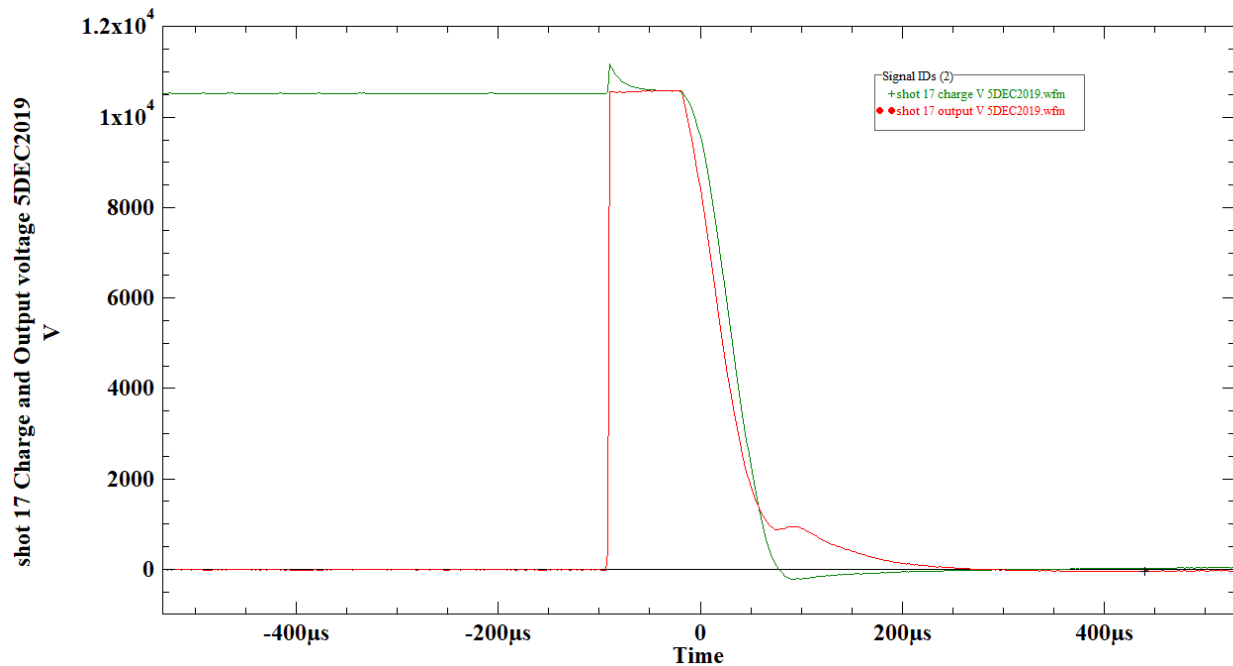


Figure 164. Shot 17 Charge and Output Voltage for Time of Trigger of EHF System

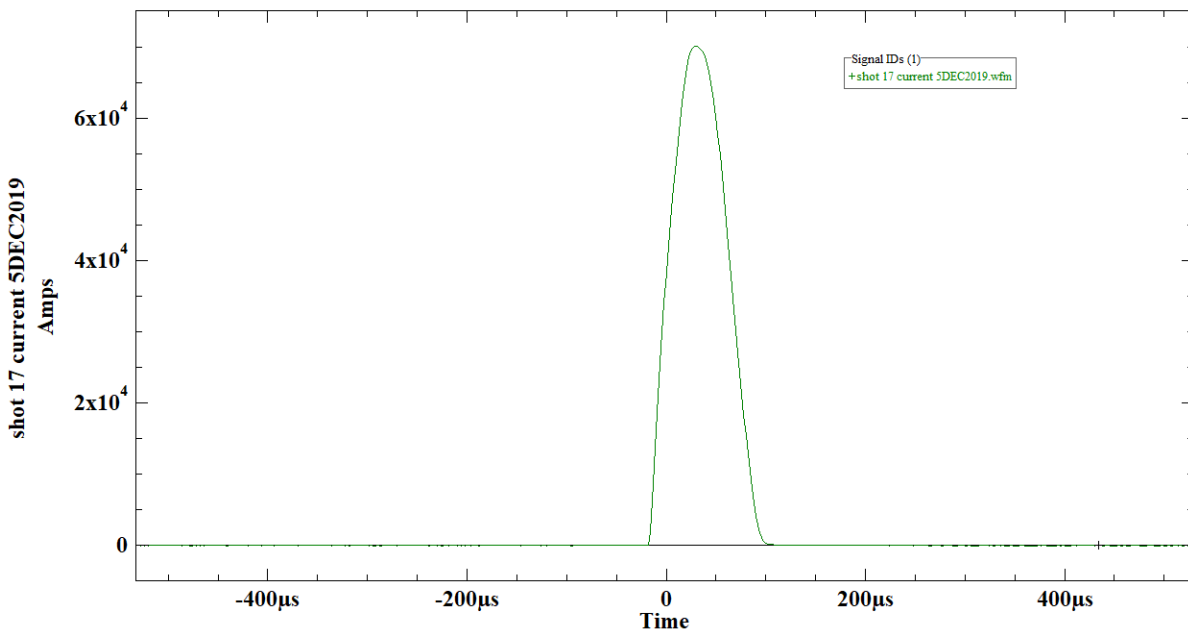


Figure 165. Shot 17: Time–Current Plot for Trigger from EHF System to Plasma Probe

As with shots 8 and 16, offset pre-cuts failed to control crack propagation path. This shot further confirms that pre-cut(s) must either intersect or terminate in or near the borehole for pre-cut to set the crack propagation path. Figure 166 and Figure 167 show results of shot 17. Probe 3 after shot 17 was in good shape. It was cleaned up and used again for shot 19.



Figure 166. Shot 17. Crack Propagation Did Not Follow Offset Pre-cut Lines



Figure 167. Shot 17. Crack Propagation Did Not Follow Offset Pre-Cut Lines

Shot 18

Shot 18 was a second test conducted to see if an exploding wire could be used to fracture the concrete test slab. The two leads of the EHF coaxial pulse transmission line were connected to the length of copper wire as shown in Figure 168. A semi-circular cut made into the concrete 13 in long, 6 in deep in the center is shown in Figure 169. A large chunk of concrete was placed flat side down over the cut containing the wire (Figure 170) in an attempt to contain the pressure pulse from the exploding wire to allow pressure to build up and break the concrete. Test setup and results for shot 18 are listed in Table 24. Voltage and current traces collected by the oscilloscope from the capacitor and output high voltage probes and output current probe are shown in Figure 171 and Figure 172



Figure 168. Shot 18: Exploding Wire for Installation in Cut in Slab



Figure 169. Shot 18:~ Cut into Concrete Test Slab 13 to Hold Exploding Wire



Figure 170. Shot 19: Chunk of Concrete over Wire and Cut to Contain Pressure Pulse

Table 24. Data for Shot 18: Test Setup and Results

Shot 18	5-Dec-19
Plasma blasting probe	Exploding wire test (cooper wire used)
EHF pulse transmission line	Coaxial design
Number of weight plates installed on plasma blasting probe	2
Test concrete slab	Concrete slab 4: Initially 6 ft x 12 ft x 12 in thick
Borehole location	N/A, shot 18 is a second test with exploding wire in semi-circular cut into the concrete slab, 6 in deep, 13 in long
Borehole depth (in)	N/A
Borehole diameter (in)	N/A
Water used in borehole	N/A
Setup precuts used for this shot	13 in lit cut ~6 in deep into concrete to hold blasting wire
First test shot on this concrete slab?	No, multiple shots made on this concrete test slab.
Plasma blasting probe insertion depth (in)	N/A
Probe intact after shot	Yes
Charge voltage (VDC)	16550
EHF system capacitance (μF)	704
Charge energy (kJ)	96.4
Peak current (kA)	40.1
Notes	Second test of exploding wire concept. Cover over wire in semi-circular cut 13 in long, center 6 in deep, blown off by pressure spike. No cracking noticed.

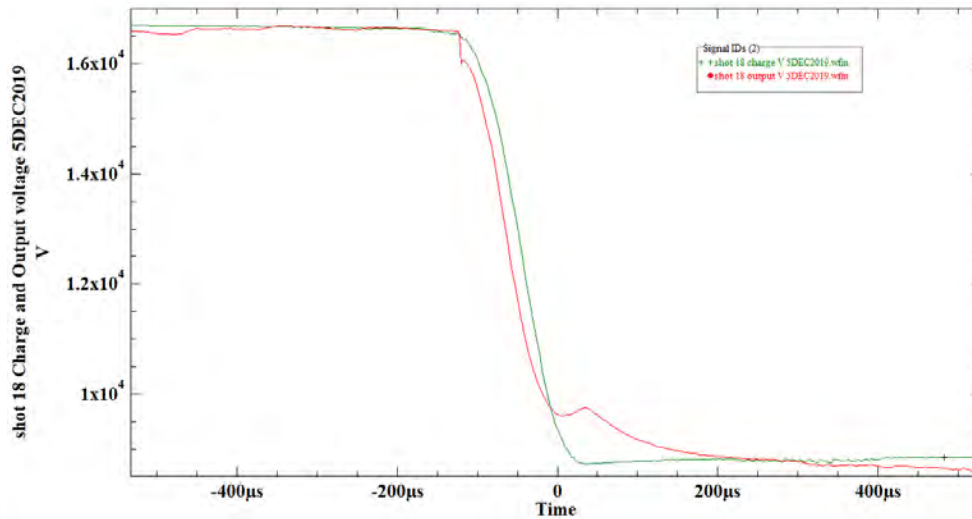


Figure 171. Shot 18: Charge and Output Voltage for Time to Trigger the EHF System

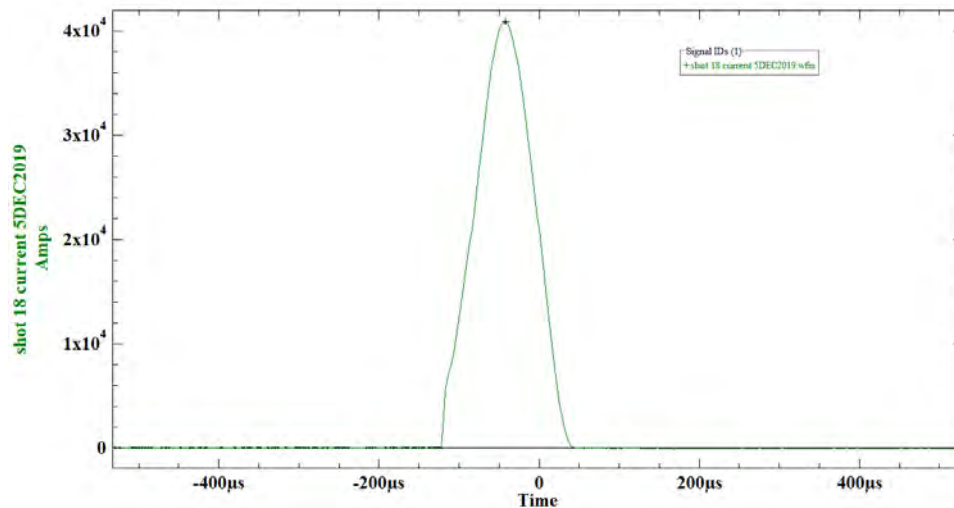


Figure 172. Shot 18: Time-Current Plot for Trigger from EHF System to Plasma Probe

Figure 173 shows the results of the shot 18 exploding wire test, which did not crack the concrete. The pressure pulse of the exploding wire pushed the concrete chunk on top of the setup off the test concrete slab. The edges of the semi-circular cut used to contain the exploding wire are slightly ablated. The exploding wire had no visible appreciable effect on the concrete test slab. The exploding wire test created a significant pressure spike, felt moving through the air ~100 ft from the test setup. As with shot 12, the wire failed to crack the concrete, because the pressure pulse created was not confined and escaped out the top of its cut in the concrete. This concept for cracking concrete may have potential but, due to time constraints, it was not pursued in further testing. Future tests of the exploding wire should attempt to better contain the pressure pulse from the exploding wire. Also, aluminum wire would be more energetic as an exploding wire: exploding wire in future tests should be made of aluminum wire or foil. In addition, placing the exploding wire in a borehole instead of a linear surface cut may be advantageous.



Figure 173. Shot 18: Pressure Pulse of Exploding Wire Only Lifted Concrete Chunk

Shot 19

Pre-cut lines used in shot 19 were the same setup as in shot 13, ~6 in deep edging a 36-in by 36-in section of the 4 concrete test slab. The borehole was placed at the intersection of the pre-cut lines, which terminated close to, but not connected to the borehole. In another effort to stop unintentional crack propagation, a second through borehole was drilled ~4 in away from the plasma blasting probe borehole in the concrete test slab. Figure 174 and Figure 175 show the test setup for shot 19.

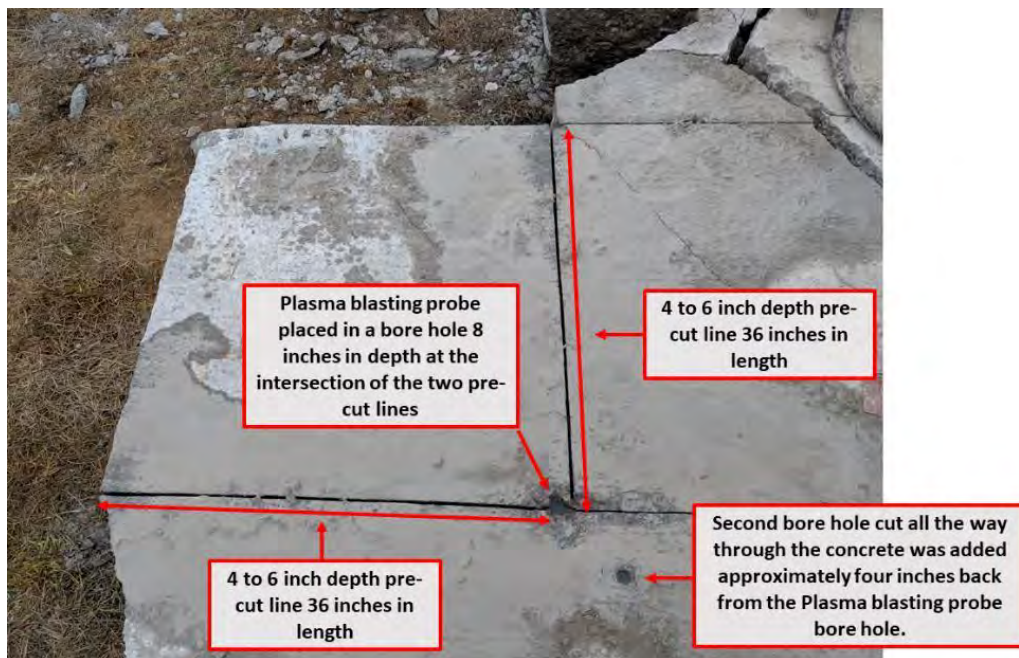


Figure 174. Shot 19: Test Setup; as for Shot 13, Plus Second Borehole to Stop Crack



Figure 175. Shot 19: Test Setup with Plasma Blasting Probe Installed

Table 25 lists Test setup and results for shot 19. Voltage and current traces collected by the oscilloscope from the capacitor and output HV probes and output current probe are shown in Figure 176 and Figure 177.

Table 25. Data for Shot 19: Test Setup and Results

Shot 19	5-Dec-19
Plasma blasting probe	Probe 3: cleaned and re-used from shot 17
EHF pulse transmission line	Coaxial design
Number of weight plates installed on the plasma blasting probe	2
Test concrete slab	Concrete slab 4: Initially 6 ft x 12 ft x 12 in thick
Borehole location	36 in from two edges of slab along pre-cut lines. Through hole added ~ 4 in from plasma blasting probe borehole in concrete test slab to stop unintentional crack propagation.
Borehole depth (in)	8
Borehole diameter (in)	1
Water used in borehole	Yes, bottled water, nothing added to the water
Setup precuts used for this shot	Deeper (~6 in) lines were pre-cut in the same layout as shot 13 marking a 36-in by 36-in section of 4 concrete test slab. precut lines ended near but not touching the probe borehole.
First test shot on this concrete slab?	No, multiple shots have been completed in this concrete test slab.
Plasma blasting probe insertion depth (in)	7
Probe intact after shot	Yes
Charge voltage (VDC)	10500
EHF system capacitance (μF)	704
Charge energy (kJ)	38.8
Peak current (kA)	77.4
Notes	Two unintentional cracks in slab, one through through hole. 6-in-deep pre-cuts directed separation of 36-in by 36-in section of concrete, pre-cuts near borehole draw crack path.

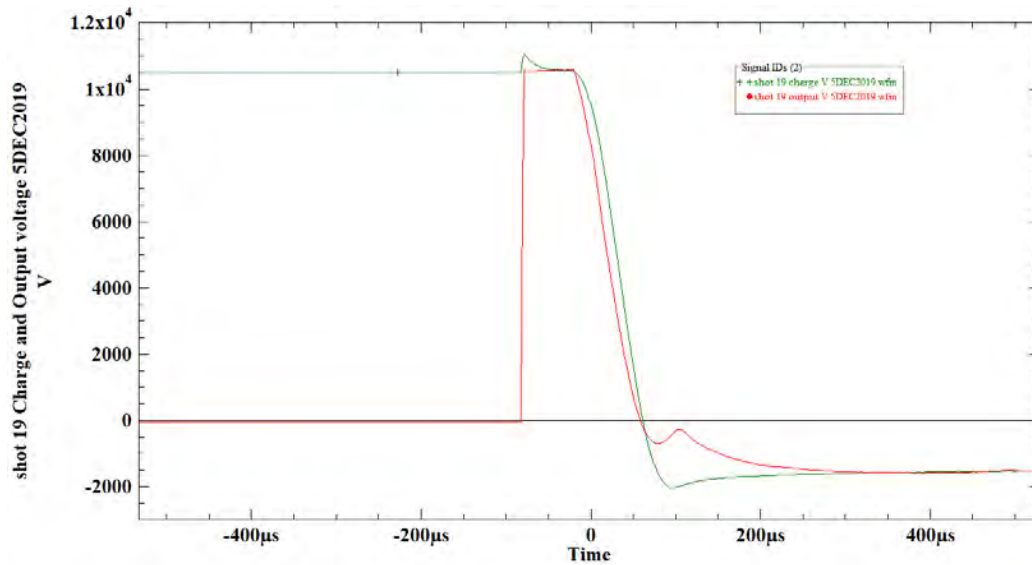


Figure 176. Shot 19 Charge and Output Voltage for Time of Trigger of EHF System

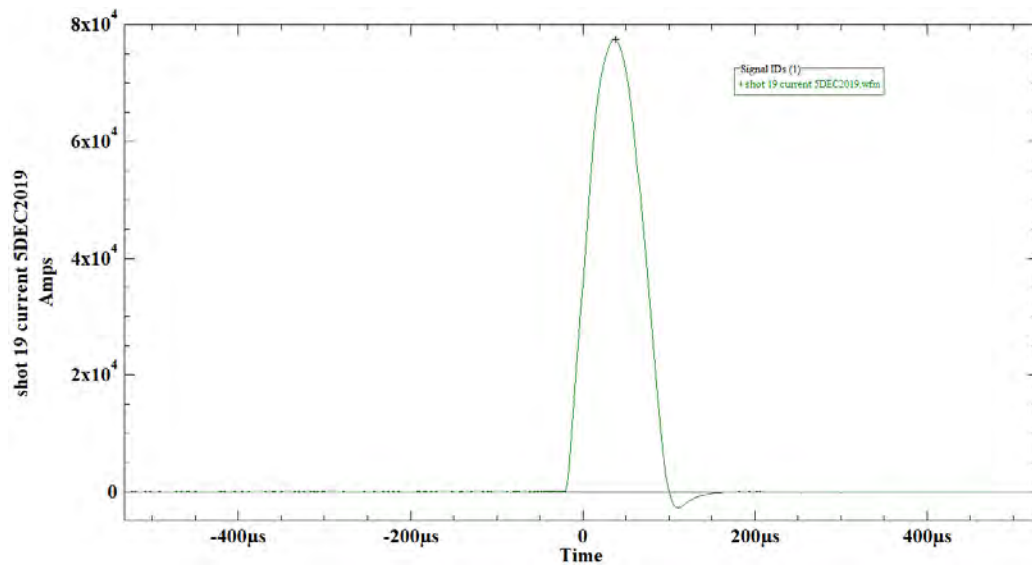


Figure 177. Shot 19: Time–Current Plot for Trigger from EHF System to Plasma Probe

Figure 178 through Figure 180 show test results for shot 19. Two unintentional cracks formed in the concrete test section (Figure 178). One of the cracks shown propagated through the hole drilled 4 in back from the probe borehole. The 6-in-deep pre-cuts for shot 19 successfully directed crack propagation from the shot to separate the 36-in by 36-in section of concrete (Figure 179). This test shot confirms that, as in similar test setups, pre-cut lines that pass through or terminate near the borehole containing the plasma blasting probe can direct crack propagation. After shot 19 Probe 3 was in good shape. It was cleaned up and used again for shot 20.

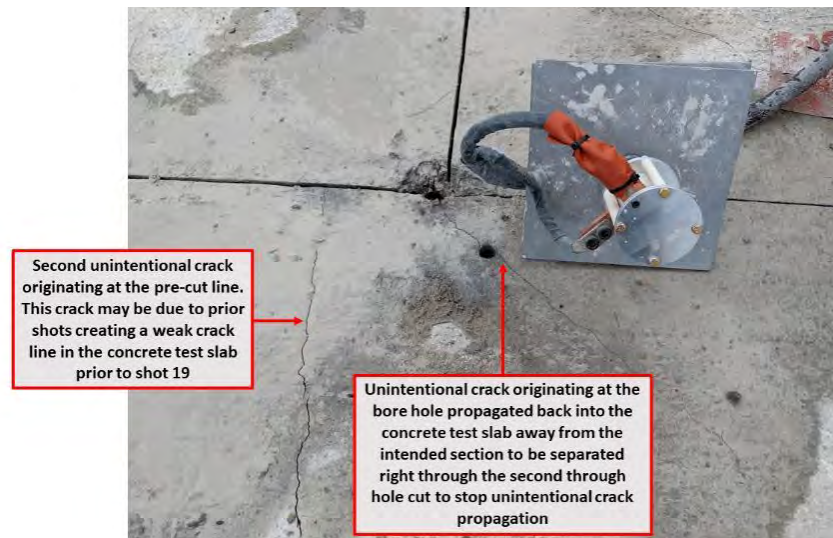


Figure 178. Shot 19: Two Unintentional Cracks Formed in the Concrete Test Section



Figure 179. 6-in-deep Pre-cuts Directed Crack Propagation



Figure 180. Shot 19: Crack Propagation along Pre-cut Lines from Borehole

Shot 20

A borehole was drilled at the center of the 36-in by 36-in section separated off concrete test slab 4 by shot 19. Figure 181 shows the test setup for shot 20. The goal of this shot was to break up the section separated in shot 19 into smaller more manageable chunks. This shot used a charge energy of 87.9 kJ to promote fragmentation of the concrete section. Test setup and results for shot 20 are summarized in Table 26. Figure 182 and Figure 183, respectively, show voltage and current traces collected by the oscilloscope from the capacitor and output HV probes.

Shot 20 successfully broke up the 36-in by 36-in separated concrete section from shot 19 into smaller chunks. High charge energy is more useful for this application as more-extensive fragmentation occurs. Figure 184 and Figure 185 show the results of shot 20. Probe 3 after shot 20 is in good shape and can be used for further shots.



Figure 181. Shot 20: Plasma Blasting Probe in Concrete Section Separated by Shot 19

Table 26. Data for Shot 20: Test Setup and Results

Shot 20	5-Dec-19
Plasma blasting probe	Probe 3: cleaned and re-used
EHF pulse transmission line	Coaxial design
Number of weight plates installed on the plasma blasting probe	2
Test concrete slab	36-in x 36-in section shot 19 sheared off 4 concrete test slab
Borehole location	Center of 36-in by 36-in section separated from 4 concrete test slab by shot 19
Borehole depth (in)	8
Borehole diameter (in)	1
Water used in borehole	Yes, bottled water, nothing added to the water
Setup precuts used for this shot	No pre-cuts; goal shot is to break the 36-in by 36-in section separated by shot 19 into smaller more manageable chunks
First test shot on this concrete slab?	No, breaking up block of concrete separated off by shot 19
Plasma blasting probe insertion depth (in)	7
Probe intact after shot	Yes
Charge voltage (VDC)	15700
EHF system capacitance (μF)	704
Charge energy (kJ)	86.8
Peak current (kA)	153.6
Notes	Goal: fragment the large section separated by shot 19 into smaller chunks. Higher pulse charge energy, 86.8 kJ, did it.

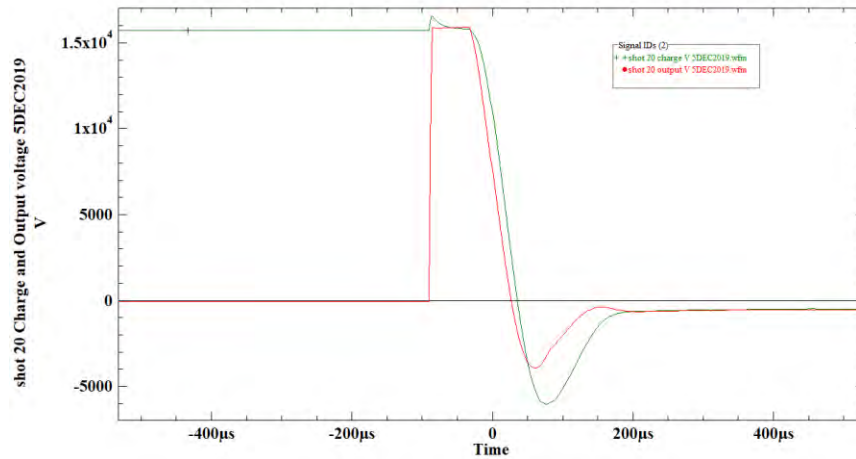


Figure 182. Shot 20: Charge and Output Voltage for Time of Trigger of EHF Ssystem

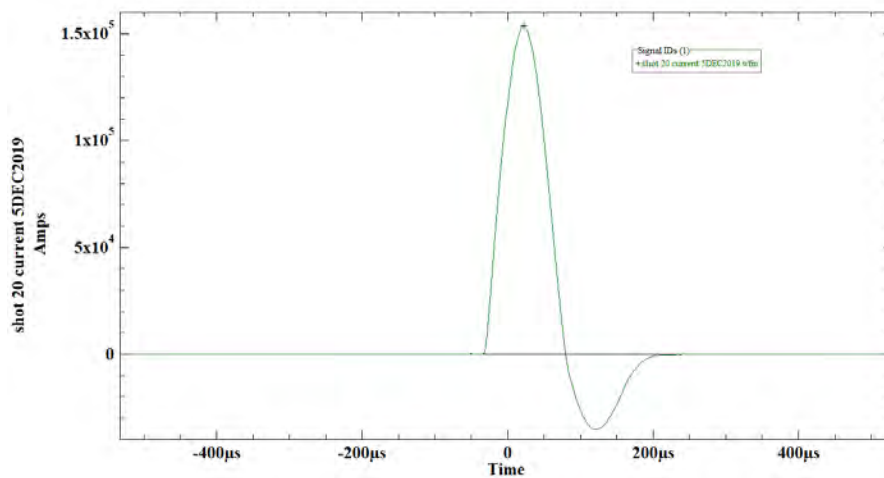


Figure 183. Shot 20: Time-Current Plot for Trigger from EHF System to Plasma Probe



Figure 184. Shot 20: Debris and Chunks from 36-in by 36-in Shot 19 Fragment



Figure 185. Shot 20: Debris and Chunks from 36-in by 36-in Shot 19 Fragment

3. CONCLUSIONS AND RECOMMENDATIONS

The EHF system was tested in the field on 3–5 December 2019 through a series of 20 test shots into four test section slabs of 12-in-thick concrete. As originally proposed for the Phase I, Hyperion intended the field demonstration to combine the use of a waterjet cutting system for pre-cutting slabs followed by use of the EHF system to fragment the cut concrete slabs into small fragments for easy handling and disposal. However, despite numerous attempts to arrange for short-term rental use of the waterjet cutting systems, at the time for the field testing that equipment was not available, as vendors were interested only in long-term use.

Hyperion modified the EHF field demonstration tests using no waterjet cutting system to show the results of having no, or only shallow pre-cuts into the concrete to be followed by EHF system plasma blasts. During these tests, the user-selectable energy applied to each blast demonstrated the extent to which an operator may control and tailor the blast mechanics to produce and limit the desired level of crack formation and fragmentation. Fragmentation occurs along a cut line only if the borehole for the plasma probe is located somewhere along the cut line, and no simple means to avoid additional cracking was identified.

These initial tests over only two field-test days (plus one half day for setup) show that the EHF causes significant fragmentation of large sections of cut concrete slabs, but that control of the direction of fragmentation may require extensive preparation of the concrete slab. Future tests during Phase II would include modifications to the EHF blasting probe intended to eliminate this effect. Further, refinement of the system and more-detailed understanding could further reduce the need or depth of “pre-scarring” to control the cutting action of the system. Phase I was intended just to be a PoP demonstration, which was accomplished without question.

4. BIBLIOGRAPHY

1. "Study of the Electrical Characteristics, Shock-Wave Pressure Characteristics, and Attenuation Law Based on Pulse Discharge in Water" (June 2016, Shock and Vibration 2016(6):1-11, DOI: 10.1155/2016/6412309;
https://www.researchgate.net/publication/303847987_Study_of_the_Electrical_Characteristics_Shock-Wave_Pressure_Characteristics_and_Attenuation_Law_Based_on_Pulse_Discharge_in_Water
2. Ioffe, A. I. "Theory of the initial stage of an electrical discharge in water." Journal of Applied Mechanics and Technical Physics 7, no. 6 (1966): 47-50.
<http://www.springerlink.com/index/R1MWHM844J201684.pdf>
3. Graneau, Peter, and P. Neal Graneau. "Electrodynamic explosions in liquids." Applied Physics Letters 46, no. 5 (1985): 468-470. <https://aip.scitation.org/doi/abs/10.1063/1.95559>
4. Qian, Jun, Ravindra P. Joshi, Karl H. Schoenbach, J. R. Woodworth, and G. S. Sarkisov. "Model analysis of self-and laser-triggered electrical breakdown of liquid water for pulsed-power applications." IEEE transactions on plasma science 34, no. 5 (2006): 1680-1691.
http://crpppc42.epfl.ch/Roma/pdf/P5_064.pdf.
5. Yan, Dong, Decun Bian, Jinchang Zhao, and Shaoqing Niu. "Study of the electrical characteristics, shock-wave pressure characteristics, and attenuation law based on pulse discharge in water." Shock and Vibration 2016 (2016).
<http://downloads.hindawi.com/journals/sv/2016/6412309.pdf>
6. Gidalevich, E., and R. L. Boxman. "Sub-and supersonic expansion of an arc channel in liquid." Journal of Physics D: Applied Physics 39, no. 4 (2006): 652.
<https://iopscience.iop.org/article/10.1088/0022-3727/39/4/010/pdf>
7. Yang, Yong, Hyounsup Kim, Andrey Starikovskiy, Alexander Fridman, and Young I. Cho. "Pulsed multichannel discharge array in water with stacked circular disk electrodes." IEEE Transactions on Plasma Science 39, no. 11 (2011): 2624-2625.
<https://ieeexplore.ieee.org/abstract/document/5762387>

LIST OF ABBREVIATIONS, SYMBOLS AND ACRONYMS

AC	alternating current
B-M	Bernardes–Merryman
CAD	computer-assisted design
CCPS	capacitor–charging power supply
COTS	commercial-off-the-shelf
dI/dt	current rise-time
EHF	electro-hydraulic fracture
ESL	equivalent series inductance
IEEE	Institute of Electrical and Electronics Engineers
GA	General Atomics
HV	high-voltage
HVPS	high-voltage power supply (
KAPRA	Korea Accelerator and Plasma Research Association
LCA	long-charge adapter
SPICE	Simulation Program with Integrated Circuit Emphasis (model)
TRL	Technology Readiness Level